Santa Clara University
Scholar Commons

Interdisciplinary Design Senior Theses | Engineering Senior Theses

6-2018

Powering a Biosensor Using Wearable Thermoelectric Technology

Anneliese Bals
Santa Clara University, abals@scu.edu

Noah Barnes
Santa Clara University, nbarnes@scu.edu

Rafael Bravo
Santa Clara University, rbravo@scu.edu

Nicolas Garcia
Santa Clara University, ngarcia@scu.edu

Joseph O'Bryan
Santa Clara University, jobryan@scu.edu

See next page for additional authors

Follow this and additional works at: https://scholarcommons.scu.edu/idp_senior

Part of the Biomedical Engineering and Bioengineering Commons, and the Mechanical Engineering Commons

Recommended Citation

Bals, Anneliese; Barnes, Noah; Bravo, Rafael; Garcia, Nicolas; O'Bryan, Joseph; and Santana, Dylan, "Powering a Biosensor Using Wearable Thermoelectric Technology" (2018). *Interdisciplinary Design Senior Theses*. 41.
https://scholarcommons.scu.edu/idp_senior/41

This Thesis is brought to you for free and open access by the Engineering Senior Theses at Scholar Commons. It has been accepted for inclusion in Interdisciplinary Design Senior Theses by an authorized administrator of Scholar Commons. For more information, please contact rscroggin@scu.edu.

Author
Anneliese Bals, Noah Barnes, Rafael Bravo, Nicolas Garcia, Joseph O'Bryan, and Dylan Santana

This thesis is available at Scholar Commons: https://scholarcommons.scu.edu/idp_senior/41

SANTA CLARA UNIVERSITY

Department of Mechanical Engineering
Department of Bioengineering

I HEREBY RECOMMEND THAT THE THESIS PREPARED
UNDER MY SUPVISION BY

Anneliese Bals, Noah Barnes, Rafael Bravo,
Nicolas Garcia, Joseph O'Bryan, and Dylan Santana

ENTITLED

POWERING A BIOSENSOR USING WEARABLE THERMOELECTRIC POWER GENERATION

BE ACCEPTED IN PARTIAL FULFILLMENT OF THE REQUIREMENTS
FOR THE DEGREE OF

BACHELOR OF SCIENCE
IN
MECHANICAL ENGINEERING
BIOENGINEERING

6/11/18
Dr. Hohyun Lee, Mechanical Engineering Advisor date

6/11/18
Dr. Terry Shoup, Mechanical Engineering Department date

6/12/18
Dr. Prashanth Asuri, Bioengineering Advisor date

06/13/18
Dr. Yuling Yan, Bioengineering Department Chair date

POWERING A BIOSENSOR USING THERMOELECTRIC POWER GENERATION

By

Anneliese Bals, Noah Barnes, Rafael Bravo,
Nicolas Garcia, Joseph O'Bryan, and Dylan Santana

SENIOR DESIGN THESIS REPORT

Submitted to
the Departments of
Mechanical Engineering and Bioengineering

of

SANTA CLARA UNIVERSITY

in Partial Fulfillment of the Requirements
for the degrees of
Bachelor of Science in Mechanical Engineering
Bachelor of Science in Bioengineering

Santa Clara, California

2018

Abstract

Wearable medical devices such as insulin pumps, glucose monitors, hearing aids, and electrocardiograms provide necessary medical aid and monitoring to millions of users worldwide. These battery powered devices require battery replacement and frequent charging that reduces the freedom and peace of mind of users. Additionally, the significant portion of the world without access to electricity is unable to use these medical devices as they have no means to power them constantly. Wearable thermoelectric power generation aims to charge these medical device batteries without a need for grid power.

Our team has developing a wristband prototype that uses body heat, ambient air, and heat sinks to create a temperature difference across thermoelectric modules thus generating ultra-low voltage electrical power. A boost converter is implemented to boost this voltage to the level required by medical device batteries. Our goal was to use this generated power to charge medical device batteries off-the-grid, increasing medical device user freedom and allowing medical device access to those without electricity. We successfully constructed a wearable prototype that generates the voltage required by an electrocardiogram battery; however, further thermoelectric module and heat dissipation optimization is necessary to generate sufficient current to charge the battery.

Acknowledgments

We sincerely thank those who have helped us along the way to achieving wearable electric power generation. From those who helped us from day one, to those who rooted for us on the final day of presentation, we are grateful for all the love and support we have received all year. We would especially like to thank:

Dr. Lee, our amazing advisor for helping us kickstart the project with amazing advise, and leading us to great success throughout the year.

Dr. Hight for keeping us organized in our efforts, allowing us to make incredible progress in just one academic year.

Dr. Asuri and Dr. Zhang for excellent advise pertaining to bioengineering concepts.

Don MacCubbin for the excellent quality of rapidly prototyped fixture and the infinite help with developing them.

Tom Watson for all the help with thermoelectrics, the amazing data, the beautiful graphs, unending knowledge of TEM-heat sink systems, and much more.

Joshua Vincent for collecting excellent data and helping with thermoelectric testing.

The Santa Clara University Department of Engineering for funding the project, making great technological progress on the undergraduate level possible.

Our friends and families for their unending support of our efforts.

Thank you!
- The Wearable Thermoelectric Team

Contents

Abstract **iii**

Acknowledgments **iv**

Table of Figures **viii**

Table of Tables **x**

1 Introduction **1**
- 1.1 Problem Statement 1
- 1.2 Solution: The Wearable Thermoelectric Generator 1
- 1.3 Literature Review 2
- 1.4 Project Objectives 3

2 Systems Level Analysis **5**
- 2.1 Customer Needs 5
  - 2.1.1 Introduction 5
  - 2.1.2 Questions and Answers 5
  - 2.1.3 Summary 6
- 2.2 System Level Physical Sketch and User Scenario 6
- 2.3 Functional Analysis 9
- 2.4 Benchmarking Results 12
- 2.5 System Level Issues 14
- 2.6 System Level Design Layout 16
- 2.7 Team and Project Management 17
  - 2.7.1 Project Challenges and Constraints 17
  - 2.7.2 Budget 18
  - 2.7.3 Timeline 18
  - 2.7.4 Design Process 18
  - 2.7.5 Risks and Mitigation 19
  - 2.7.6 Team Management 20

3 Power Generation Subsystem **21**
- 3.1 Options and Trades 21
  - 3.1.1 Heat Sinks 21
  - 3.1.2 Thermoelectric Modules 23
- 3.2 Heat Sink and Thermoelectric Module Analysis and Selection 25
  - 3.2.1 Heat Sink Analysis and Selection 25
  - 3.2.2 Heat Sink Modification 28
  - 3.2.3 Thermoelectric Module Analysis and Selection 29
- 3.3 Design Description 34

3.4 Prototype Results . . . 35
3.5 Subsystem Testing and Verification . . . 35
3.5.1 Theoretical Maximum Power Tests . . . 35
3.5.2 Seebeck Tests . . . 38

4 Voltage Boosting Subsystem 40
4.1 Choosing a Boost Converter . . . 40
4.2 Circuit Design . . . 41
4.3 Subsystem Optimization . . . 42

5 Battery Charging Subsystem 45
5.1 Options and Trades . . . 45
5.2 Design Description . . . 47
5.3 Prototype Results . . . 47
5.4 Subsystem Testing and Verification . . . 48

6 Wearability Subsystem 50
6.1 Wristband . . . 50
6.1.1 Options and Trades . . . 50
6.1.2 Design Description . . . 51
6.2 Prototype Results . . . 53
6.3 Housing Fixture . . . 54
6.3.1 Rationale . . . 54
6.3.2 Design Criteria . . . 54
6.3.3 Design Iterations . . . 54
6.4 Prototype Results . . . 57

7 System Integration, Test, and Results 58
7.1 Experimental Protocol and Results . . . 59
7.1.1 Voltage and Current Testing . . . 59
7.1.2 Battery Charge Testing . . . 60
7.1.3 Customer Needs Testing . . . 61
7.1.4 Moisture and Durability Testing . . . 62

8 Cost Analysis 63

9 Patent Search 66
9.1 Executive Summary . . . 66
9.2 Scope of Design Concept . . . 66
9.3 Invention Description . . . 67
9.4 Mechanical Drawings . . . 69
9.5 Patent Classification . . . 70
9.6 Review of Prior Art . . . 70

9.7 Conclusion 72

10 Engineering Standards and Realistic Constraints 73
10.1 Cost 73
10.2 Health and Safety 73
10.3 Manufacturability and Repairability 73
10.4 Sustainability 74
10.5 Ethical Considerations 74

11 Conclusion 76
11.1 Summary 76
11.2 Future Improvements 76
11.3 Final Thoughts 77

Appenidx A: Selection Matrices 81

Appendix B: PDS 83

Appendix C: Timeline 84

Appendix D: Calculations 85
Heat Sink Hand Calculations 85
Heat Sink FEA Analysis 87

Appendix E: Drawings 89
Heat Sink 89
Thermoelectric Module 90
Housing 91
Assembly Drawing 92
Miscellaneous Drawings 93

Appendix F: Budget Details 100

Appendix G: Senior Design Conference Presentation 103

Appendix H: Relevant Patents 111

Table of Figures

1 System sketch, top side of device. 7
2 System sketch, bottom side of device. 8
3 Seiko Thermic [16]. 12
4 Matrix Powerwatch [20]. 13
5 Wristband prototype with integrated EKG monitor on topside. 16
6 Wristband prototype with integrated TEMs 17
7 Fin type, pin type, and natural convection heat sinks [13]. 22
8 Non-potted TEM versus potted TEM. 24
9 Heat sink testing and evaluation setup schematic. 26
10 Heat sink testing and evaluation setup detail. 27
11 Heat sink testing and evaluation results. 28
12 FEA heat sink heat flux distribution. 29
13 TE technology TEM schematic and dimensions. 30
14 TEM theoretical power output versus effective B factor, courtesy of Tom Watson, SCU. 32
15 Dimensioned schematic of TE-65-0.6-1.5. 34
16 Power generation prototype. 35
17 Power generation VI curve. 37
18 Power generation Seebeck curve. 39
19 Optimal LTC3108 circuit [10]. 41
20 Efficiency vs. Voltage In for LTC3108. 43
21 Voltage Out vs. Voltage In graph for LTC3108. 43
22 EKG and its charger. 46
23 Battery charging prototype. 48
24 Battery voltage over 2 hour charging period, courtesy of Joshua Vincent, SCU. 49
25 Initial concept for wristband prototype. 52
26 Wristband prototype. 53
27 Snap-fit housing design. 55
28 Screw-and-bolt housing design. 56
29 Final housing design, Modular TEM-Heat Sink Interface. 57
30 Wearable thermoelectric power generation system. 58
31 Wearable thermoelectric power generation system prototype. 59
32 Detailed Mechanical Drawing of Modular TEM-Heat Sink Interface. . 69
33 TEM theoretical power output versus N versus B$_{eff}$, courtesy of Tom Watson, SCU. 77
34 Subsystem factor weighting matrix. 81
35 Subsystem concept ranking matrix. 82
36 Gantt charts for Fall, Winter, and Spring. 84
37 N19-10B heat dissipation hand calculations. 85

38 N19-10B surface area and heat flux hand calculations. 86
39 FEA temperature distribution model. 88
40 FEA heat flux model. 88
41 N19-10B mechanical specifications, courtesy of Alpha Nova Tech. . . 89
42 TE-65-0.6-1.5 detail drawing. 90
43 TEM-heat sink housing detail drawing. 91
44 TEM, heat sink, and housing assembly drawing. 92
45 Assembly-in-wristband drawing, uncovered and covered, on left and right, respectively. 93
46 System sketch, top side of device. 94
47 System sketch, bottom side of device. 95
48 Screw-and-nut housing concept, hand sketch. 96
49 Thermoelectric power generator powering a medical device, hand sketch. 97
50 A watch band-esque thermoelectric power generator, hand sketch. . . 98
51 Orthographic view of full TEM, heat sink, and fixture assembly. . . . 99
52 Patent of TEM module used for low power generation. 111
53 Patent of wrist wearable EKG device. 112
54 Patent of thermoelectric assembly using cardtridge support fixture. . 113
55 Patent of thermoelectric heat pump. 114

Table of Tables

1 Subsystem inputs, outputs, and constraints. 11
2 Benchmarking Results 14
3 Theoretical maximum power test results. 31
4 Power generation testing and verification data. 37
5 Output voltage and current experimental results. 60
6 Wristband dimensions and mass. 61
7 Aesthetics and comfort/ergonomics ratings. 62
8 Detailed project costs. 64
9 Detailed prototype costs. 65
10 PDS. Rev. 3, May 7, 2018. 83
11 Detailed proposed project budget. 100
12 Detailed project costs. 101
13 Detailed prototype costs. 102

Chapter 1

Introduction

1.1 Problem Statement

Millions of people around the world live with the assistance of medical technology that improves the quality and length of their lives. Many of these people rely on these technologies daily, some are so necessary for the patient that the proper functionality of such a device could mean life or death. These devices include insulin pumps, glucose monitors, hearing aids, portable heart rate monitors, and more. One of the main concerns for users of these medical devices is keeping their devices powered. Having to worry about charging or replacing batteries can limit the freedom of the user and cause additional stress. Extended outdoor activities such as camping trips or off-the-grid excursions may not be accessible to one who has to worry about powering their medical device. Additionally, nearly 13% of the world lives without access to electricity [1]. This prevents these people from benefiting from life prolonging and life saving medical device technologies as they have no means to power these devices consistently. The medical device field has never had a thermoelectric-generation-based device make it to market, and with most portable medical devices optimized for running on very low voltage power sources, there is high potential for thermoelectric power generation for battery charging or power supply.

1.2 Solution: The Wearable Thermoelectric Generator

Wearable thermoelectric power generation is a solution to bring peace of mind to those using these medical devices and bring medical device access to those without electricity. It is a wearable device harvesting the heat of one's own body to produce electricity through the use of thermoelectric technology. The power generated by this device is used to charge a medical device battery.

Our goal is to improve the quality of life for people using medical devices by allowing them to charge their devices wherever and whenever with the heat of their own body. We strive to provide a wearable thermoelectric generator that can charge the battery of a medical device such that a user does not have to charge the device by other means as often or at all. This awards the freedom of extended mobility away from a power outlet, and allows medical devices to be used in regions with no access to electricity.

Our technical goal is to successfully charge a 3.7V / 80mA battery common in low-voltage medical devices.

1.3 Literature Review

The device produced by the team is a wearable power generator, utilizing the power generation capabilities of thermoelectric modules (TEMs) and the heat dissipating capabilities of heat sinks. When a temperature difference is present across the TEMs, a voltage is produced proportional to this temperature difference by a constant ratio unique to the specific TEM. The voltage is collected in an electrical circuit and used to power low-voltage medical devices, the whole system being held in a wearable fixture. Heating a "hot side" by the heat of one's body and cooling the "cold side" by attaching heat sinks to reduce the temperature to as close to room temperature as possible will improve the consistency of this temperature difference present across the TEM. There are many factors that go into how the system of TEMs and heat sinks performs and each variable can affect the performance differently. And it is especially difficult with the variable of the human body temperature being added. The article "Modeling, Fabrication, and Experimental Testing of a Heatsink-free Wearable Thermoelectric Generator" published in the journal *Energy Conversion & Management* in 2017 discusses the variables that determine performance of wearable thermoelectric generators excluding the use of a heat sink. However, because adding a heat sink to the cold side of a TEM in wearable generation is almost always beneficial, optimizing the TEM, electrical circuitry, and wearability subsystems will improve the function of the device [6].

Despite this, heat sinks are an important subsystem of the design of the generator, as cooling the temperature of the "cold side" towards the temperature of ambient room temperature air is very important for the device's proper and efficient function. Therefore, optimizing the heat sink to dissipate the proper amount of heat, remain low-profile, and fit comfortable on one's body is very important. The article "Design of Heat Sink for Improving the performance of Thermoelectric Generators Using Two-Stage Optimization" published in *Sustainable Energy and Environmental Protection* in 2010 breaks down the optimization process by stages, specifically for use with thermoelectric modules, for the purpose of power generation. Heat sinks are an important aspect of the project and information on well-organized optimization methods can greatly increase the performance and speed of the process [23].

With both the knowledge of efficient thermoelectric generation methods in wearable situation, and that of heat sink optimization for TEMs, putting these two systems together into one assembly can prove difficult. There are many variables that go into account when combining TEMs and heat sinks that will determine the heat dissipated, heat accumulated, power output, and other determining factors. The article

"Parametric Optimization of Thermoelectric Generators for Waste Heat Recovery" published in the *Journal of Electronic Materials* in 2016 discusses this combination in detail, describing methods for optimizing each step of the generation process from heat source to heat waste. This includes maximizing power output via methods for minimum heat dissipation from the hot side and presented numerical models for thermoelectric generator coupled heat transfer and electrical power output [9].

With knowledge of TEM optimization for the specific purpose of wearables, heat sink optimization for the specific purpose of thermoelectric generation, and optimization of the two combined systems for generation, the final step is optimization of the electrical components of the device. The paper "Equivalent Electrical Circuits of Thermoelectric Generators under Different Operating Conditions" published in *Energies* in 2017 discusses the factors that go towards optimizing the electrical system with the goal of reaching voltage thresholds, maximizing current, minimizing resistance, and optimizing power efficiency. Boost converters and optimal resistance loads convert amperage into additional voltage in methods of balancing the two electrical characteristics in order to meet the requirements of the powered device. Series and parallel configurations are discussed with different electrical outcomes, as well as ways of maximizing power output and meeting all electrical requirements with as few TEMs as possible [18].

And finally the whole field of wearable thermoelectric power generation is discussed in "A Review of the State of the Science on Wearable Thermoelectric Power Generators (TEGs) and their Existing Challenges" published in *Renewable and Sustainable Energy Reviews* in 2017. With developing any technologies, one cannot become too firmly ingrained in the minutia without a deep understanding of the field in its entirety. There are many groups that are working on the same problem of wearable thermoelectrics and the field has proved difficult. But learning from the mistakes and difficulties of other researchers across the field can ensure Wearable Thermoelectric Power Generation does not fall into the same traps. Thus, the paper is important for us to understand the current limitations of the technology, the areas of possible improvement, faster optimization based on recommendations in the paper, and the steps to be taken when it seems the project is at a stand-still. The information covers many projects done over the past decades, and the ways in which the field itself can best be improved.

1.4 Project Objectives

The main objectives of the project are to produce sufficient electrical power to charge the battery of a low-voltage medical device. The voltage threshold defined is 3.7V, standard for a device charged through a USB connector cable.

The device is to work properly in a room temperature environment or colder, meaning an ambient air temperature of 23°C or an environment colder than this.

The device is to be safe to the wearer and all components of the device for constant charging while wearing.

The device is to be low-profile and appealing to the customer in terms of comfort and aesthetics.

Chapter 2

Systems Level Analysis

2.1 Customer Needs

2.1.1 Introduction

Wearable thermoelectric power generation can appeal to various types of customers because it can be implemented in numerous applications. However, our targeted consumer base were individuals who use medical devices. In November of 2017 we conducted a survey to ask participants about their preferences for a wearable power generator. Friends, family, and fellow students were asked to complete the survey, and we received 42 responses. Survey questions were designed to determine the demographic of the participants as well as the physical constraints of the wristband.

2.1.2 Questions and Answers

We were interested to know the geographic and academic demographic of our survey participants so that we could determine whether these factors affected the wristband preferences of the customer and the level of adjustability that the wristband would need to appeal to different demographics.

Q: Where are you located? How old are you? What is your level of education?

A: A majority of survey participants were between the ages of 18 and 25. About half identified as female and half as male. A majority of survey participants were located in the Bay Area; however, results from Massachusetts, Wisconsin, Missouri, Kansas, Minnesota, Oregon, and Germany were received as well. 46.7% of survey participants marked bachelor's degree as their highest level of academics.

Since the device is worn on the wrist there are specific requirements that it must fulfill in order to be appealing to the customer. Knowing that the design requirements of the wristband would be a balance between aesthetic and performance, we wanted to identify the priorities of the customer.

Q: What width of a power generating wristband would you be comfortable with? What height, of a power generating wristband, off the top of the wrist would you be comfortable with? How heavy of a power generating wristband would you be comfortable with?

A: The preference of aesthetic over performance was very slim as 51.5% of participants reported that aesthetic is more important and 48.5% valued functionality more. However, participants had overwhelming opinions on the width, height, and weight of the wristband favoring the physical characteristics of typical wrist accessories such as smart watches and electrocardiogram wristbands.

2.1.3 Summary

As a result of our survey, we concluded that the age, location, and educational background of the customer did not affect their likelihood to wear or their preferences for a wearable power generator. Our response to the preferences of the customer, as expressed by the results of the survey, was to set strict size contraints. The entire device was to be no taller than 10 mm, no wider than 80 mm, and no heavier than 200 grams. In addition to the size, we considered cost, usability, adjustability, and durability to be design requirements to make the device appealing to the customer. Values for these characteristics are listed in the PDS in the appendix, Table 10, along with design requirements for performance, safety, and maintenance.

2.2 System Level Physical Sketch and User Scenario

The device will be used by health care practitioners (or the equivalent) in areas without consistent grid power, areas of the world that are coincidentally highly susceptible to cardiovascular diseases. The device would ideally be used to monitor the heart health of individuals over a set amount of time, particularly individuals at higher risk due to family history, poor nutrition, or any number of other factors which would be determined at the discretion of the areas doctors. The device will take electrocardiogram readings of a patient using an EKG monitor, shown in Figure 1, which will be stored and analyzed using algorithms designed to predict the onset of cardiovascular diseases. Harnessing the patient's body heat using a thermoelectric module circuit, shown in Figure 2, has the potential to provide a continuously running predictive health device even in areas that cannot supply consistent power. Predicting and diagnosing cardiovascular diseases in these remote locations will dramatically help improve the life expectancy of many individuals who likely have never set foot inside a hospital.

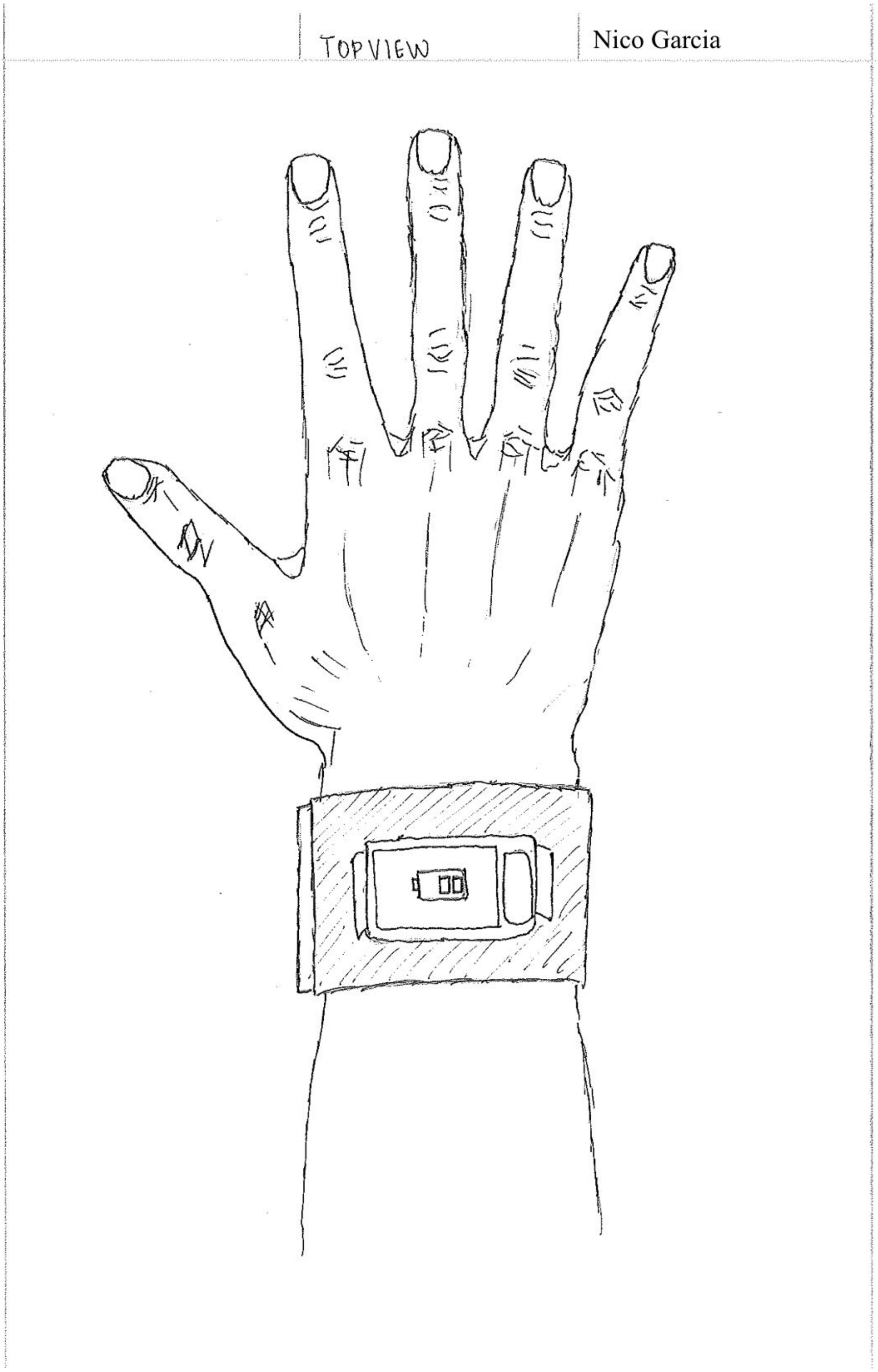

Figure 1: System sketch, top side of device.

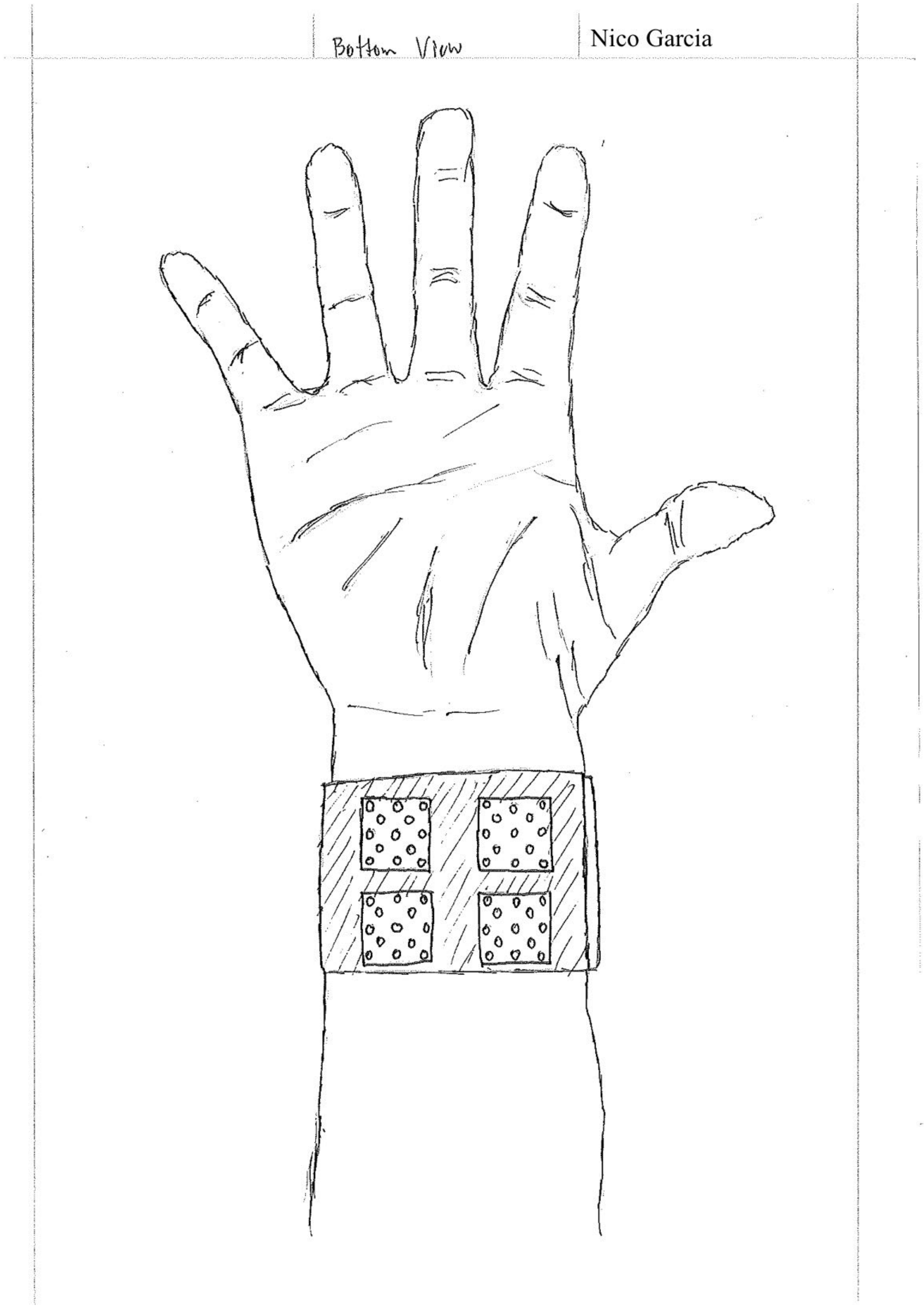

Figure 2: System sketch, bottom side of device.

2.3 Functional Analysis

The main function of this device is to convert a temperature difference created by body heat and ambient air into a voltage output sufficient to charge the battery of a wearable electrocardiogram, or EKG, (and other low-input medical devices). We chose to charge an EKG battery in our prototype because it is worn on the wrist, an accessible point on the body for thermoelectric power generation and a place where users are familiar with wearing accessories. Additionally, wearable EKGs offer the user the ability to measure their heart rate, allowing those with heart conditions to have better heart monitoring. EKG cardiovascular data can also be analyzed by machine learning algorithms to predict risk for heart disease [24]. This is especially important to those without access to electricity as over 75% of the 17.7 million cardiovascular deaths each year occur in low and middle income countries[4].

The device itself consists of four subsystems of Power Generation, Voltage Boost, Battery Charging, and Wearability which all have their own sub-functions in the design.

The Power Generation subsystem consists of a circuit of TEMs, heat sinks, and the heat source (wrist/forearm body heat) and its main function is converting the temperature difference across the TEMs into a small voltage output on the order of mV. The actual power generation is specifically the role of the TEMs while the role of the heat sinks is to dissipate heat and maintain sufficient temperature differences. Since the devices overall function is to charge the battery of a low-input medical device, the voltage output from Power Generation must be increased before it can be utilized. So, this power generated is then sent to the next subsystem, Voltage Boost. The function of Voltage Boost is to take the small voltage output from Power Generation and increase it to a much higher, usable value of 4.1 [V] while sacrificing a significant amount of the current. It utilizes an electrical component called a boost converter to do so. This boosted voltage of 4.1 [V] satisfies the charging requirements for the battery of the wearable EKG. The EKG itself and any associated miscellaneous wiring that make up the Battery Charging subsystem. Lastly, all of these subsystems and their components need to be integrated into a single, wearable wristband. This is the function of the Wearability subsystem. Wearability consists of 3D printed housings for the TEM and heat sink modules as well as the wristband itself, made of multiple fabric types.

Along with their functions, each subsystem has its own inputs, outputs, and constraints. These are described in detail in Table 1. The information provided for the four major subsystems are summarized as the following: the power generation subsystems input is simply a temperature difference across the TEM. This subsystem has size constraints that require a low profile design with a small form factor. It must also work effectively for small ΔTs. Power Generation outputs a small voltage output, on the order of mV which doubles as the input for the Voltage Boost subsystem. This subsystem outputs a usable level of voltage (about 4.1 [V]). This subsystems main constraint is the boost converters voltage input requirement of 20 [mV]. Once again, voltage boosts boosted voltage output doubles as the input for the next subsystem, battery charging. This subsystem's output is the active charging of the EKG (or other low-input medical device) battery. This subsystem faces size constraints, as usual, as well as current constraints (the lower the current, the slower the battery charges). Lastly, the wearability subsystem takes the various components of the system as inputs and integrates them into a wearable, functional wristband as an output while facing size, comfortability, and ergonomic constraints. The inputs, outputs, and constraints for all of the subsystems in the Wearable Thermoelectric Power Generation design are compiled and organized in Table 1 below.

Table 1: Subsystem inputs, outputs, and constraints.

Subsystem	Input	Output	Constraints
Power Generation	Temperature difference across the TEMs hot and cold sides.	Small power (voltage and current) output through TEM leads.	Must have small form factor and be low profile. Must work effectively for small ΔTs.
Voltage Boost	Low voltage and current output from TEM circuit.	Higher, usable voltage output, significant decrease in current.	Voltage input requirement must be met to achieve boost.
Battery Charging	Generated power via boosted voltage and current from Voltage Boost	Charging the EKG battery.	Needs sufficient amount of current to charge. Must integrate comfortably into wristband design.
Wearability	TEMs, heat sinks, boost converter, EKG, and miscellaneous wiring components	Wearable wristband that integrates the other 3 subsystems components. Consists of 3D print housings, miscellaneous wiring, wristband materials.	Must maintain sufficient contact between TEM and skin. Must allow sufficient heat dissipation. Must be comfortable and ergonomic for the user.

2.4 Benchmarking Results

In the current market only a few wearable thermoelectric power generation devices have been developed. One such device was the Seiko Thermic watch developed by Japanese watch company Seiko in 1998. The watch, depicted in Figure 3, used thermoelectric technology to charge an auxiliary battery with the wearer's body heat. [16].

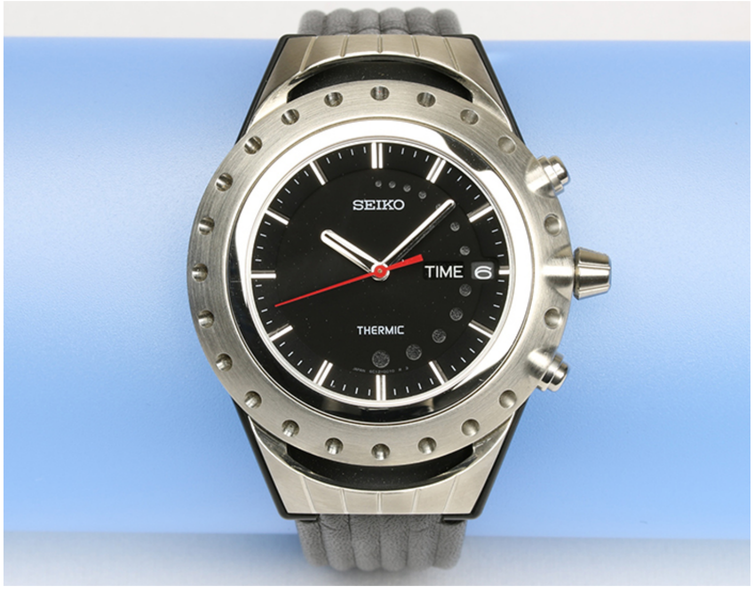

Figure 3: Seiko Thermic [16].

A more recent wearable thermoelectric power generation device is the Matrix Powerwatch, seen below in Figure 4. The Powerwatch is a smartwatch powered by body heat using thermoelectric technology [20].

Figure 4: Matrix Powerwatch [20].

Aside from these watches, no wearable thermoelectric power generation devices exist in the consumer electronics market. The results of research in the field of thermoelectric generation available on the market, to compare with the the goals of the project, can be seen in Table 2.

Table 2: Benchmarking Results

Existing Technology	Details	Cost	Room for Improvement
SEIKO Thermic Watch	A luxury watch powered by thermoelectric modules placed where a traditional battery watch would be. Did not work in hot environments such as Malaysia.	\$1911	Improve efficiency of product to work in warmer environments and power something more meaningful than a wristwatch.
MATRIX PowerWatch	A smartwatch powered by body heat capable of measuring calories burned, activity level, and sleep characteristics. It also includes a power meter displaying current power generation.	\$199	Costs of parts and production would be minimized to reach a more affordable price point.

2.5 System Level Issues

The Wearable Thermoelectric Power Generation system is made up of four subsystems: power generation, voltage boost, battery charging, and wearability. The two main elements of the power generation subsystem are the thermoelectric modules and heat sinks. During testing, various configurations of thermoelectric modules and heat sinks were used. Options for heat sinks varied in dimensions and fin length. Initially, the power efficiency of each configuration was weighted with the highest factor, as seen in Figure 34 in the appendix. However, the device is designed to be worn on the wrist and therefore configurations with higher power efficiency, but which exceeded the size requirement, 40mm by 40 mm by 10 mm, were ranked lower than those that fell within the size requirement.

Voltage boost and battery charging make up the electrical portion of the project. The most significant electrical component considered in the design of this device is the boost converter. The boost converter takes an input voltage supplied by the thermoelectric modules and boosts it to a output voltage of at least 3.7 V to power an EKG or other portable medical device. Both high and ultra-low input voltage boost converters were considered during testing. However, based on the output voltages of the TEM and heat sink configurations, ultra-low input voltage boost converters were prioritized. Boost converters from Linear Technologies and Texas Instruments were considered. Linear Technologies boost converters were ranked higher because of their wider range of options for ultra-low converters. Figure 34 shows that boost converter efficiency is weighted the highest. However, efficiency is again traded off for compactness if the size requirement is exceeded. Our priority is to use a boost converter that has the highest efficiency in sustaining an output of at least 3.7 V while operating within a realistic input voltage range. If input voltage is required to be high, more thermoelectric modules are needed, causing the overall size requirements to be exceeded. The other element of the device's electrical portion is the circuitry from the boost converter to the EKG or medical device which charges the battery. The options, such as direct or USB connection, depend on whether device adaptability and functionality or aesthetic value is more important .

The wearability subsystem of the device mainly consists of the fixture band that will hold the power generation components, hold the electrical components, and be worn around the wrist. Based on the needs of the customer, the comfort and aesthetic of the band are weighted the highest for selection criteria, shown in Figure 34 in the appendix. Although many materials satisfy the lightweight and durability requirements, based on cost, silicone, Velcro, and elastic were considered for the fixture band composition. In theory, a silicone band would provide adequate comfort, contact pressure, and weight. It would also provide a factor of safety by isolating static electricity. However, a silicone band would not be able to contain or hide the wiring of the electrical components easily and therefore would not have the cleanest aesthetic. If silicone was used for the fixture, it would most likely be a continuous band and therefore would not be adjustable. A Velcro band would be adjustable, robust, and provide sufficient contact pressure, however, would not have the ideal level of comfort or weight. Although it would be possible to sew Velcro and keep the wiring of the electrical components hidden, it would be very thick and not have the ideal sleek aesthetic that would appeal to customers. Lastly, an elastic band would provide the ideal comfort, light weight, and adjustablility. However, the adjustability of the elastic is traded off with a low capability to provide sufficient contact pressure. Elastic is also the least robust. Scoring each option based on the selection matrix depicted in Figure 35 in the appendix, silicone would be the best option for the fixture band. However, as it will be discussed further in the wearability subsystem chapter, prototyping revealed that some of the strengths and weaknesses of these materials can be circumvented by the fixture band design.

2.6 System Level Design Layout

The system level design has multiple components that work together to accomplish the systems overall function. The system takes excess body heat and creates a voltage output using the TEMs and heat sinks in the Power Generation subsystem. This voltage output is increased to a usable level by a boost converter within the Voltage Boost subsystem. This boost voltage output is then used to charge the battery of the wearable EKG in the Battery Charging subsystem. Lastly, the Wearability subsystem integrates all of the previously mentioned components into a single, wearable wristband. Figures 5 and 6 depict this system level design layout.

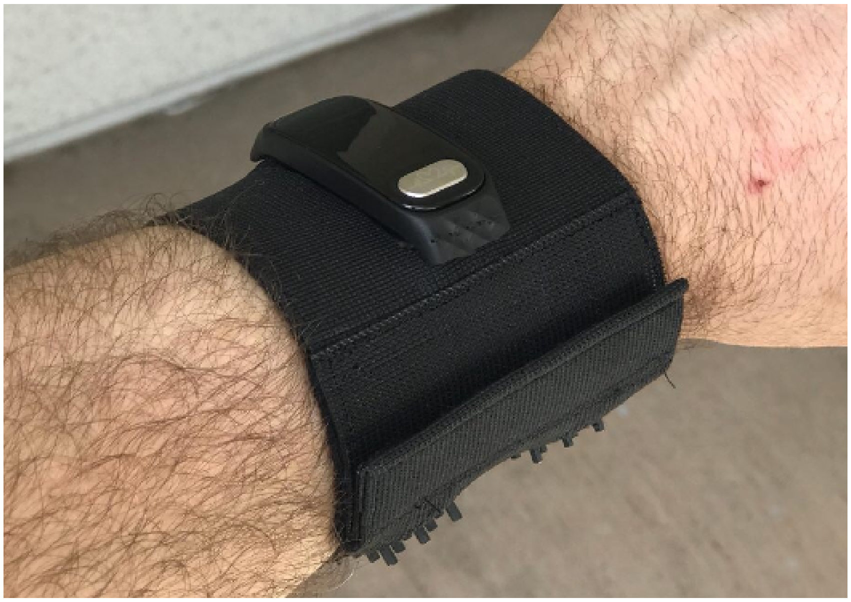

Figure 5: Wristband prototype with integrated EKG monitor on topside.

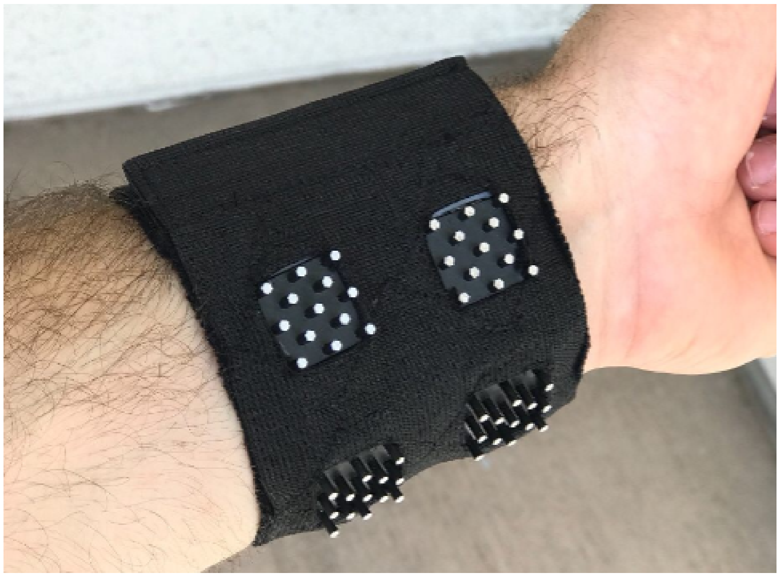

Figure 6: Wristband prototype with integrated TEMs .

2.7 Team and Project Management

2.7.1 Project Challenges and Constraints

The obvious challenges and constraints encountered in this project are those presented by size and cost of the device. Theoretically, any desired power output could be achieved with enough thermoelectric modules and proper heat dissipation. However, the device must be designed to be worn on the wrist and be similar in size to other wrist-based accessories like watches and fitness trackers. Additionally, the price must be reasonable, which limits thermoelectric modules that can be used. In order to keep the design low profile, lightweight, compact, and cheap to manufacture while still meeting performance requirements, the sizes of thermoelectric modules must be optimized to minimize the number of modules used and maximize the size of module while still having good contact with the skin. In areas where the wrist has larger flatter area, larger modules could be used. However, if modules are placed in areas with more curvature, smaller modules must be used to ensure good contact with the skin. It is imperative that the surface of the wrist is considered during module selection.

An additional challenge that will be discussed further in their respective subsystem chapters is this issue of performance trade-offs between the thermoelectric modules and their circuit configuration, heat sinks, boost converter, battery to be charged, and overall size of the device. The boost converter has requirements of a minimum input voltage and a maximum input resistance which corresponds to and varies with input voltage. As input voltage increases due to the temperature difference across the thermoelectric module (which is influenced by the heat sink properties), input resistance increases. Additionally, the circuit configuration of the thermoelectric modules can be used to manipulate how much input voltage, current, and resistance the boost converter sees. However, the greater these areas are optimized, the more space is needed for the thermoelectric modules and their heat sinks. The battery to be charged also has minimum voltage and current requirements. This additional challenge is difficult to overcome because increasing voltage decreases current and vise-versa. These interdependent challenges require difficult and complex optimization to be successful.

2.7.2 Budget

A main budget concern for this project is allowing enough money to purchase thermoelectric modules and heat sinks for evaluation and prototyping. After the appropriate thermoelectric modules and heat sinks are selected, 10-20 (depending on design configuration) modules and sinks must be purchased. Additionally, the cost of a boost converter evaluation board is a significant budget concern. Although boost converters themselves are inexpensive, an evaluation board used to develop a prototype can cost over $100. Please see Table 11 in the appendix for a detailed description of proposed project budget, and refer to Table 12 for actual costs of developing our prototype.

2.7.3 Timeline

The main issue for the timeline of our project is familiarizing the team with the technologies as early as possible. This project leans heavily on the use of thermoelectric modules and boost converters, technology that is not explored in the regular curriculum at Santa Clara University. After achieving adequate levels of familiarity with the technologies utilized in our design, the next immediate concern is performance testing a variety of thermoelectric modules, heat sinks, and boost converters to identify which models of these items will be used in prototyping. Modules, heat sinks, and boost converters which are in the lab were tested and evaluated and used as a baseline to refer to when ordering modules, heat sinks, and boost converters for further testing and evaluation. It was necessary that this be completed in the first half of the year to allow time for prototyping, design changes, and troubleshooting. The final timeline concern was scheduling amongst the group. Because all group members have busy schedules with limited availability, it was difficult to find meeting times that worked for all members. To address this concern, the subsystems within the project were assigned to different group members so that members working on the same subsystems could meet more easily than the whole group meeting. Please see Figure 36 for the Gantt Charts for Fall, Winter, and Spring quarter.

2.7.4 Design Process

Our approach to design for this project can be outlined in the following steps:

1. Define problem to be solved.

2. Specify requirements for the solution.
3. Identify possible solutions, evaluate solutions, choose a suitable solution.
4. Break up the solution into subsystems.
5. Identify requirements for subsystems, design a solution that fulfills these requirements.
6. Construct a prototype of each subsystem, evaluate subsystem prototypes against their goals.
7. Make subsystem design changes if necessary, re-evaluate updated subsystem design changes.
8. Assemble complete prototype, evaluate prototype against its goals.
9. Make design changes if necessary, re-evaluate updated prototype.

2.7.5 Risks and Mitigation

The main risks in this project are safety risks, and the risk of breaking materials and equipment. The main safety risks for this project lie in the use of equipment such as power tools, soldering irons, and tools with sharp blades. To mitigate risk here, group members must wear proper lab attire (closed toed shoes, longs pants, hair tied up, etc.) when performing experiments and construction work on the project. Additionally group members must be properly trained to use any equipment, and are not permitted to work in the lab alone. When using equipment such as sharp bladed tools, group members must cut away from their bodies and be cutting on top of a surface, rather than holding an object in their hands and cutting it. Another safety risk is risk of electric shock. Although the voltage and currents generated by the thermoelectric modules are well below thresholds that pose danger to those handling them, certain performance tests and experiments with electrical equipment could involve larger voltages and currents from DC power supplies. To ensure safety when working with electronics, all electrical connections must be ensured to be secure, and electrical power supplied to loads must not exceed their power limits. Power should not be applied to a circuit until it is confirmed that the circuit is complete and all connections are made properly, and all electrical systems must be properly grounded.

Because our power generation device is to be used with medical devices, the risk of medical device failure is introduced. We must ensure that power to the medical device is never lost, even if our power generator fails. This can be accomplished by supplying a backup battery which the medical device defaults to if the power generation device fails.

Some of the equipment used in this project can also be easily damaged, such as thermoelectric modules, boost converters, and electrical resistors. To mitigate risk of damaging these items, they must be handled with care. When they are to be supplied with electrical power, the power must not exceed their limits so that the electrical elements of the equipment are not damaged.

2.7.6 Team Management

Team management for this project follows a simple approach. Each member of the team is primarily responsible for one area of the project (heat sinks, thermoelectric modules, electrical circuits, wristband design, etc.) and secondarily responsible for another area of the project. This allows each person to contribute significantly to the project and have support in their area if needed. We meet bi-weekly as an entire group to discuss progress, goals, and issues encountered, and smaller groups within the team meet at various times in the week to complete work on the project. Conflict resolution is handled by directly addressing the problem. Although we did not encounter any conflicts, if there was a serious disagreement, the conflict would have first been acknowledged and discussed with the group. All sides of the conflict would have a chance to explain their side, and the group would decide on a compromise that puts the goal of the team first.

Chapter 3

Power Generation Subsystem

The role of the power generation subsystem is to produce a small voltage output using excess body heat of the user. The subsystem implements a circuit of TEMs in conjunction with heat sinks to accomplish the function of power generation. The TEMs are responsible for the actual power generation while the heat sinks are employed to help with heat dissipation.

The power generation subsystem's most critical requirement is that there must be a sufficient temperature difference present across the two sides of the TEM (skin side and ambient air side). This falls hand in hand with the requirement that it must produce enough voltage to satisfy the input requirements of the voltage boost subsystem (20 [mV]). TEMs operate on the Seebeck effect, which states that an electric current will be produced when two dissimilar metals (the TEM legs) are exposed to a temperature difference [3]. This effect is further characterized by the Seebeck coefficient, $S = \Delta V / \Delta T$, which shows that the voltage produced by a TEM is directly proportional to the temperature difference its subjected to. Due to the nature of the TEMs' operating principles, subjecting the thermoelectric modules to a sufficient temperature difference is critical to the function of the device. This is why the heat sinks' role of heat dissipation is essential to the project; it satisfies the subsystems most critical requirement. By dissipating excess heat away from the cold side of the TEM, the heat sink helps maintain the temperature difference across the thermoelectric module. Without the heat sinks, excess heat would build up in the TEM legs and eventually bring the hot and cold side temperatures closer to each other resulting in a lowered power output. The remaining requirement of the power generation subsystem is concerning size, and it applies to both the TEMs and heat sinks. Both components must be low profile with small form factors to increase the devices wearability while still being able to meet performance requirements.

The roles and requirements of the power generation system are critical to the functionality of the wearable device and overall success of the project. These were considered heavily when making design decisions regarding TEM selection and heat sink optimization, as will be explained in the following sections.

3.1 Options and Trades

3.1.1 Heat Sinks

Heat sink selection was completed before TEM selection due to the importance of considering heat sink size when selecting a TEM. Due to the time constraints of this project, it was determined that purchasing stock heat sinks designed for natural convection applications was the best option for obtaining heat sinks. Although designing and manufacturing custom heat sinks offers the opportunity to integrate the heat dissipation into structural elements of the device, it was necessary to allocate more time to developing the electrical components of the device. Fin and pin type heat sinks were identified as the ideal geometries for our application. Heat sinks are often used in conjunction with fans for forced convection; however, our application relies on still air and natural convection, and adequate space between fins or pins is needed to allow free air to flow between them. Figure 7 depicts the three types of heat sinks considered for use in this project: Alpha Nova Tech's fin type series, pin type series, and specialized natural convection series.

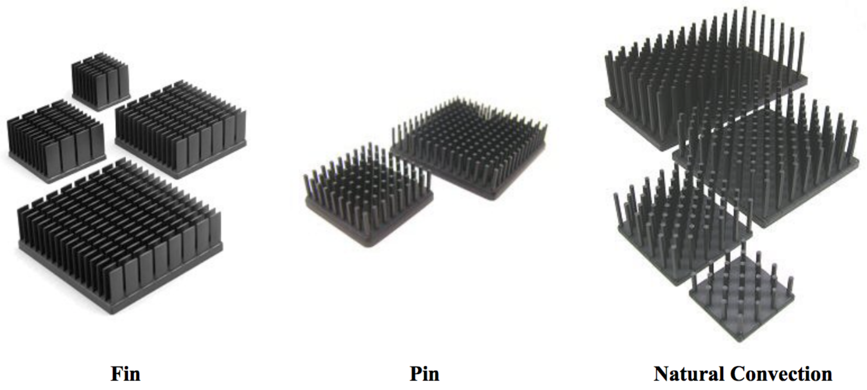

Figure 7: Fin type, pin type, and natural convection heat sinks [13].

Heat sink geometry played an important role in heat sink selection because size constraints limited their performance. A larger heat sink allows more heat to be dissipated which increases TEM performance; however, because our device is worn on the wrist, heat sinks were required to be less than approximately 25mm. When that size is exceeded, multiple TEMs and their heat sinks are unable to fit on a wristband that fits a variety of wrist sizes. Additionally, because the wrist is not a perfectly flat surface, bending and turning often throughout the day, the heat sink may contact the skin itself when the wrist is bent or turned if the heat sink is much larger than the TEM. This interferes with the contact between the skin and TEM. Therefore, some performance increase must be traded for size reduction.

3.1.2 Thermoelectric Modules

The implementation of the TEMs into the power generation subsystem required a few decisions and trade offs as well. Though designing and manufacturing our own TEMs would be ideal, as was the case with the heat sinks, we decided to order and use available market TEMs due to the time constraints of this project. While this sacrifices the potential performance of our TEM and device, it allows for much more time for assembly, testing, and troubleshooting that would be otherwise spent waiting for TEMs to be manufactured. Since we decided to move forward in our design with market TEMs, we had to weigh our options and make trade offs when purchasing different TEM models.

The two main decisions we made regarding TEM selection were choosing between generators and coolers (TEM types) as well as between potted and non-potted TEMs. A generator TEM is one that takes a given temperature difference and generates a power output while a cooler TEM takes a given power input and produces a temperature difference (used in cooling applications), showing the reversibility of the Seebeck effect. Theoretically, generators and coolers with the same Seebeck coefficient should perform identically under either application (e.g. using a generator for cooling, vice versa). However, coolers are designed to operate around room temperature while generators tend to be optimized for much higher temperatures [5]. Since room temperature closely matches our expected ambient air operating conditions, we focused on purchasing cooling TEMs to implement into our design.

The second trade off, between potted and non-potted TEMs, was not an obvious choice at first. A potted TEM has a rubber-like material surrounding and in between the legs of the module. This allows for slightly better conduction and additional robustness. Figure 8 depicts the the difference between non-potted, seen on top, and potted, seen on bottom, modules. Initially, we ordered non-potted TEMs because they were slightly less expensive and boasted nearly the same performance characteristics as their potted counterparts. However, it became quickly apparent that the non-potted TEMs were extremely fragile, especially the TEM legs, as many of them broke during testing, assembly, and even gentle handling. We ordered potted TEMs for our final design to obtain components that would be much more durable.

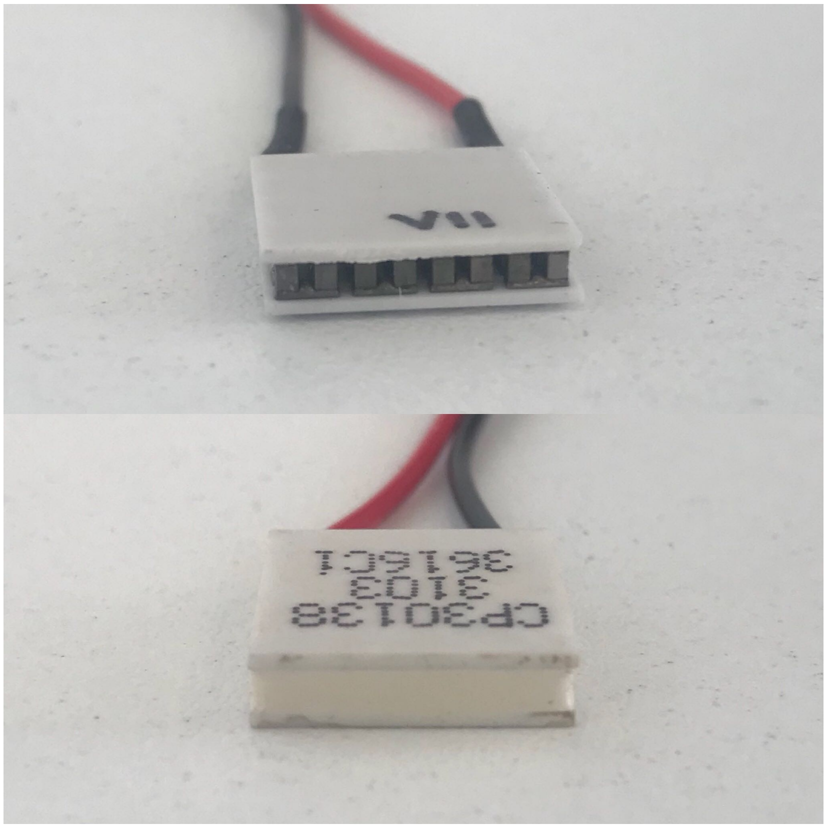

Figure 8: Non-potted TEM versus potted TEM.

The last trade off regarding TEM implementation was the actual size of the module. Most TEMs are designed for industrial use and have relatively large module areas (typical dimensions would be 40 mm by 40 mm). TEM power output typically increases with module area which allows for the use of less TEMs in the final design. However, despite increased performance characteristics and saved costs, large TEMs greatly hinder the wearability and modularity of the device. Because of this, we decided to make the performance trade off and implement the use of small TEMs (side lengths less than 20 mm). Though it is slightly more expensive, the space saved by using smaller modules allows for flexibility in the wristband design (regarding the TEM circuit configuration) as well as increased wearability. Similar trade offs pertaining to more detailed geometric characteristics of the TEMs are explained in further detail in Section 3.2.3.

3.2 Heat Sink and Thermoelectric Module Analysis and Selection

3.2.1 Heat Sink Analysis and Selection

As it was previously stated, the heat sink's role in the power generation subsystem is to remove heat from the top side of the TEM, helping to generate a temperature difference across the TEM. There are many types of heat sinks used in a variety of applications, such as thermoelectric coolers and computer components. Heat sinks are made up up of two main categories: active and passive. Active heat sinks are typically equipped with a fan to help remove heat, whereas passive heat sinks stand alone, although they function best with consistent airflow over their surfaces [2]. Because our device is intended to be low profile, small, passive heat sinks, such as those used with circuit components, were ideal. Additionally, because our device is to be worn on the wrist and consistent forced convection is not a given, heat sinks with considerable space between fins or pins were considered because this favors natural convection [8].

Several heat sinks geometries of various base areas and fin/pin heights that fit within our size constraints were chosen to be evaluated and both ordered from Alpha Nova Tech, a local heat sink manufacturer, and obtained from available supply in lab. They were:

- LPD19-4B (fin type, 19 [mm] x 19 [mm] base, 4 [mm] tall)
- LPD19-6B (fin type, 19 [mm] x 19 [mm] base, 6 [mm] tall)
- LPD30-4B (fin type, 30 [mm] x 30 [mm] base, 4 [mm] tall)
- LPD40-4B (fin type, 40 [mm] x 40 [mm] base, 4 [mm] tall)
- N19-10B (natural convection type, 19 [mm] x 19 [mm] base, 10 [mm] tall)
- ST19-4B (pin type, 19 [mm] x 19 [mm] base, 4 [mm] tall)
- ST19-6B (pin type, 19 [mm] x 19 [mm] base, 6 [mm] tall)

In order to evaluate the performance of the heat sinks, they were each paired with the best perfoming TEM available in our lab, the TK19 module, and these TEM-heat sink pairs were placed under a temperature difference, producing a power output. This power output, specifically the voltage component, was used to evaluate heat sink performance. TEM selection was also based off of this "ideal" TK19 TEM.

The schematic below in Figure 9 depicts the setup for evaluating heat sink performance. Similar to the way in which electrical power is generated when there is a temperature difference across a TEM, when power is supplied to a TEM, a temperature difference is created across the TEM. This creates both hot and cold sides of the TEM. The hot side of an auxiliary TEM was used as the heat source for creating a temperature difference across the test TEM in this experimental procedure. A DC power supply provided power to the "hot plate" TEM, and the power input to this TEM was increased until the hot plate TEM's hot side measured approximately 35°C. A large heat sink was placed under the hot plate TEM to ensure the temperature difference across the hot plate TEM remains consistent. The test TEM, TK19, and the heat sink to be evaluated were placed on top of this heat source. The open circuit voltage output (voltage when no load is applied to the circuit) from this single TEM-heat sink combination was measured by reading the voltage across the leads of the test TEM using a National Instruments NI-DAQ 9215 (serving as the multimeter), and this data was recorded in Labview software. The data was recorded at a sampling rate of 75 [Hz] for 100 samples. The NI-DAQ 9215 has a measurement uncertainty of 0.02%. This procedure was repeated for three trials for each heat sink. Figure 10 depicts testing of the ST19-6B heat sink.

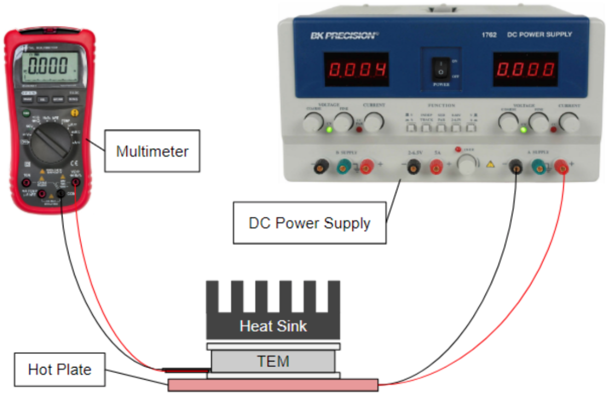

Figure 9: Heat sink testing and evaluation setup schematic.

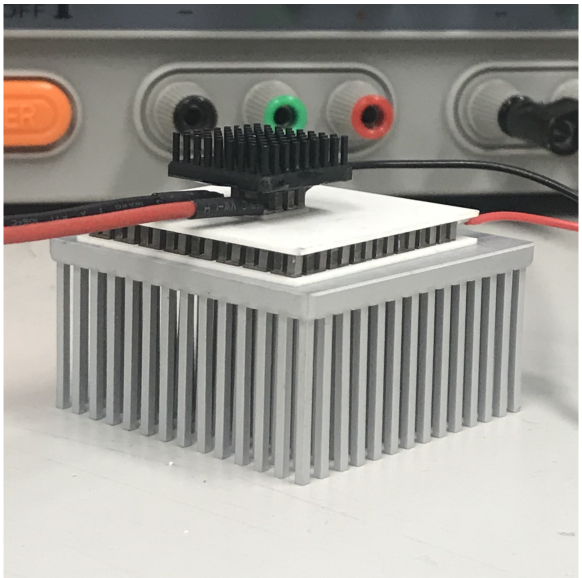

Figure 10: Heat sink testing and evaluation setup detail.

Higher open circuit voltage indicates a higher temperature difference due to the Seebeck effect, indicating that the heat sink is doing its job. Although comparing thermal resistance values provided by the manufacturer for each heat sink at our device's operating temperature is an effective method of comparing each heat sink's ability to pass heat through themselves, it does not take the effect that TEM geometry and its interaction with the heat sink have on performance. Therefore, comparing open circuit voltage for each heat sink with a control TEM that is similar in geometric properties to the TEM we will select is the most effective method of evaluating and comparing heat sink performance. Figure 11 below depicts the open circuit voltage of each heat sink with the TK19 TEM. Each column represents the average open circuit voltage for 300 data points. N19-10B is highlighted as it was the heat sink chosen to be used in our device.

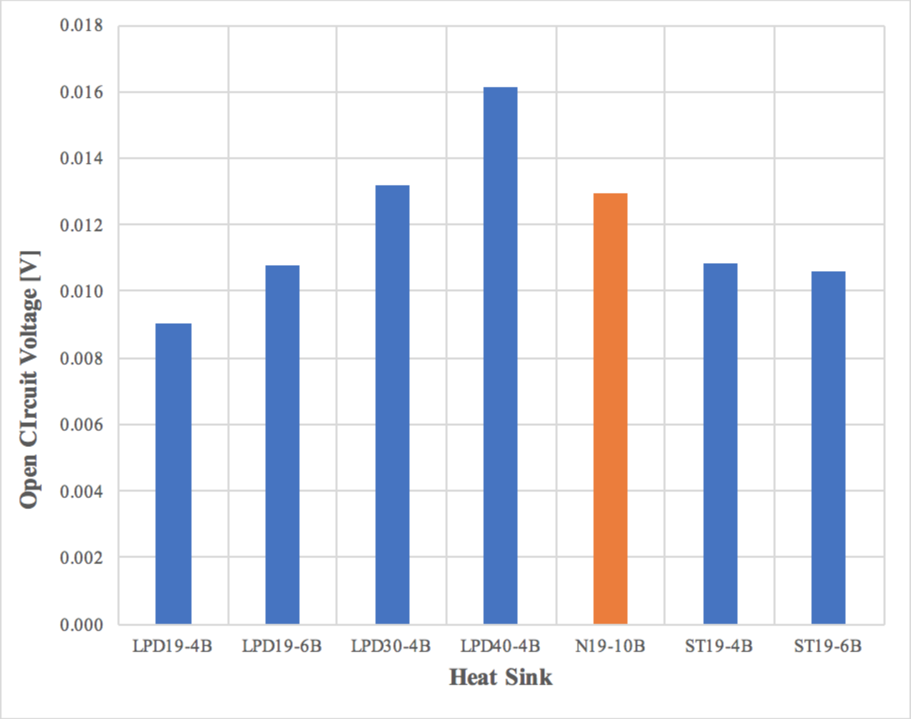

Figure 11: Heat sink testing and evaluation results.

As is evident in the figure above, LPD30-4B, LPD40-4B, and N19-10B performed best. Although LPD40-4B is the top performer, its large base size severely hurts the wearability of the device as integrating these large heat sinks into the design would mean either sacrificing the amount of TEMs used, which would hurt performance, or violating the size constraints defined in the PDS. Although the LPD30-4B is slightly smaller, it still poses a size issue, and its performance is only slightly greater than the much smaller N19-10B heat sink. Therefore, the N19-10B heat sink was selected due to its superior performance and small base area, allowing more TEMs to be utilized in the design of the device. Additionally, it is specialized for natural convection, which is ideal for our application.

3.2.2 Heat Sink Modification

Since the device is worn on the wrist, it is ideal for it to have a low profile. In order to determine whether or not we could shorten heat sink pins without a sacrifice in performance, we conducted finite element analysis using Abaqus CAE software to determine the heat flux and temperature distribution of the heat sink. Using the software, we simulated conditions similar to operating conditions. Since the heat sink mainly experiences natural convection, it was given a convection coefficient of 40 $\frac{W}{m^2K}$ and an ambient air temperature of 21°C, which is typical room temperature. The simulated heat sink was given a heat source temperature of 30°C, which is the typical temperature of the side of the TEM that the heat sink contacts. The heat sink is made of the aluminum alloy A6063 so the heat sink was set to have a conductivity of 200 $\frac{W}{mK}$. As a result of our finite element analysis, it was determined that a majority of the heat flux occurs at the base of the heat sink pins, seen in figure 12 which depicts heat flux distribution of the heat sink simulated to experience conditions similar to operating conditions in Abaqus CAE software. With this information, we were able to cut the pins of the heat sink to only 5 [mm] long with negligible effect on the performance of the heat sink. The pins of the heat sink were cut using a diamond cutter in the material science lab, room 515 of the Mechanical Engineering building on the Santa Clara University campus.

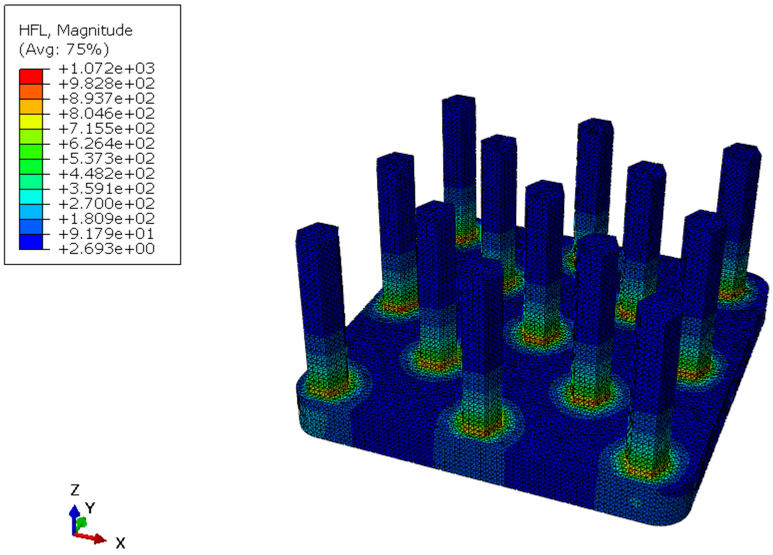

Figure 12: FEA heat sink heat flux distribution.

3.2.3 Thermoelectric Module Analysis and Selection

Due to time constraints restricting our ability to design and manufacture our own thermoelectric modules, we relied heavily on theoretical analysis and geometric characterization throughout our TEM selection process. Nearly the entire process was based on a geometric characterization of TEMs known as the B factor. A TEM's B factor is calculated using geometric dimensions of the module, as shown in Equation 1, and characterizes the module's performance in terms of its mechanical design [[14].

$$B = \frac{LL}{FF} = \frac{LL * A_{TEM}}{A_{L,tot}} \tag{1}$$

where LL = Leg Length [m], FF = Fill Factor, A_{TEM} is the area of the TEM's ceramic plates, and $A_{L,tot}$ is the total cross-sectional area of the TEM's legs. The dimensions required to calculate the B factor are shown below in Figure 13 in the context of a generic TEM schematic, provided by TE Tech [21]. The dashed squares within the top view represent the individual TEM legs.

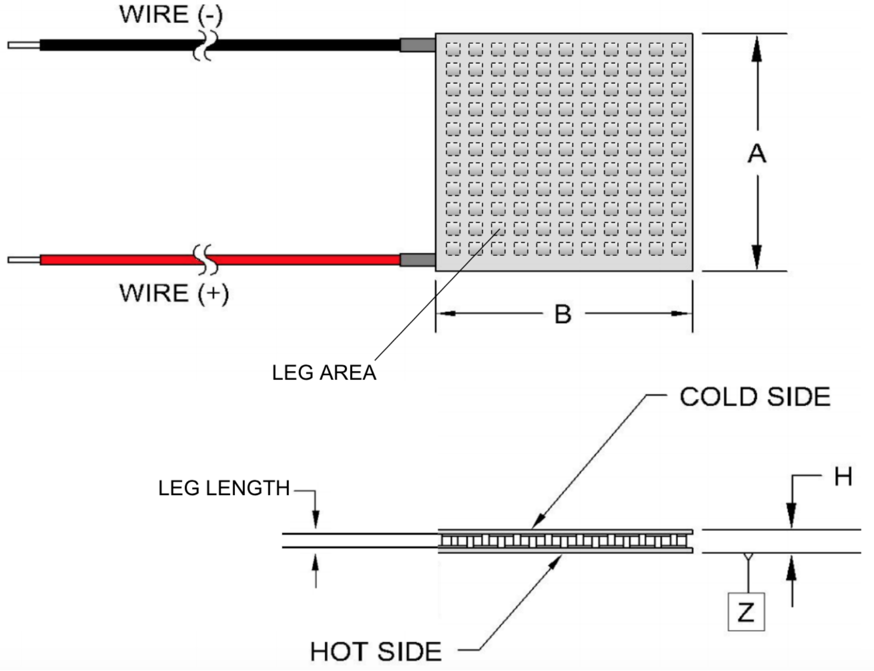

Figure 13: TE technology TEM schematic and dimensions.

In our design, and in most TEM applications, the TEM operates in conjunction with a heat sink to increase heat dissipation from the cold side. The size of the heat sink directly correlates with its heat dissipation capabilities and therefore correlates with the performance of the TEM itself. A larger heat sink allows for more heat dissipation, a higher temperature difference, and an increase in power output from the TEM. Because of its direct role in TEM performance, the heat sink should be taken into consideration when characterizing the TEM. To do so, the original B factor of the TEM (1) is multiplied by the ratio between the heat sink and TEM areas (A_{HS} and A_{TEM}) to obtain the effective B factor, B_{eff}, as shown in Equation 2. This effective B factor concept was used for our TEM analysis and selection process instead of the original B factor shown in Equation 1 to allow for more accurate characterization of TEM performance based on module geometries and heat sink size.

$$B_{eff} = \left(\frac{LL * A_{TEM}}{A_{L,tot}}\right) * \left(\frac{A_{HS}}{A_{TEM}}\right) = \frac{LL * A_{HS}}{A_{L,tot}} \tag{2}$$

To begin TEM selection process, we performed theoretical maximum power tests on the various TEMs we already had available in our lab. This was an effort to quickly gain an understanding on how different TEM models and geometries performed at our expected operating conditions. The experimental setup and procedure for these tests was the same as that described in section 3.2.1 with a few modifications. In order to calculate maximum theoretical power, open circuit voltage and short circuit current must be measured. The procedure for open circuit voltage measurement was identical to that described in section 3.2.1 except that the heat sink was kept consistent while testing a number of TEMs available in our lab. Since heat sink evaluation resulted in N19-10B being chosen as the model used in our final design, these tests were performed using N19-10B as the designated heat sink.

The procedure for short circuit current measurement was nearly identical to this open circuit voltage measurement. Rather than measure the voltage across the leads, a 0.1 [Ω] precision resistor was placed in series between the positive and negative leads of the TEM being evaluated. The voltage across this precision resistor was then measured using the same equipment detailed previously. Using the method described in section 3.5.1, this measurement was used calculate the short circuit current. The open circuit voltage and short circuit current values were then used to calculate maximum theoretical power using methods detailed in section 3.5.1. Just like measurements made in heat sink evaluation, these TEM evaluation measurements were sampled at a rate of 75 [Hz] for 100 samples.

5 trials were of this test were performed and the averages of the individual measurements and results were used for analysis. The results from the initial theoretical maximum power tests are shown below in Table 3 for each TEM. From these tests, we identified a TEM labeled 'TK-19' as the top performer. TK-19 had the largest theoretical power output and was identified as the top performer.

Table 3: Theoretical maximum power test results.

TEM	Hot Side Temperature [C]	Power Max [W]	Voltage OC [V]	Voltage OC [V]
CP30138	34.9	1.77 E -3	3.47 E -2	2.04 E -1
TJ26	33.9	1.61 E -3	2.66 E -2	2.42 E -1
TK19	35.5	1.82 E -3	1.65 E -2	4.41 E -1
UE09	33.0	6.99 E -4	2.86 E -2	9.79 E -2
UL24	33.1	1.43 E -3	4.03 E -2	1.42 E -1
X1	34.0	9.47 E -4	2.48 E -2	1.53 E -1

With TK-19 identified as our top performer, we moved on to the next step in our process: shopping for new TEMs based on TK-19's geometries. Of course, using TK-19 as our TEM for our final design would have been ideal, but it was an old model which had been discontinued by its manufacturer, Laird Technology, and was no longer available for purchase. In order to obtain a TEM that performed similarly to TK-19 under the same operating conditions, we searched for models with effective B factors closely matching that of TK-19. The effective B factors of the potential TEMs to be purchased were calculated based on heat sink N19-10B, the heat sink chosen for our final design as explained earlier in Section 3.2.1. Since there were no detailed schematics of TK-19 available from Laird Technology, the dimensions required for the B_{eff} calculation were measured with calipers. For TK-19, $B_{eff,TK-19} = 0.03216$.

In our shopping process, in addition to meeting TEM design size constraints, we specifically focused on searching for TEMs with effective B factors that were as close to our desired value ($B_{eff,TK-19}$) as possible to try and avoid an issue known as bottlenecking. The effects of bottlenecking are easily recognizable on the Power versus Effective B Factor plot shown in Figure 14. TK-19's performance point is marked.

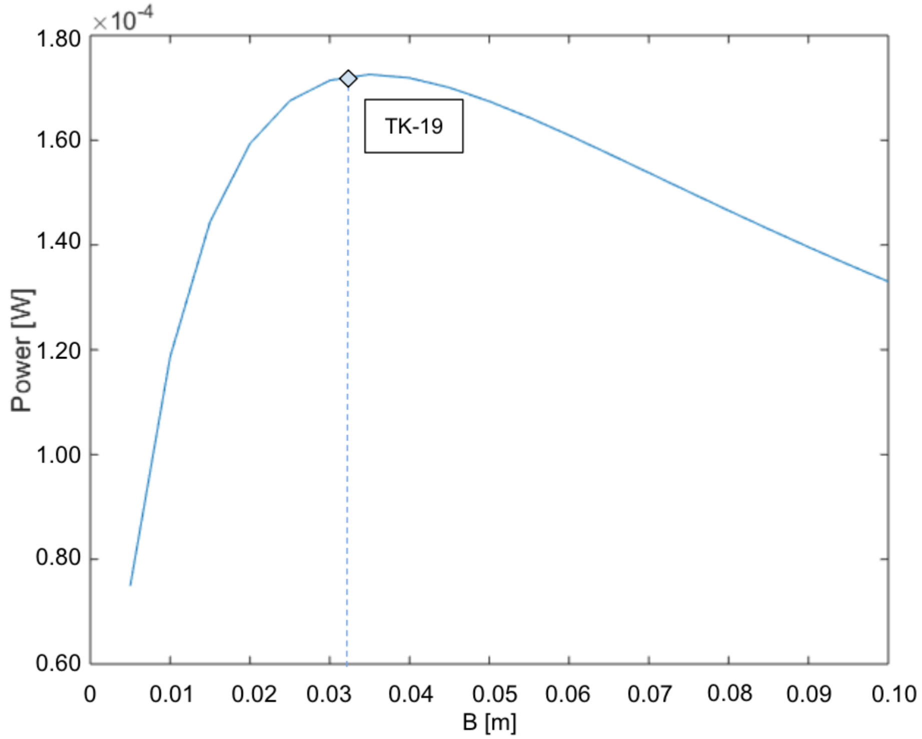

Figure 14: TEM theoretical power output versus effective B factor, courtesy of Tom Watson, SCU.

As can be seen in Figure 14, as the effective B factor increases, the theoretical power output increases and eventually peaks just about where TK-19 lands on the curve. Though at a slower rate, the power output then decreases as the effective B factor continues to increase. These dips in performance on the right side of the optimal

B_{eff} value are results of bottlenecking. Bottlenecking is when heat transfer between two surfaces (heat sink and TEM) is restricted due to small contact area, usually as a result of one surface being much smaller than the other. Since B_{eff} is directly proportional to the ratio between A_{HS} and A_{TEM}, increase in B_{eff} can be associated with a size increase of the heat sink in comparison to the TEM, and vice versa. As the heat sink size decreases in comparison to the TEM, it is less and less capable of dissipating enough heat to maintain desired temperature differences, thus resulting in the sharp decrease in theoretical power output as B_{eff} decreases (moving left from the peak point). However, as the B_{eff} increases past the optimal point, the heat sink reaches and passes a size large enough in comparison to the TEM that bottlenecking will begin to occur which causes the gradual decrease in theoretical power output.

The decline in performance caused by bottlenecking is the reason why our shopping process involves searching for TEMs with effective B factors close to TK-19's. By calculating the B_{eff} of potential TEMs based on our N19-10B heat sink and comparing it to the desired $B_{eff,TK-19}$, we are confirming that the potential TEMs will perform optimally when implemented into our final design.

The TEM shopping process ran into some issues along the way, such as limited market availability and lack of TEM information provided by manufacturers and vendors. Often times, we would find a TEM model with our desired effective B factor but would not be able to purchase it due to the item being out of stock or having a lead time too large for our project's time constraints. Other times, we were unable to even calculate a TEM model's effective B factor because the manufacturer or vendor would not disclose the necessary dimensions. Companies such as TE Technology and Laird Technology used model numbering systems which incorporated TEM dimensions as well as provided detailed schematics with the remaining dimensions required to calculate B_{eff}. For example, TE Technology employed the following model numbering system: TE-NN-XX-YY, where NN is the number of leg pairs, XX is the leg width [mm], and YY is the leg length [mm]. The combination of the market availability issues and lack of information regarding TEM dimensions limited our options for a selecting TEM to purchase implement into our final design.

By the end of the shopping process, we selected a TEM named TE-65-0.6-1.5 (TE-65) with an effective B factor, $B_{eff,TE-65} = 0.01157$. Due to the market limitations, while TE-65 is certainly not ideal, it's effective B factor is the closest to $B_{eff,TK-19}$ we could find for a TEM which satisfied the design size constraints. Even with a much lower effective B factor, according to the plot in Figure 14, TE-65 has a theoretical power output of about 0.12 [mW], which is still 75% of TK-19's power output.

3.3 Design Description

Because the N19-10B heat sink is a stock item, our group had no input on its design. It consists of 13 hexagonal pins spaced evenly on a 19 [mm] x 19 [mm] base. As stated previously, the pins were cut down to yield a total height of 7mm. Detailed mechanical drawings and properties can be found in Figure 41 in the appendix.

Similar to the heat sink, our chosen module TE-65-0.6-1.5 is a stock item and was designed and manufactured by TE Technology. The module consists of 65 leg pairs sandwiched between two 13 [mm] by 13 [mm] ceramic plates [21]. Figure 15 shows TE Tech's generic TEM schematic with dimensions pertaining to our specific model, TE-65-0.6-1.5. The dashed squares within the top view represent the individual legs of the TEM.

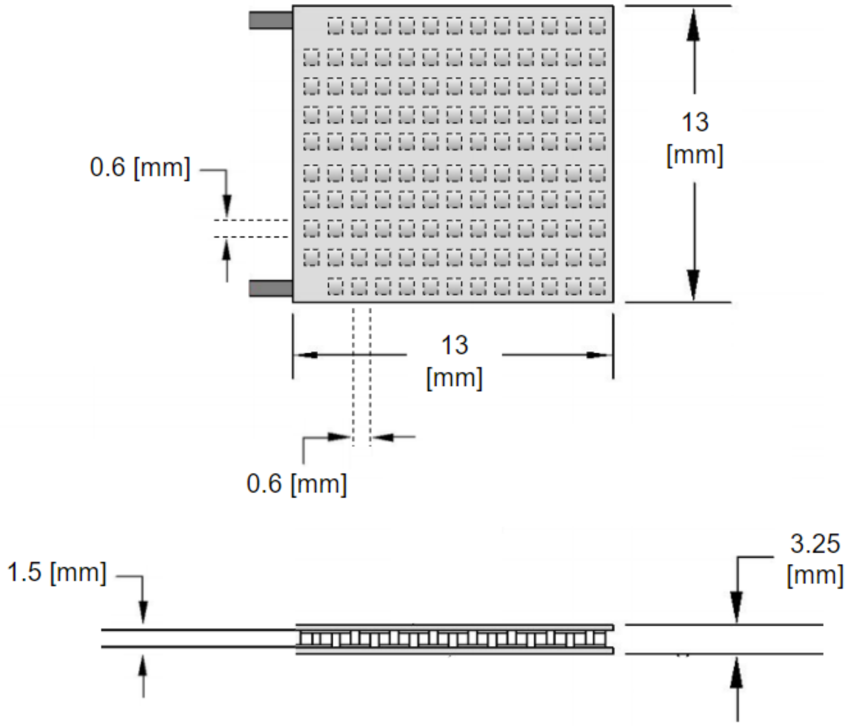

Figure 15: Dimensioned schematic of TE-65-0.6-1.5.

In order for the power generation subsystem to successfully function, the TEM and heat sink must be held together securely with sufficient contact pressure. Additionally, the heat sink must not be significantly obstructed, and the subsystem must be easily integrated into a wearable device. To do this, the TEM and heat sink are held together using a plastic, 3D-printed housing. The housing has a three-sided groove at its bottom which the TEM slides into and a recessed portion on top in which the heat sink sits. Mounting wax was used as a thermally conductive adhesive to hold the TEM and heat sink together and inside the housing with sufficient contact pressure. The housing also has two bars on opposite sides, similar to a watch face, to allow them to be easily integrated into our wristband. This housing will be described in more detail in the wearability subsystem section, Chapter 6.

3.4 Prototype Results

Depicted in the Figure 16 below, the selected TEM and heat sink combination held by mounting wax in a plastic, 3D-printed housing make up the power generation subsystem prototype.

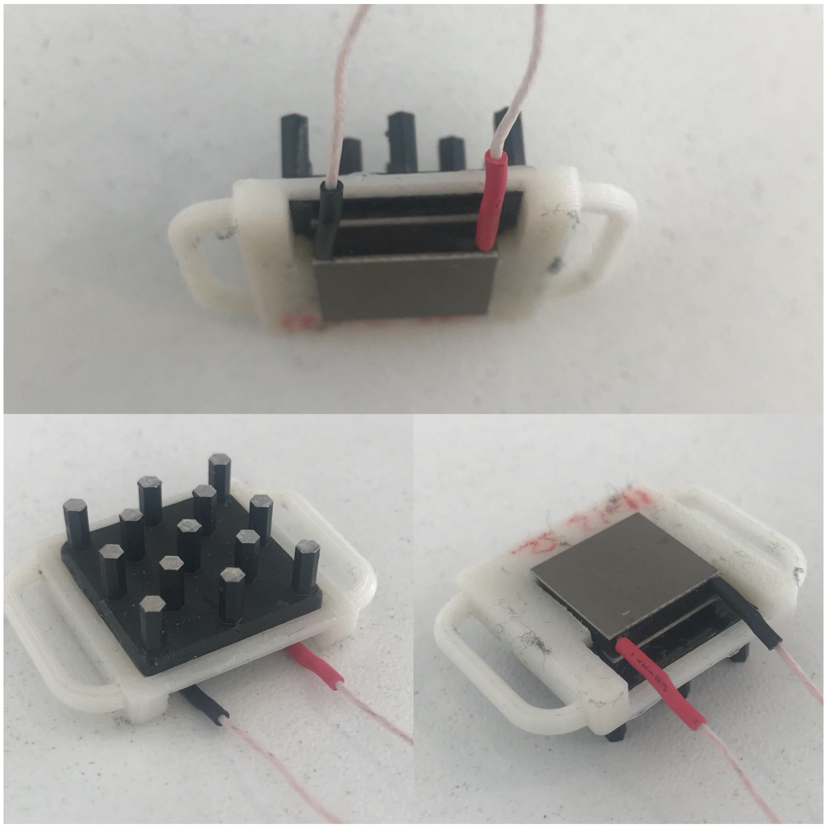

Figure 16: Power generation prototype.

3.5 Subsystem Testing and Verification

3.5.1 Theoretical Maximum Power Tests

Testing and verification of the power generation subsystem was performed by way of measuring the open circuit voltage and short circuit current in order to calculate the theoretical maximum power. Open circuit voltage occurs when the circuit is in an “open” state and no current is flowing. To measure this, voltage across the positive and negative leads of the TEM, V_{OC}, was measured. Short circuit current occurs when the circuit is in a “shorted” state and is closed but has no load. It is technically not possible to measure the short circuit because current is obtained by measuring the voltage across a low resistance precision resistor in series with the circuit (R = 0.1Ω) and using Ohm’s Law, I = V/R, to calculate current I. However, a current value very close to the short circuit current can be obtained by connecting sole a 0.1Ω precision resistor in series with the positive and negative leads of the TEM and measuring the voltage across this resistor, V_{PR}, and calculating the current through the resistor, I_{PR}. The short circuit current, I_{SC}, can then be extrapolated from the linear VI curve generated from these two measurements.

The test setup for this consisted of a single TEM and heat sink secured in the housing with mounting wax. The bars on the housing were used to wear this TEM-heat sink combination on the wrist. The approximately 32°C body heat from the wrist served as the heat source for power generation. The open circuit voltage and precision resistor voltage and current were measured and recorded with Labview using the procedure described previously in section 3.2.3. Samples were once again taken at a rate of 75 [Hz] for 100 samples, and measurement uncertainty of the NI-DAW 9215 was 0.02%.

Using this testing procedure, the following linear voltage versus current, or VI, curve was obtained using the average V_{OC} and V_{PR} values from 500 data points. The slope of this line is used to extrapolate the short circuit current using the equation,

$$I_{SC} = \frac{V_{OC}}{M}, \tag{3}$$

where I_{SC} is short circuit current in Amps, V_{OC} is open circuit voltage in Volts, and M is the slope of the VI curve.

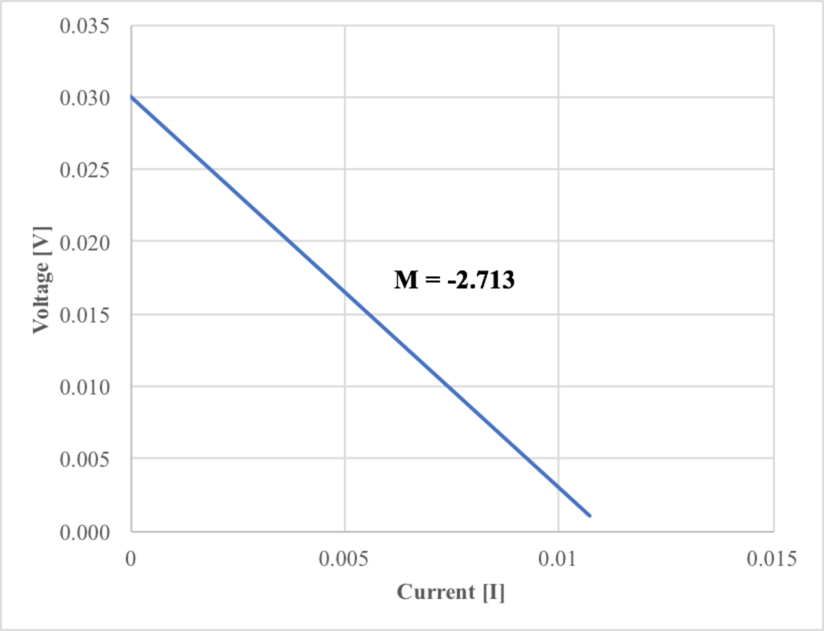

Figure 17: Power generation VI curve.

The average open circuit voltage V_{OC}, precision resistor voltage V_{PR}, precision resistor currentI_{PR}, and slope M for the power generation subsystem are depicted in Table 4 below. They were obtained from 500 data points and were used to calculate the short circuit current.

Table 4: Power generation testing and verification data.

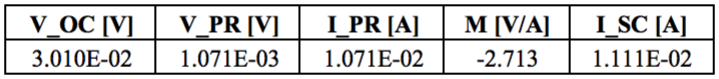

V_OC [V]	V_PR [V]	I_PR [A]	M [V/A]	I_SC [A]
3.010E-02	1.071E-03	1.071E-02	-2.713	1.111E-02

Because power P is equal to $V * I$, it is evident that the theoretical maximum power that could occur along the VI curve is a product of half of the maximum or open circuit voltage and half of the maximum or short circuit current. Therefore, the theoretical maximum power is equal to $\frac{1}{4} V_{OC} * I_{SC}$. According to the principle of maximum power transfer, the maximum voltage, current, and power occur when the circuit's load is equal to the internal impedence of the power source, in this case, the power generation subsystem [11]. Using the data found in Table 4, it is found that the maximum theoretical voltage, current, and power for a single TEM-heat sink pair are $V = 1.505E-2$ $[V]$, $I = 0.556E-2$ $[A]$, and $P = 8.360E-5$ $[W]$. Since the boost converter has a minimum input voltage of $2.0E-2$ $[V]$, assuming that load matching conditions are ideal, it is necessary to connect at least two TEM-heat sink pairs in series so that the voltage output may be doubled to be approximately $3.0E-2$ $[V]$, meeting the minimum input voltage requirement. This will be discussed further in the voltage boosting subsystem section, Chapter 4.

3.5.2 Seebeck Tests

An additional component of the testing and verification of the power generation subsystem was the calculation of the subsystem's Seebeck coefficient. This test was performed by subjecting our TEM-heat sink pair to a number of increasing temperature differences, from approximately 0 to 20°C. The procedure for this was similar to that of evaluating heat sink performance. A hot plate TEM was used as the heat source, and the DC power supply's power input was gradually increased to increase the temperature of the hot plate. Temperature measurements were recorded at approximately 25°C intervals. Thermocouples were used with the NI-DAQ 9215 to take the temperature across the TEM, and open circuit voltage across the TEM was also measured using the NI-DAQ 9215. These temperature measurements and their corresponding open circuit voltages were recorded using Labview at a rate of 75 [Hz] for 100 samples. The uncertainty for NI-DAQ 9215 temperature and voltage measurements was 0.02%. The slope of the curve obtained from this data represents the Seebeck coefficient of a single TEM-heat sink pair. As seen in Figure 18 below, the Seebeck coefficient was found to be S = $3.73E-3$ $[V/°C]$. Therefore, a TEM-heat sink pair is capable of generating $3.73E-3$ $[V]$, open circuit, per $°C$ temperature difference across the TEM. The projected value of about 30 [mV], open circuit, produced at expected operating conditions (indicated by the highlighted region on Figure 18) agrees with measurements taken in the theoretical maximum power tests.

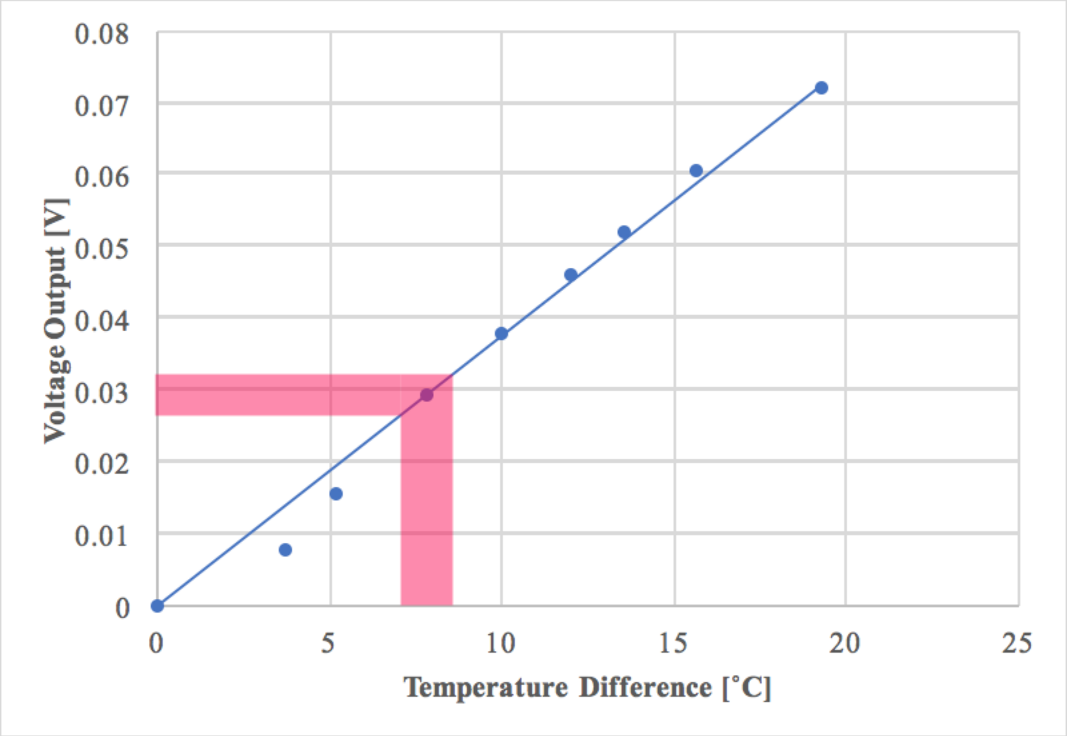

Figure 18: Power generation Seebeck curve.

Chapter 4

Voltage Boosting Subsystem

For the voltage boost subsystem, the primary role was to accept the fluctuating ultra-low input voltage being output from the thermoelectric modules and supply an output voltage at a constant, higher stepped up voltage that could power a wearable EKG. As mentioned in our system requirements, the voltage boost subsystem was required to output a voltage of at least 3.7V in order to charge the battery for our specific EKG monitor. The closest setting for our system is 4.1V which works well with the EKG battery.

4.1 Choosing a Boost Converter

The primary component of the voltage boost subsystem is a boost converter which plays the role of stepping up this voltage. When deciding on what type of boost converter to use we were limited to models specifically designed to take ultra-low inputs that our thermoelectric modules would output. Due to the limited market saturation of these types of boost converters, we were limited to a few models from Linear Technologies and Texas Instruments. Linear technologies had a model with two different versions depending on the voltage output settings required called the LTC3108, which accepted input voltages as low as 20mV under no load conditions [10]. Texas Instrument models such as the TPS61200 had input voltages that only went as low as 300mV. With our circuit combinations of thermoelectric modules in the 20-150mV range from initial testing we were able to easily determine that the linear technologies model would be the only viable option given our input requirements. The optimal low-voltage input circuit for LTC3108 is shown below in Figure 19.

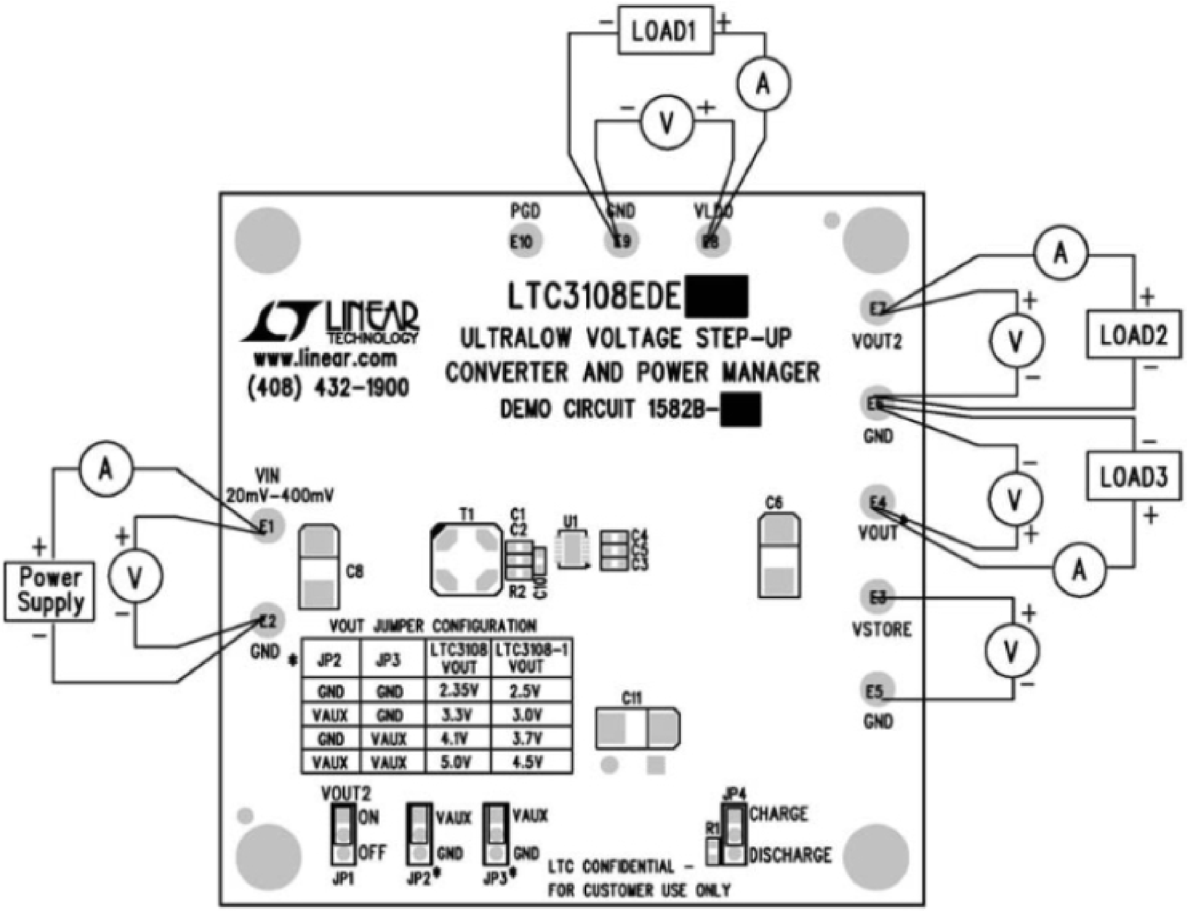

Figure 19: Optimal LTC3108 circuit [10].

4.2 Circuit Design

To meet the requirements of the LTC3108 module we quickly determined that a single assembly (which will be referred to as a module in this chapter) would not be able to provide adequate power for our charging application. The supplied power in watts from a circuit is equal to the voltage difference multiplied by the current (I) flowing to the output, as shown in equation 4.

$$P_{supplied} = V * I \tag{4}$$

A portion of this power is absorbed or lost within the circuit as heat due to the electrical resistance (R) of the modules and connecting wires, as seen in the second relation for power dissipated, as shown in equation 5.

$$P_{dissipated} = I^2 * R \tag{5}$$

Due to these power relations, our optimal circuit design maximizes voltage and current while minimizing the resistance (and power loss) of the circuit.

In order to optimize these three inversely related variables, voltage, current and resistance we experimented with different numbers of modules with series and parallel connections. Adding a module in series theoretically leads to an unchanged current, increased output voltage, and increased circuit resistance. Adding modules in parallel theoretically gives an unchanged voltage, increased current, and decreased resistance for the circuit. To take advantage of the beneficial portions of each connection type, we determined that the optimum configuration of modules for our application has 4 modules with a single parallel connection between two pairs of modules in series. It should be noted that this optimization was further complicated by fact that the resistance of the modules is directly related to their temperature difference, a higher temperature difference gives a higher module resistance.

4.3 Subsystem Optimization

Our four module approach was also determined using efficiency data found by testing our boost converter using low inputs provided directly by a DC power supply. The efficiency of a boost converter is found by dividing the power output from the boost converter by the power that is input into it (multiplied by 100 to get a percentage), as shown in equation 6.

$$Efficiency = (P_{out}/P_{in}) * 100 \tag{6}$$

As shown in Figure 20 in the peak in the efficiency vs. voltage in to the boost converter provided by a DC power supply at constant voltages, a peak efficiency of approximately 25% was found for our boost converter at an input of approximately 100mV. We designed our circuit to output as close to this optimal 100mV point as possible with a temperature difference across our modules similar to that of human skin and room temperature.

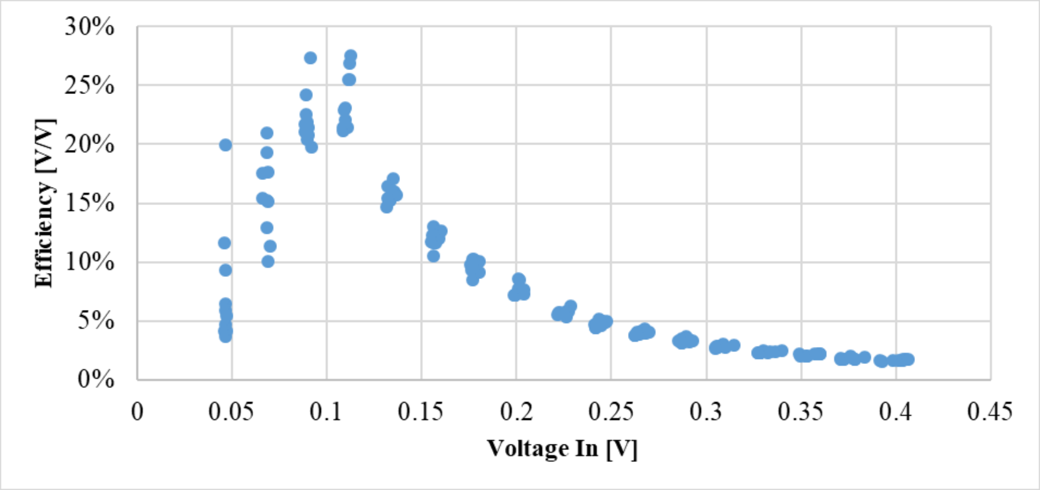

Figure 20: Efficiency vs. Voltage In for LTC3108.

We were able to successfully boost up to beyond the necessary 3.7V using both a DC power supply as the input as well as our circuit configuration as the input. A voltage input vs voltage output graph demonstrating this using a DC power supply is shown in Figure 21. Around the 100mV in this graph the boost converter was able to reach an output level of 5V which it consistently held for higher inputs, confirming the 100mV as a peak efficiency point for the boost converter.

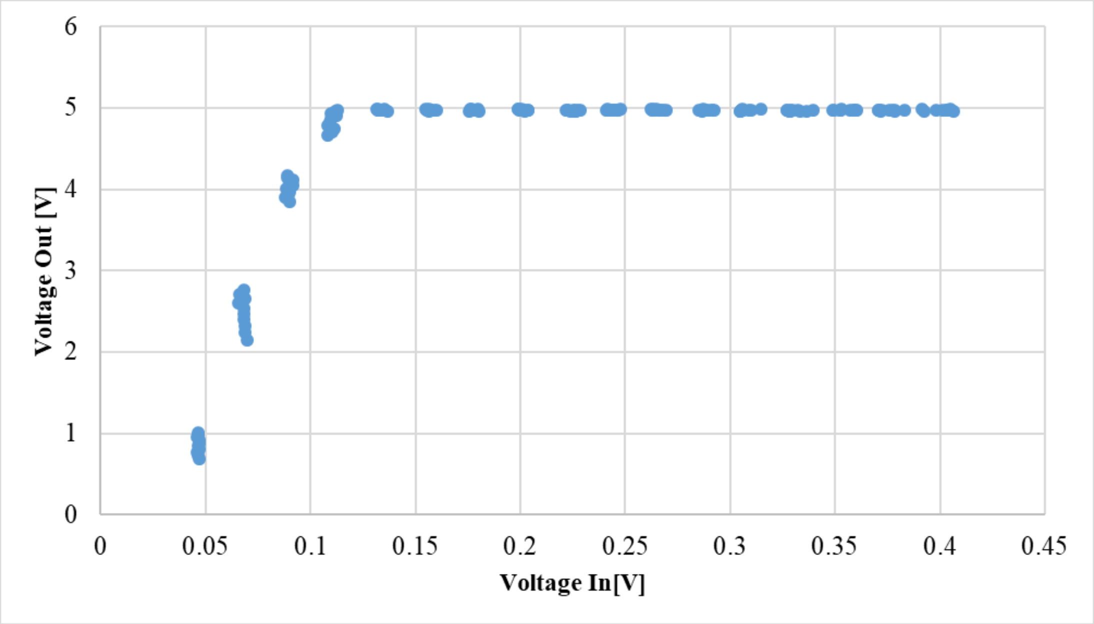

Figure 21: Voltage Out vs. Voltage In graph for LTC3108.

The testing procedure for the LTC3108 boost converter used the National Instruments NI-DAQ 9215 modules with connected BNC cables acting as voltmeters and sampled at 75[Hz] for 100 samples within Labview. The measurement uncertainty for the NI-DAQ 9215 was 0.02%. To power the boost converter, we used an Agilent 66000A DC power supply which we set controlling voltages of through Labview. For each setup we put a 0.1 [Ω] precision resistor in series with both the input(Vin) and output of boost converter (Vout) and its load so that we could measure the voltage drop across them allowing for an accurate measurement of current into and out of the boost converter. Two other voltmeters measured through Labview were also connected directly between the output and input voltage ports and ground to measure the voltage going into and out of the boost converter. Being able to knowing voltage and current at the input allowed us to easily power input and output using equation 4 and in turn get the efficiency of the boost converter using equation 6.

For the boost converter to operate efficiently, resistive loads were connected between the output voltage port of the boost converter and ground. Based on testing with loads between 10[Ω] and 100[kΩ] we found the most efficient load to occur at approximately 22[kΩ] which is the load that was used in both figure 20 and figure 21. When testing Labview was used to take 10 voltage samples for each BNC cable at each interval of input voltage supplied by the DC power supply. This is the reason for the scattered nature of the graphs for both figure 20 and figure 21 since the current readings out were very low and caused some variation due to the accuracy limits of the voltmeters. The voltage setting for the power supply was varied between 50 and 450 [mV] with intervals of 50[mV] for all testing.

Chapter 5

Battery Charging Subsystem

One of the key elements of the device is its ability to power the EKG battery. Without constant and reliable grid power, being able to charge the EKG portably is crucial to the success of our device. In our hopes to expand the wearable device market, the ability to power various types of wearable devices is also important. This includes different connections to respective devices. While the scope of this subsystem will focus on meeting the power requirements of a low voltage wearable device specifically to our EKG application, adaptability is still an important aspect of the subsystem. The device battery requires 3.7V and sufficient current to produce an indication of charging. Considering that this threshold might be different for other low voltage applications, the efficiency of our device to charge its respective wearable may fluctuate.

5.1 Options and Trades

The EKG has three charging contacts on its underside. The included USB charge cable has a claw design that presses its own contacts onto those on the EKG. This interaction is seen below in Figure 22.The left side of the figure depicts the underside of the EKG; its three gold charging contacts are seen at the top. The center of the figure depicts the "claw" charger with its three corresponding contacts. The right side of the figure depicts the claw charger clamped onto the EKG charging contacts. Because the boost converter has charge controlling capabilities that limit the output current and voltage, charge controlling was not necessary to consider in the battery charging subsystem.

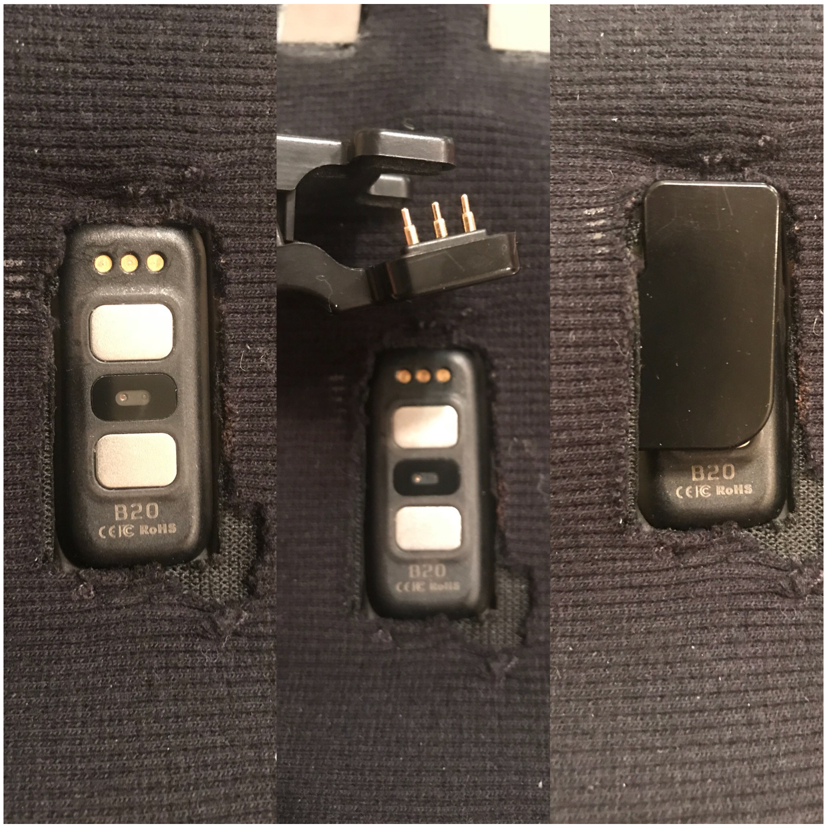

Figure 22: EKG and its charger.

When designing the method of charging a battery with the boost converter electrical output, three options were considered:

1. Connect boost converter output directly to EKG charging contacts via wire and solder.
2. Connect boost converter output directly to EKG chare cable, continue to use the claw charger.
3. Connect boost converter output to female USB port, plug USB EKG charge cable into USB port.

The third option, connecting the boost converter output to a USB port, was the most simple, adaptable, and safe method of charging the battery, and it was selected for these reasons. By connecting a female USB port to the boost converter, the power output from our device can charge a number of USB devices rather than be limited to the EKG. The only drawback to this design is that using the claw charger while wearing the EKG somewhat interferes with contact between the EKG and wrist. However, the EKG is still able to function. A slightly different EKG or other USB wearable medical device with a charge port located on its outer sides would alleviate this issue.

5.2 Design Description

As it was mentioned before, the design of this subsystem is very simple because the boost converter regulates output voltage current, protecting the battery from being overcharged. The battery charging subsystem simply must connect the boost converter output to the EKG's rechargeable battery. To do this, the power and ground connections of a female USB port were connected to the boost converter voltage output and ground leads. An evaluation board was used in this project rather than a much smaller printed boost converter circuit board, so this USB port was not integrated into our wristband design. The USB EKG charge cable was plugged into this USB port and the charging claw was placed around the EKG (which is integrated into the wristband). The EKG itself displays an animated battery charging indicator when it is being charged.

5.3 Prototype Results

The boost converter output was connected to a female USB port, and The EKG and its charge cable were plugged into this USB port. The battery indicator on the EKG monitor verifies that the battery is successfully charging. This prototype is depicted below in Figure 23

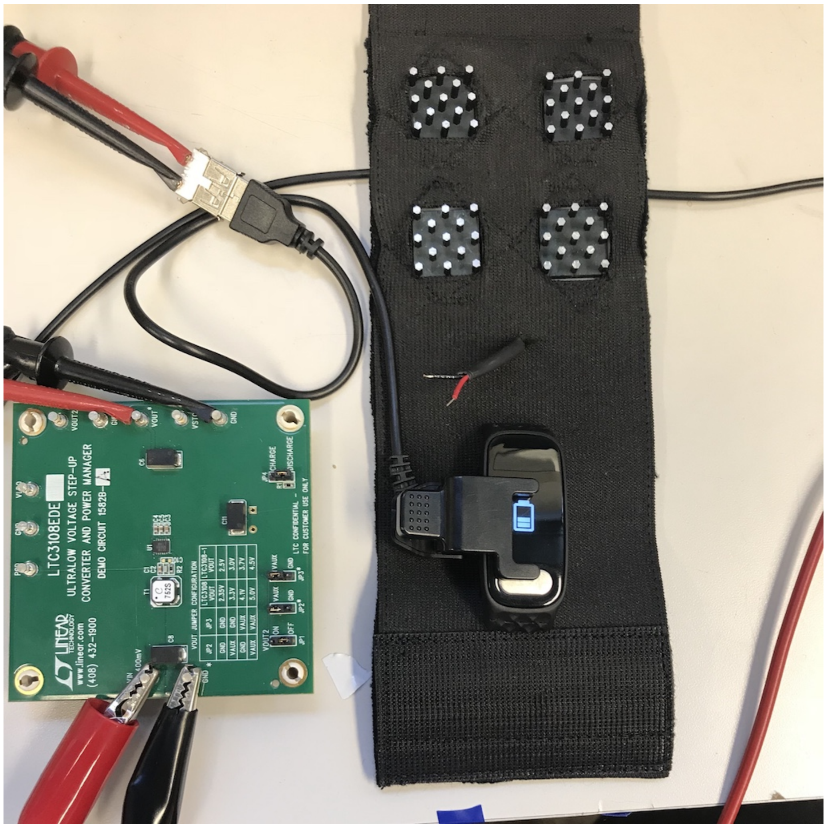

Figure 23: Battery charging prototype.

5.4 Subsystem Testing and Verification

The testing and verification of the battery charging subsystem, independent from other subsystems, was a simple process. It consisted of testing and verifying that the connection between the female USB port, EKG charge cable, and EKG was successful in transmitting power to the EKG battery. To do this, a DC power supply was tuned to 4.1V to simulate the boost converter output, and it was connected to the female USB port. The animated battery charging indicator on the EKG was used as verification that the connection was successful. The EKG indicated that its battery was charging when the 4.1V (0.2A) DC power supply was connected to the USB port and the EKG and its charge cable were plugged into this USB port, verifying that the female USB port design was valid and successful.

A proof of concept test was also performed to characterize battery charging using a boost converter and thermoelectric module. A Laird 40 [mm] x 40 [mm] thermoelectric module was placed under a 12°C temperature difference using an 80 [mm] x 80 [mm] heat sink with 40 [mm] tall pins. The heat source was the hot side of another Laird module, and a DC power supply was used to power this heat source thermoelectric module. The power output generated from the thermoelectric module was fed to a Linear Technologies LTC3109 boost converter, which has very similar characteristics to the boost converter used in this project, LTC3108. The output from the boost converter charged a 3.7V 150mAh lithium polymer rechargeable batter, which is similar to the 3.7V 80mAh battery in the EKG.

The voltage across the battery was measured over two hours using a NI-DAQ 9215 connected to the batteries positive and negative leads, and Labview recorded measurements at a sampling rate of 75 [Hz] for 100 samples. Once again, the NI-DAQ 9215 measured with an uncertainty of 0.02%. Through this experimental procedure, the charging pattern for this battery using thermoelectric power generation and a boost converter was obtained. The battery was charged using the boosted power output from a thermoelectric module placed under a 12°C temperature difference. The battery charging is characterized by sharp increases in voltage across the battery followed by longer plateau periods. This pattern continues until the voltage and current capacities of the battery are reached. Figure 24 below depicts this pattern.

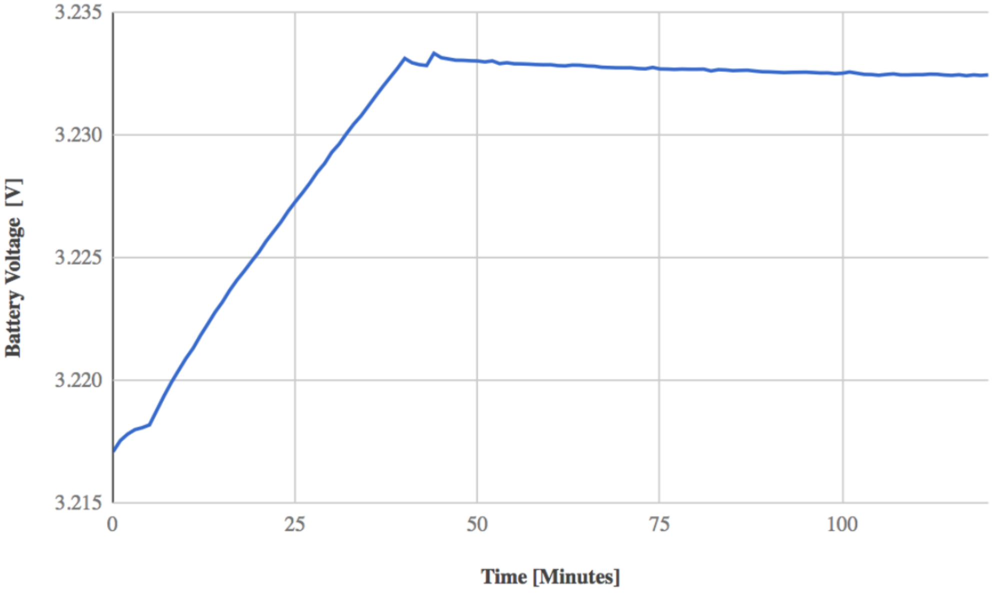

Figure 24: Battery voltage over 2 hour charging period, courtesy of Joshua Vincent, SCU.

Chapter 6

Wearability Subsystem

The wearability subsystem is what allows for the power generation device to be worn on the wrist. Its two main components are a wristband and a fixture to hold the thermoelectric modules and heat sinks together. The design of the wristband and fixture were constrained by performance and aesthetic requirements outlined by customer needs. This included size, comfort, and weight constraints as listed in the PDS table in the appendix.

6.1 Wristband

The purpose of the wristband is to create sufficient contact between the hot side of the thermoelectric module and the user's skin so that the thermoelectric modules can use the body as a heat source, as well as providing the capability of the device to be comfortably worn and easily put on and taken off.

6.1.1 Options and Trades

When initially designing the wristband, we considered three different materials that would be appropriate for the wearability subsystem: elastic, silicone, and velcro. The wristband material needed to be able to provide comfort, contact pressure, robustness, and adjustability as well as be aesthetically pleasing and light weight. Velcro was able to provide sufficient contact pressure, robustness, and adjustability; however, the side in contact with the skin created friction and discomfort, and the lack of stretch also was detrimental to both comfort and functionality. In order to use a velcro band, both a male and female layer are needed. This increased the overall height of the wristband and decreased its aesthetic attributes. A silicone wristband had the qualities of comfort, robustness, and aesthetic value. However, it was a challenge to find a clasp or buckle to make the band significantly adjustable without interfering with TEM, heat sink, and EKG layout. Additionally, the lack of breathability of the silicone decreased comfort for long-term wear. In addition, silicone wristbands are not readily available and is expensive when custom ordered. A wristband made of elastic provided comfort, sufficient contact pressure, robustness, and adjustability. Elastic is also readily available in solid colors and easy to sew, making it more attainable to design an aesthetically pleasing wristband. It is also thin, lightweight, and inexpensive.

6.1.2 Design Description

After evaluating the pros and cons of our options we decided to construct our wristband prototype out of 3 inch elastic. Four 20 mm by 20 mm holes were cut in a 2 by 2 grid to expose the heat sink to ambient air, facilitating natural convection. The thermoelectric modules were placed in the fixture and the heat sinks were then waxed to the fixture and thermoelectric module. The fixture was then sewn to the elastic through the side bars. A layer of thin, rib knit cloth with a 2 by 2 grid of 10 mm by 10 mm holes was sewn to the bottom of the elastic to expose the hot side of the thermoelectric module to the skin while concealing the wiring connections and fixtures. This layer of rib knit cloth also increases the comfort of the wristband. The EKG was also sewn into the wristband using part of its own original wristband as the frame to hold it in place. corresponding holes in the elastic and Velcro allow the EKG to contact the skin and function properly. The initial design for the wristband prototype is seen below.

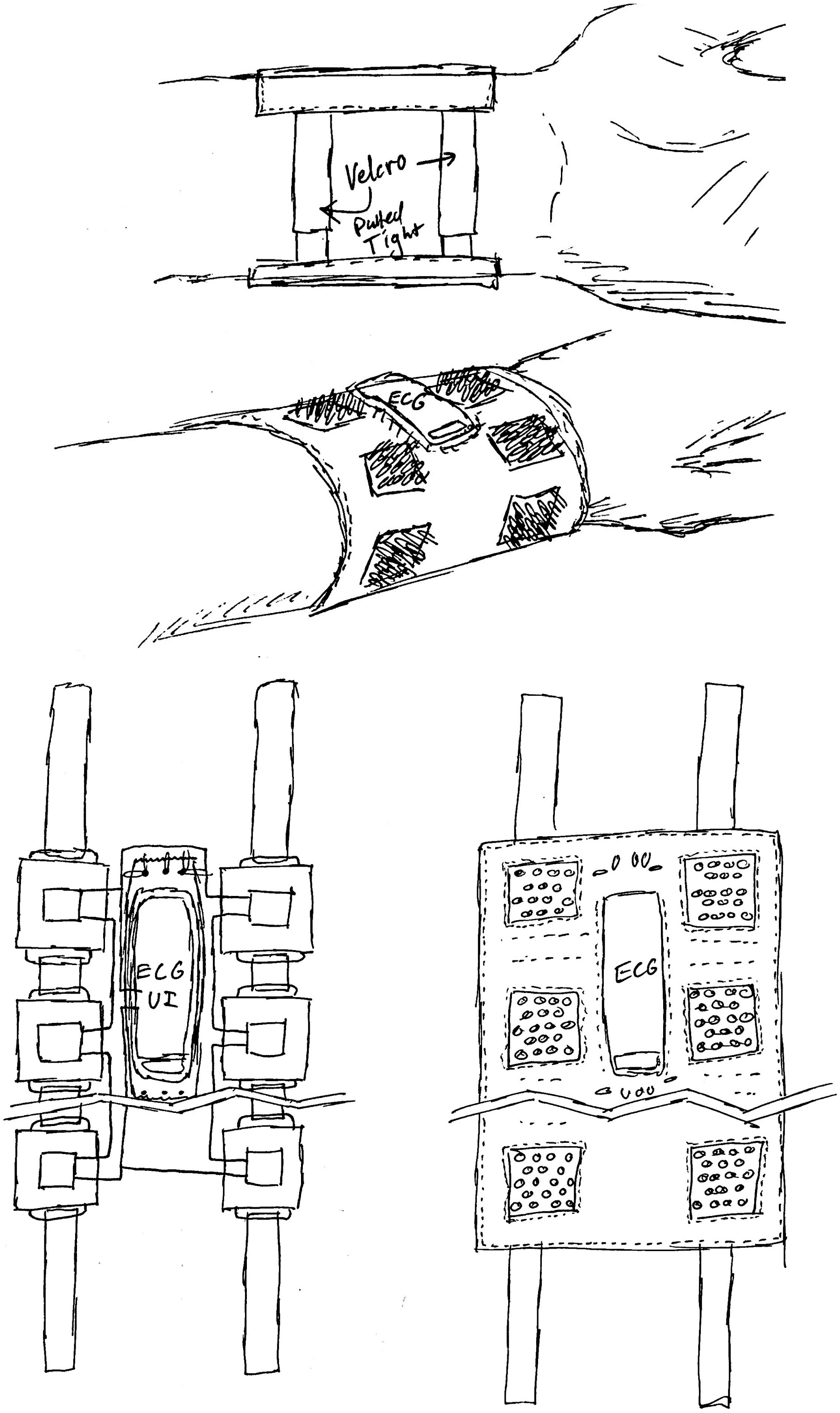

Figure 25: Initial concept for wristband prototype.

6.2 Prototype Results

When actual prototyping began, it was evident there was not enough space for the EKG and TEMs, heat sinks, and housings to be on the same side. Therefore, the TEMs, heat sinks, and housings were moved to the bottom side of the wristband. A small amount of glue placed between the rib knit cloth and housings was used to keep rib knit cloth in the correct position. Because an evaluation board separate from the wristband was used for the boost converter circuit, the power generation subsystem output protrudes from the wristband in insulated, heat shrinked wires. This wristband prototype is seen below.

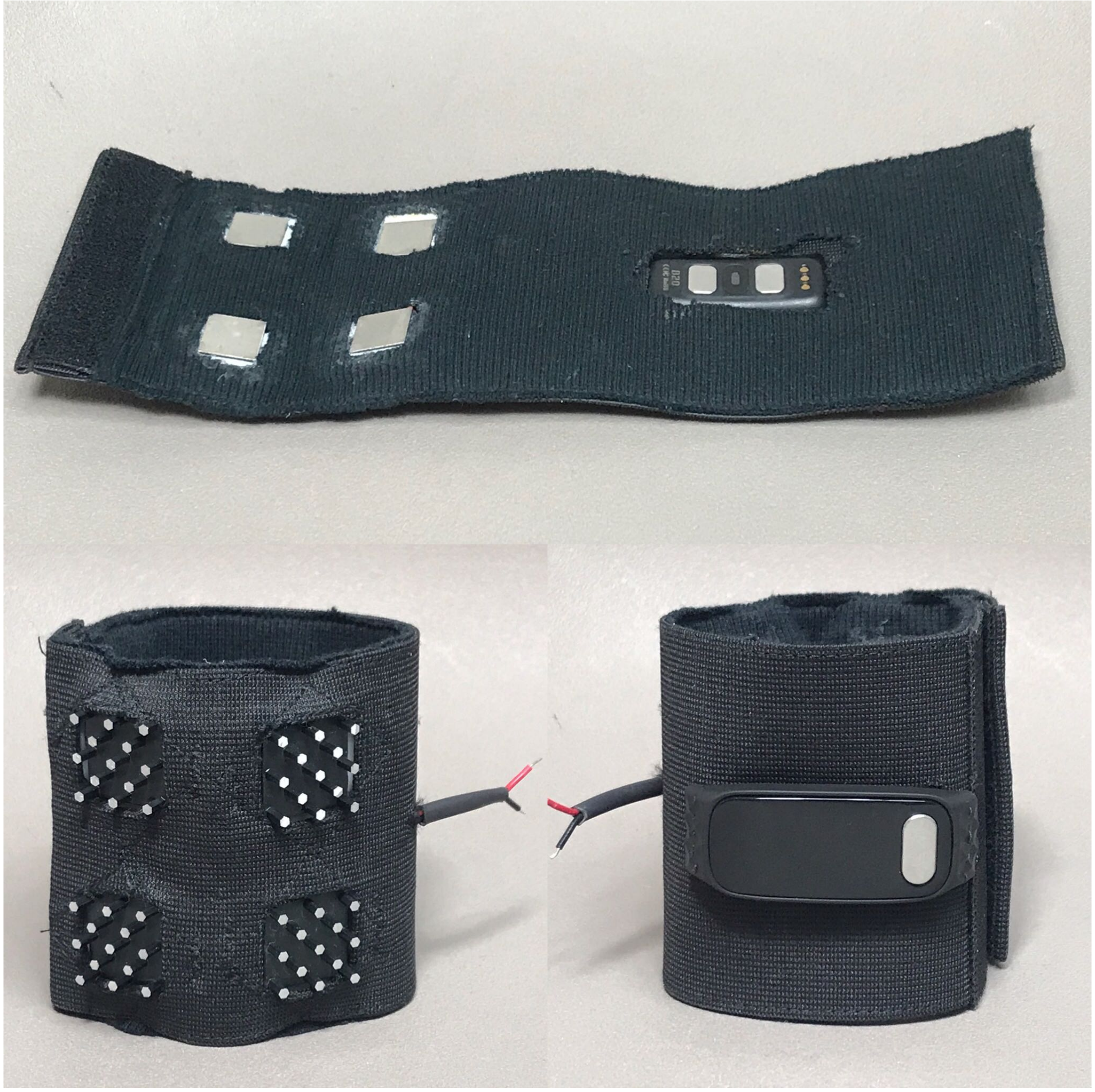

Figure 26: Wristband prototype.

6.3 Housing Fixture

The housing fixture is a plastic fixture developed with the purpose of holding the heat sink in contact with the thermoelectric module with sufficient pressure to provide efficient contact between the two pieces. This is necessary for optimal heat dissipation. The fixture can be seen in Figure 29. The heat sink and thermoelectric module are adhered to the fixture with a reversible thermoset wax that holds the three pieces of the assembly together in the configuration shown in Figure 44 in the appendix.

6.3.1 Rationale

The housing fixture was developed because, as we were beginning to construct the first wearable thermoelectric generation prototype, we came to the conclusion that directly installing heat sinks and thermoelectric modules into the wristband prototype without some sort of housing was very dangerous for the small and fragile TEMs, produced inconsistent heat sink efficiency due to inconsistent contact with TEMs, and exposed the thermal circuit to potential interference. The high work cost for adapting the device for more voltage or amperage, or for different devices, and complication of the build were unideal. The fixture was developed to address these issues and provide a solution that met the desired functionality requirements of the device.

6.3.2 Design Criteria

The criteria for the design is as follows:

- Provides both physical and thermal protection for the TEM and heat sink.
- Improves the adaptability of the device.
- Maintains sufficient pressure between the heat sink and TEM for optimal thermal conductivity.
- Improves power output consistency for TEM-heat sink combinations.

6.3.3 Design Iterations

The first iteration of the housing fixture is pictured in Figure [27]. Initially, the main concern in the design was ensuring a tight seal between the TEM and heat sink, while minimizing the number individual pieces for greater adaptability. The design was a two-piece, snap-fit fixture where the top piece would snap onto the lower piece, holding the heat sink by the outermost pins onto the TEM with a high pressure for efficient heat dissipation. The material chosen was a resin set material named ”Tough V4” used by the FormLabs Form 2 SLA 3D printer. The material was chosen along with the 3D printing approach to fabrication because it allowed for the time between iterations to be greatly reduced, the fabrication had a high material placement accuracy of within 0.1mm, and the material provided enough strength and durability to withstand impacts and protected the internal devices well. However, the material was too flexible to provide a consistent snap-fit hold of reliable pressures between separate assemblies. Thus the snap-fit design was retired.

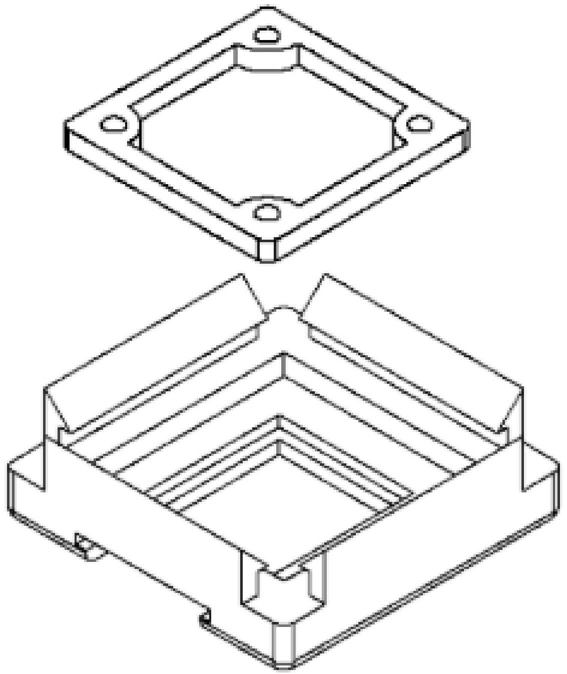

Figure 27: Snap-fit housing design.

The second iteration of the housing fixture is pictured in Figure [28]. It is a two-piece, screw-and-nut design that pressed the heat sink onto the TEM by the four outermost pins. This provided sufficient pressure and provided a reliable fit that was very consistent between assemblies, but the top piece of the housing fixture impeded the convective ability of the heat sink by obstructing the pins. The option of extending the pins to compensate was found to interfere with the overall design requirement of the device being low-profile. Therefore it was decided to retire the two-piece fixture concept altogether.

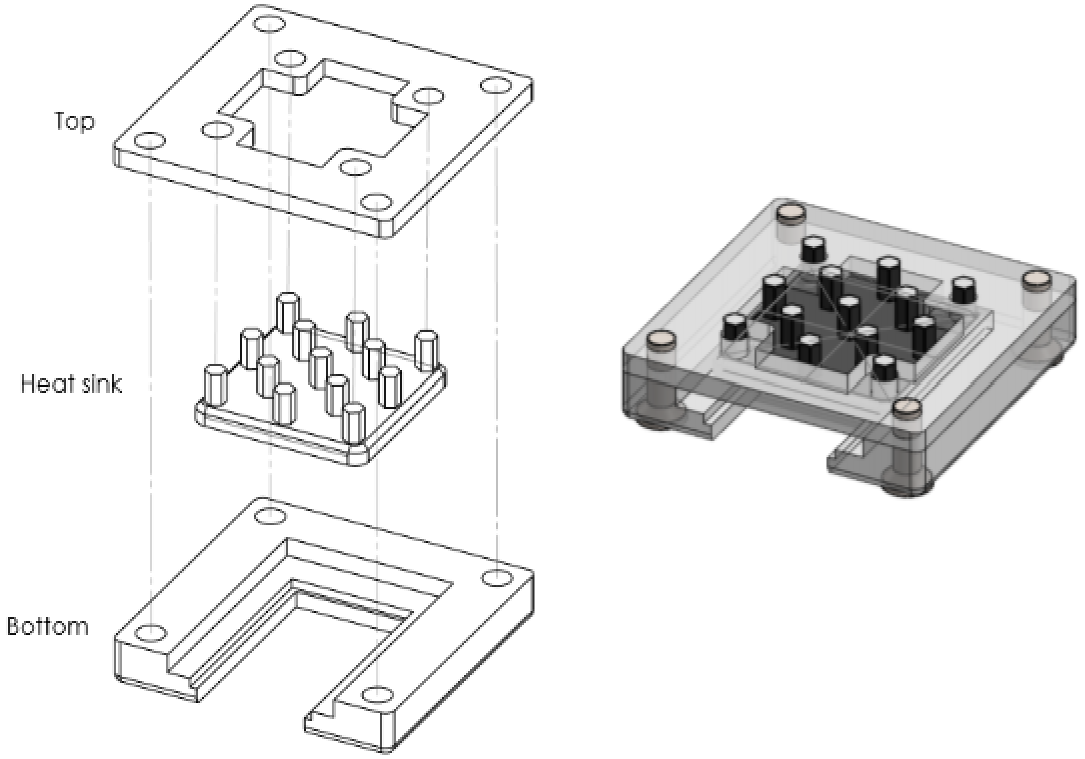

Figure 28: Screw-and-bolt housing design.

The third and final design of the housing fixture is pictured in Figure [29]. It is a single-piece fixture that serves fixes the heat sink and TEM in place with an adhesive wax. It was found that the pressure required to reach a suitable conductivity between the TEM and heat sink could be reached simply by pressing the heat sink onto the TEM together thermoset wax was setting. It was found that the wax maintained the pressure given to the assembly, maintaining the thermal conductivity as well between the heat sink and TEM. Additionally, bars were added to two opposite sides of the fixture to allow for a number of assemblies to be strung together and very easily create a circuit suitable for a required voltage. This final design meets all criteria set for a housing fixture.

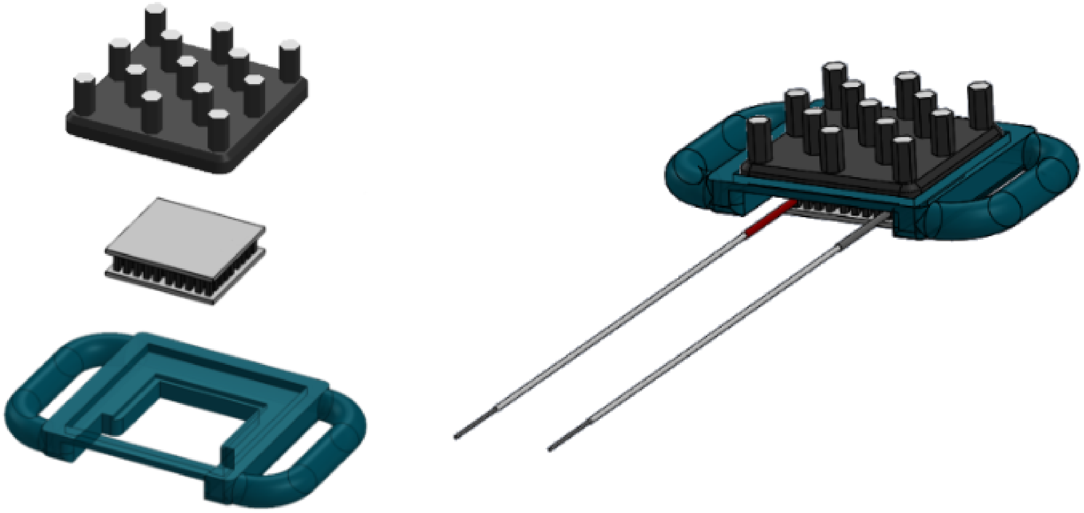

Figure 29: Final housing design, Modular TEM-Heat Sink Interface.

6.4 Prototype Results

The prototype results for the housing can be seen in Figure 16 in the prototype results section of Chapter 3.

Chapter 7

System Integration, Test, and Results

The overall wearable thermoelectric power generation system consists of the power generation subsystem connected to the voltage boosting subsystem connected to the battery charging subsystem, and these subsystems are all integrated into the wearability subsystem. Figure 30 depicts this system integration.

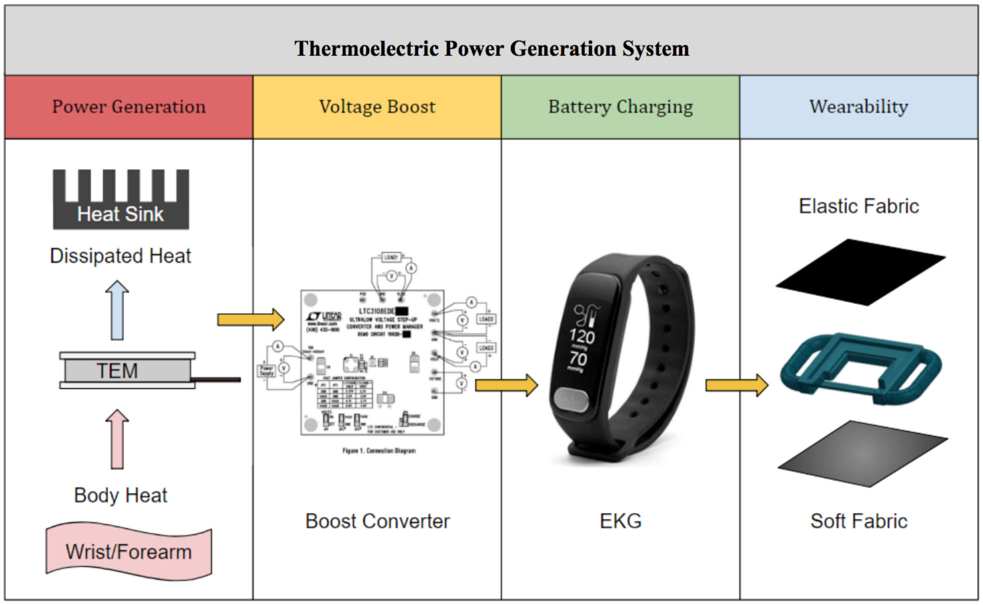

Figure 30: Wearable thermoelectric power generation system.

In order to test and evaluate our device, all the subsystems were integrated into the overall system through the construction of our prototype. After each subsytem was individually verified to function properly, the first step of construction was to integrate the power generation subsystem into the wearability subsystem. As previously described, the housings were sewn into the elastic layer of of the wristband, and the TEM leads were connected in a circuit configuration of two modules in series connected in parallel with another two modules in series. The wriring was insulated and hidden between the elastic and rib knit cloth wristband layers. The power generation positive and negative output leads protrude from the wristband and are connected to the boost converter evaluation board.

For the purpose of prototyping, the evaluation board was not included in the wristband design as it would be replaced by an extremely small printed circuit board that can easily be hidden between the wristband layers. The evaluation board's positive and ground output leads were connected to the female USB port as previously described, and the EKG and its charge cable are plugged into the USB port. The EKG can be worn while the charger is connected. It was installed in the wristband by sewing its included rubber housing into the wristband with a hole cutout so that its bottom surface could contact the skin. Figure 31 below depicts the constructed wearable thermoelectric power generation system prototype while being worn.

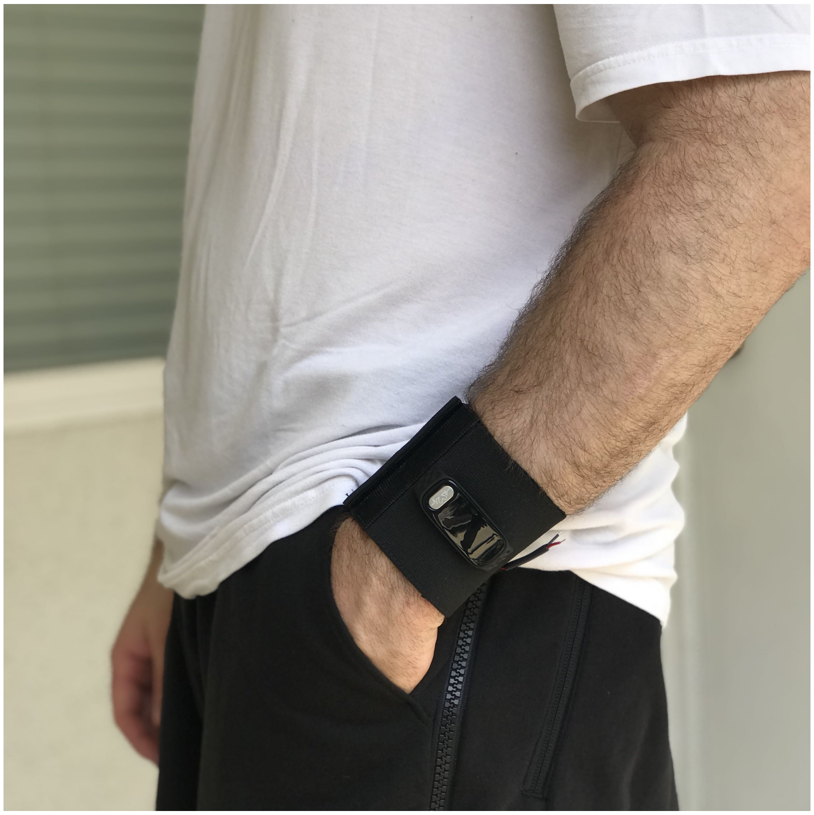

Figure 31: Wearable thermoelectric power generation system prototype.

7.1 Experimental Protocol and Results

7.1.1 Voltage and Current Testing

Voltage and current testing was performed inside at a room temperature of 21°C. The wristband was worn on the left wrist, with a wrist temperature of 34°C. This provided the heat source for power generation. Voltage into the boost converter evaluation board, V_{IN}, was measured using a NI-DAQ 9215 which measured the voltage across the boost converter input leads. Because the output of the power generation TEM circuit is connected to the boost converter input leads, this voltage measurement at this junction is NOT open circuit. The voltage measurement recorded was the voltage that the boost converter "sees." Due to the very small amount of current generated by the power generation subsystem, current into the boost converter was not able to be measured without affecting boost converter performance. Therefore, the short circuit current from the TEM circuit, $I_{SC_{IN}}$, was measured. The procedure for measuring and calculating short circuit current was identical to that described in section 3.5.1, except the the current output was from the two leads of the entire TEM circuit rather than one single TEM.

Voltage out of the boost converter evaluation board output, V_{OUT}, was also measured. Because a battery is essentially a current sink, there is no load for the boost converter output, and the open circuit voltage is voltage the battery receives. This open circuit voltage was measured using a similar procedure to that outlined in chapter three; the difference being that open circuit voltage was measured across boost converter output leads rather than a those of a TEM. Once again, the current output was extremely small and unable to be measured in-circuit. Therefore, the short circuit current out of the boost converter, $I_{SC_{OUT}}$, was measured. All measurements were sampled at a rate of 75 [Hz] for 100 samples, and the NI-DAQ 9215 measured with an uncertainty of 0.02%.

Experimental Results:

Table 5: Output voltage and current experimental results.

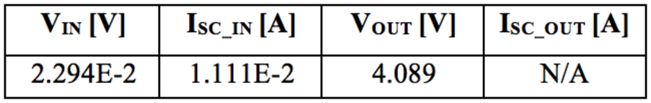

V_{IN} [V]	I_{SC_IN} [A]	V_{OUT} [V]	I_{SC_OUT} [A]
2.294E-2	1.111E-2	4.089	N/A

The device performed as expected for voltage boostage. $2.294E-2$ $[V]$ was a sufficient input voltage to achieve voltage boostage, as is evident with the output voltage value of 4.089. However, The output short circuit current was unable to be read. This was likely because it was expected to be on the magnitude of microamps, and the impedance of the 0.1Ω precision resistor was too large for the small current to overcome. Unfortunately, this was the lowest impedance precision resistor available in the lab.

7.1.2 Battery Charge Testing

The procedure for battery charge testing was to deplete the battery of the ECG, connect the interface and battery of the ECG to the prototype, and wear the device throughout the day taking note of when charging began and when it was complete.

This charge time measurement would be compared the to that specified in the PDS.

Experimental Results:
The device did not perform as expected in battery charge testing as the boost converter output was not successful in charging the battery. Although the voltage output from the boost converter met the EKG battery's requirements, we found that the extremely low current was not sufficient to indicate battery charging. Although a battery is a current sink and should accept any amount of current, our output current was too low to add significant charge to the battery over the time intervals in which the EKG checks battery level to determine if the battery is charging or not. An output current closer to the order of milliamps is desired to achieve significant battery charging.

7.1.3 Customer Needs Testing

In order to verify that the device met customer needs, measurements and user evaluations were performed. The wristband mass, width, and height off the wrist of the final prototype were measured and compared with those established in the PDS target range. These dimensions were measured with a Neiko 01407A digital caliper with an uncertainty of 0.02 [mm]. The mass was measured with an unknown model postal scale. To quantify aesthetics and comfort/ergonomics of wristband, participants not involved with the project wore the device for a period of 15 minutes and rated its aesthetic and ergonomic features relative to a standard wristwatch. A score of 1 is much worse than a standard wristwatch, 5 is equal to a standard wristwatch, and 10 is much better than standard wristwatch. Because the boost converter evaluation board would be replaced by an extremely small printed circuit board in the final product, the boost converter evaluation board was omitted from Customer Needs Testing.

Experimental Results:

Table 6: Wristband dimensions and mass.

Width [mm]	Height Off Wrist (at EKG) [mm]	Height Off Wrist (at Heat Sink) [mm]	Height Off Wrist (at wristband) [mm]	Mass (including charge cable) [g]
76.11	11.10	10.54	1.77	70

Table 7: Aesthetics and comfort/ergonomics ratings.

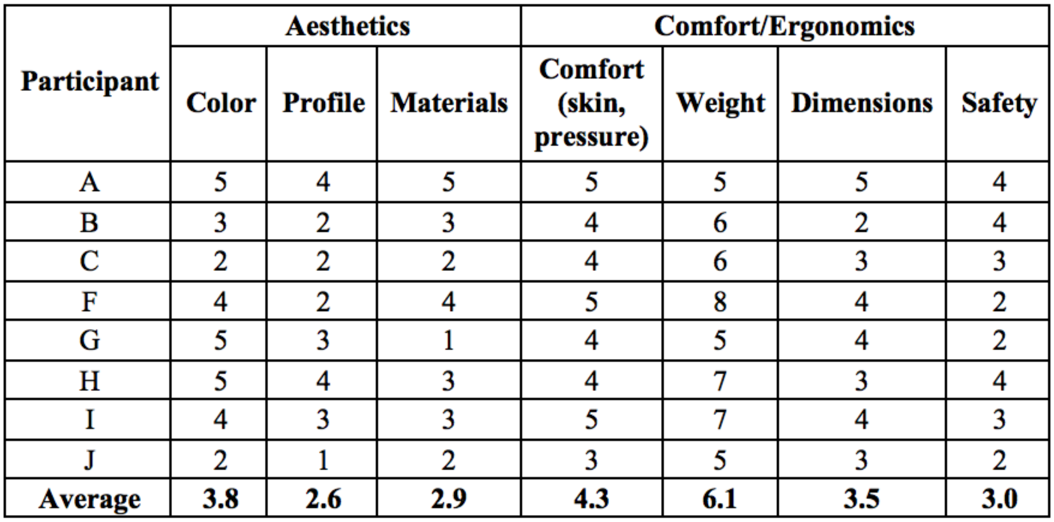

Participant	Aesthetics			Comfort/Ergonomics			
	Color	Profile	Materials	Comfort (skin, pressure)	Weight	Dimensions	Safety
A	5	4	5	5	5	5	4
B	3	2	3	4	6	2	4
C	2	2	2	4	6	3	3
F	4	2	4	5	8	4	2
G	5	3	1	4	5	4	2
H	5	4	3	4	7	3	4
I	4	3	3	5	7	4	3
J	2	1	2	3	5	3	2
Average	**3.8**	**2.6**	**2.9**	**4.3**	**6.1**	**3.5**	**3.0**

The device's width is significantly greater than the 50 [mm] specified in the PDS. This addition in size was necessary to accommodate the four TEMs and heat sinks needed for power requirements. The device's height is extremely close to the 10 [mm] specified in the PDS. The slight excess height at the heat sink is due to lack of precision in the method used for cutting heat sink pins. Although the EKG itself exceeds the height requirement by a millimeter, it is a stock item and its dimensions are out of our control. The mass of the wristband is much lower than the 200 [g] specified in the PDS. This is due to the lightweight materials that were used in the wristband.

Based off of the ratings received in aesthetic and comfort/ergonomic categories, it can be determined that users found the wristband to be less aesthetically pleasing and ergonomically comfortable than a standard wristwatch. The rather industrial profile and materials used in the wristband were not favorable among users. Overall, users found the device to be close in comfort to a standard watch; however, they were also displeased by the larger than normal width. Additionally, although users were not concerned about electrical safety, they were concerned about the heat sinks scratching themselves and surrounding objects. The weight of the prototype was a bright spot as users found it to feel lighter than a standard wristwatch.

7.1.4 Moisture and Durability Testing

Although moisture and durability tests were desirable to determine how much damage the device could withstand, these tests were not performed as the device is to be used for further testing and experimentation. Subjecting the device to impact and moisture could damage the electronic components inside, preventing them from use in further work.

Chapter 8

Cost Analysis

As it was stated in the budget section of Chapter 2, the proposed budget for this project was $\$1,875.00$. After completion of the project, a total of $\$1,330.38$ was spent on development of the wearable thermoelectric power generation wristband prototype. The most significant costs came from the purchase of TEMs. Many modules were damaged during testing, requiring more to be purchased for prototyping. The detailed overall project costs are seen below.

Table 8: Detailed project costs.

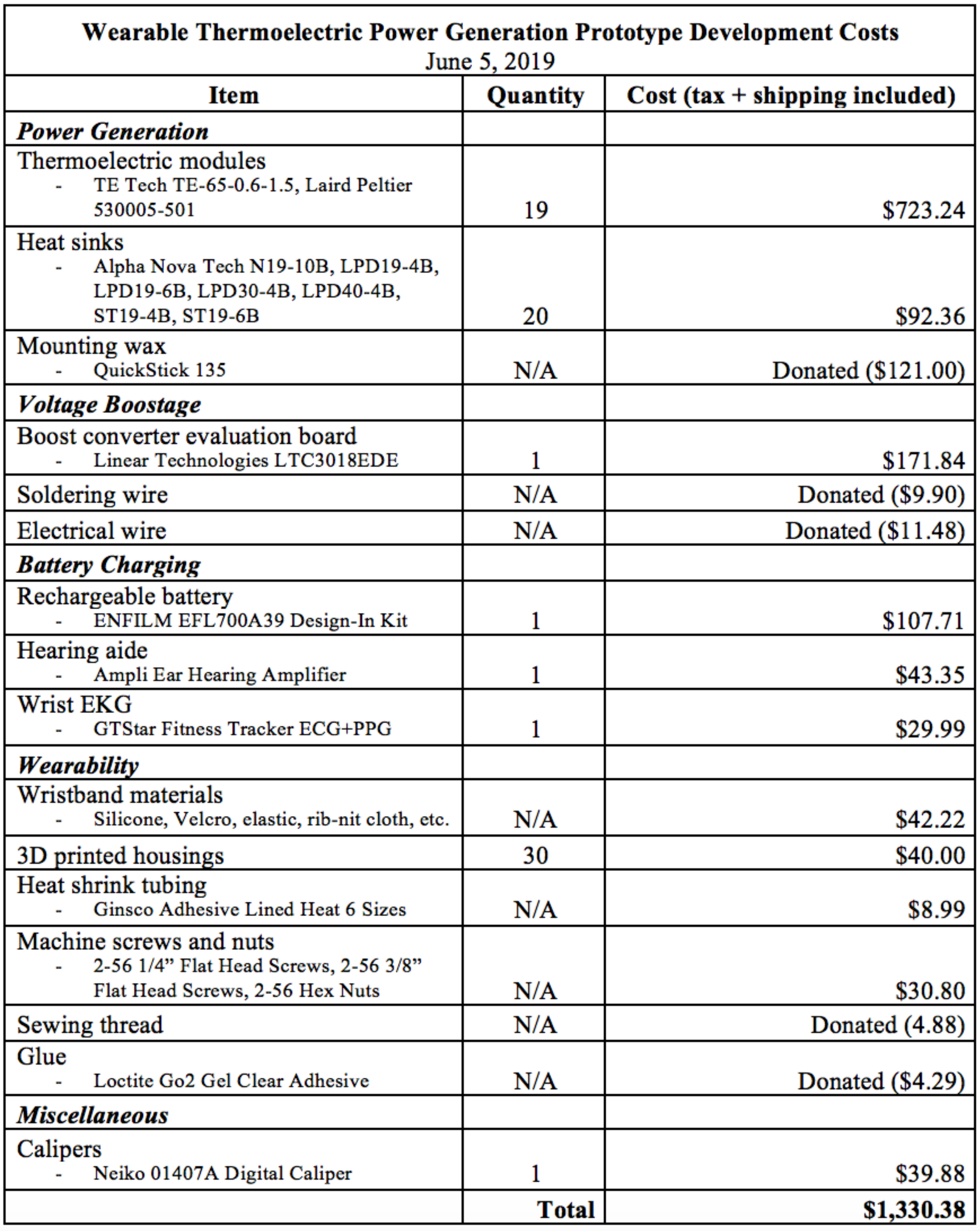

Wearable Thermoelectric Power Generation Prototype Development Costs
June 5, 2019

Item	Quantity	Cost (tax + shipping included)
Power Generation		
Thermoelectric modules - TE Tech TE-65-0.6-1.5, Laird Peltier 530005-501	19	$723.24
Heat sinks - Alpha Nova Tech N19-10B, LPD19-4B, LPD19-6B, LPD30-4B, LPD40-4B, ST19-4B, ST19-6B	20	$92.36
Mounting wax - QuickStick 135	N/A	Donated ($121.00)
Voltage Boostage		
Boost converter evaluation board - Linear Technologies LTC3018EDE	1	$171.84
Soldering wire	N/A	Donated ($9.90)
Electrical wire	N/A	Donated ($11.48)
Battery Charging		
Rechargeable battery - ENFILM EFL700A39 Design-In Kit	1	$107.71
Hearing aide - Ampli Ear Hearing Amplifier	1	$43.35
Wrist EKG - GTStar Fitness Tracker ECG+PPG	1	$29.99
Wearability		
Wristband materials - Silicone, Velcro, elastic, rib-nit cloth, etc.	N/A	$42.22
3D printed housings	30	$40.00
Heat shrink tubing - Ginsco Adhesive Lined Heat 6 Sizes	N/A	$8.99
Machine screws and nuts - 2-56 1/4" Flat Head Screws, 2-56 3/8" Flat Head Screws, 2-56 Hex Nuts	N/A	$30.80
Sewing thread	N/A	Donated (4.88)
Glue - Loctite Go2 Gel Clear Adhesive	N/A	Donated ($4.29)
Miscellaneous		
Calipers - Neiko 01407A Digital Caliper	1	$39.88
	Total	**$1,330.38**

The prototype itself costs $386.67, not including labor costs. The boost converter evaluation board was the most significant cost in producing the prototype. Boost converters and the circuit components that are needed to use them are very inexpensive; however, an evaluation board was necessary to tune the boost converter circuit to our project's needs, and it is much more expensive. In a final product, the boost converter circuit would be printed on a circuit board for a much lower cost. Bulk order purchasing could also significantly reduce the cost of TEMs, heat sinks, and wristband materials. The detailed prototype costs are seen below.

Table 9: Detailed prototype costs.

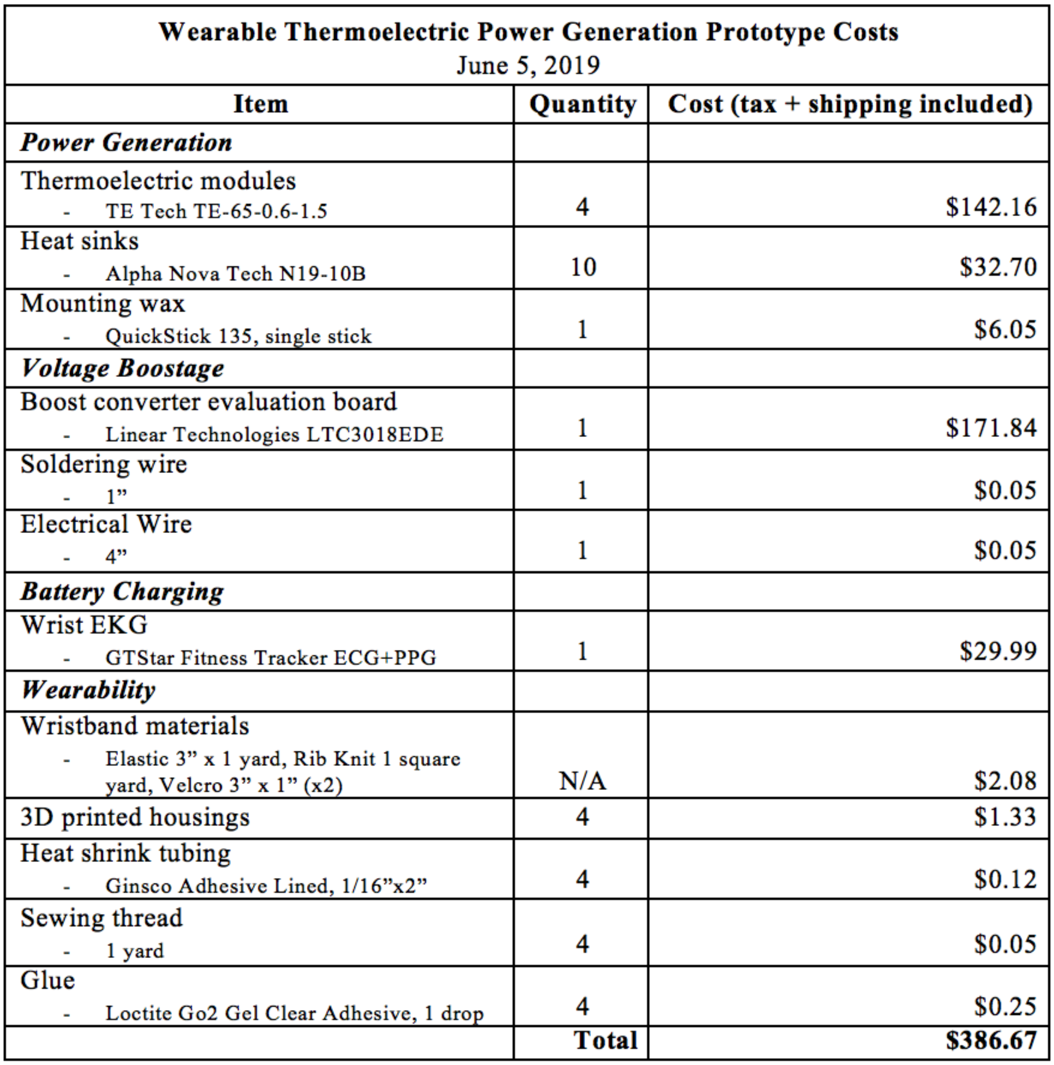

Wearable Thermoelectric Power Generation Prototype Costs
June 5, 2019

Item	**Quantity**	**Cost (tax + shipping included)**
Power Generation		
Thermoelectric modules - TE Tech TE-65-0.6-1.5	4	$142.16
Heat sinks - Alpha Nova Tech N19-10B	10	$32.70
Mounting wax - QuickStick 135, single stick	1	$6.05
Voltage Boostage		
Boost converter evaluation board - Linear Technologies LTC3018EDE	1	$171.84
Soldering wire - 1”	1	$0.05
Electrical Wire - 4”	1	$0.05
Battery Charging		
Wrist EKG - GTStar Fitness Tracker ECG+PPG	1	$29.99
Wearability		
Wristband materials - Elastic 3” x 1 yard, Rib Knit 1 square yard, Velcro 3” x 1” (x2)	N/A	$2.08
3D printed housings	4	$1.33
Heat shrink tubing - Ginsco Adhesive Lined, 1/16”x2”	4	$0.12
Sewing thread - 1 yard	4	$0.05
Glue - Loctite Go2 Gel Clear Adhesive, 1 drop	4	$0.25
	Total	**$386.67**

Chapter 9

Patent Search

9.1 Executive Summary

Through our patent investigation for our device we concluded that our housing is the basis for our patentable design. Our housing uniquely fastens together a thermoelectric module and heat sink using 3D printed plastic. The novel portions of our design include the ridges used to hold the heat sink in place, bars for easy connectability in series or parallel patterns, and the robustness of the housing which protects and electrically insulates delicate thermoelectric module leads.

9.2 Scope of Design Concept

Our project's focus is creating a wearable device capable of charging a bio-medical sensor (e.g. a wearable EKG) using body heat. In order to do so, the device utilizes thermoelectric power generation technology, specifically thermoelectric modules (TEMs), to convert excess body heat into a power output. However, more than just excess heat, the TEMs need to experience a temperature difference across its two contact sides in order to generate power. This implies that the TEM has both a hot and cold side, while also indicating a clear need for heat dissipation on the non-skin (or cold) side of the TEM. To dissipate heat from the cold side and maintain a sufficient temperature difference, heat sinks are implemented into the wearable device in conjunction with the TEMs.

The nature of the TEM and heat sinks roles of power generation and heat dissipation essentially dictate the orientation of the devices mechanical design. In order to achieve sufficient heat flux from skin, there must be consistent and firm contact between the TEMs hot side and the users wrist/ forearm. Simultaneously, there must be consistent and firm contact between the TEMs cold side and the the base of the heat sink to ensure sufficient heat dissipation. This indicates a clear need for a reliable method of securing the heat sink to the cold side of the TEM. We explored multiple different methods including velcro, wax adhesives, and various 3-D printed housing designs.

After performance tests, we determined that a single piece, 3-D printed housing design would not only secure the device components reliably, but allowed for optimal performance of both the heat sink and TEM. The specific design of this TEM-Heat Sink housing allows for sufficient free convection across the heat sink, holds sufficient contact between the heat sink and TEM, and has a relatively small form factor. These three housing characteristics allow for increased heat transfer and dissipation as well as increased modularity and wearability of the overall device which are all critical to the performance of the overall device. These specific design considerations are the reasons why the TEM-Heat Sink housing design is so important to the overall functionality of our device and essentially, the reason we chose to explore patents for the housing design.

9.3 Invention Description

The TEM-heat sink housing we designed was an invention unique to our device with the capability to be adapted to a number of different applications. Titled "Modular TEM-Heat Sink Interface," the housing's main purpose is to hold the TEM and heat sink together with sufficient contact for conduction. It must do this while allowing free air to pass over the heat sink for natural convection, having a low profile, and allowing for easy connection to other housings and integration into a wearable device.

The problem of holding a TEM and heat sink together at a scale of this size (20mm x 20mm heat sink and 12mm x 13mm TEM) is difficult because good contact pressure between the TEM and heat sink must be ensured without obstructing the exposed side of the TEM or heat sink. Additionally the connected TEM and heat sink must be comfortably wearable. In small scale heat sink applications, such as removing heat from a circuit board, thermal adhesives are used to fix heat sinks to electrical components. However, a thermal adhesive alone would not be sufficient in our case as that does not address the wearability requirement.

In order to meet these design requirements, we designed a plastic housing that holds the TEM on three sides, allowing its leads to be accessed, and has a recess on its top where the heat sink is placed. A thermally conductive adhesive, mounting wax in our case, is used to adhere the heat sink and TEM and hold them in place within the housing. The housing holds the heat sink using the ridge between the top and bottom plates of the heat sink which allows the heat sink to easily slide into the housing. In order to allow for wearability, circular bars are fixed to two opposite sides of the housing (similar to those seen on a watch face). These can be used to connect multiple housings together via a band or to fix the housings into an article of clothing or accessory such as a wristband, headband, T-shirt, or backpack strap. In the case of our device, we used the bars to sew housings into an elastic wristband. Within the small market of wearable thermoelectric power generation, products have methods of holding TEMs and heat sinks together that are specific to those devices. For example, the Matrix Powerwatch uses its external aluminum body as the heat sink and the TEM is in contact with this surface [20].

Our housing has the advantage of adaptability, allowing it to be used in a number of wearable thermoelectric power generation applications. The housings can be arranged connected in a line to be worn in a wristband or headband, or a large number can be connected in a grid pattern on a compression T-shirt or arm sleeve. By allowing free access to the TEM leads in our housing design, complex circuits can be arranged with the TEMs without modification of the housings. Additionally, our housings can also be used in wearable thermoelectric heating and cooling applications if power is supplied to the modules rather than generated by them. The housings could be used to provide heat inside gloves or cooling on the back of the neck in a T-shirt.

There are multiple commercialization opportunities for the Modular TEM-Heat Sink Interface. It could be sold as a standalone item that comes in multiple sizes for different TEMs and heat sinks. The buyer could then use this technology for any desired application. The technology could also be licensed to manufacturers for use in products, which would allow manufacturers to make design modifications to the housing, ensuring optimum functionality.

The Modular TEM-Heat Sink Interface was invented by Dylan Santana and Joseph O'Bryan on March 21, 2018. It was first manufactured via 3D print and used in wristband prototyping on March 23, 2018. It was publicized April 14, 2018 on Santa Clara University Preview Day.

9.4 Mechanical Drawings

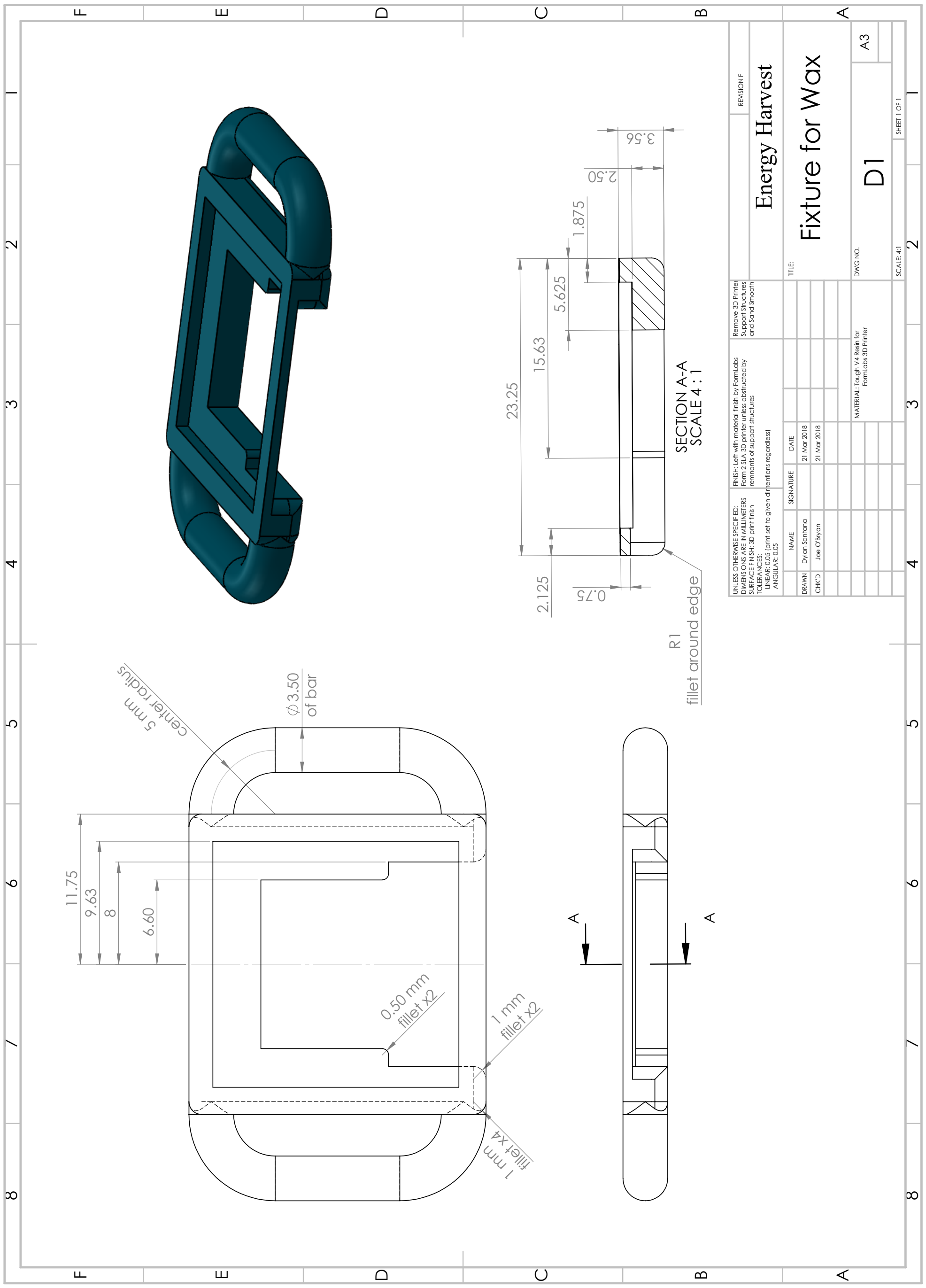
SECTION A-A
SCALE 4 : 1
3.56
2.50
1.875
5.625
15.63
23.25
2.125
0.75
R1
fillet around edge
Ø3.50
of bar
5 mm
center radius
11.75
9.63
8
6.60
0.50 mm
fillet x2
1 mm
fillet x2
1 mm
fillet x4
A
A
UNLESS OTHERWISE SPECIFIED:
DIMENSIONS ARE IN MILLIMETERS
SURFACE FINISH: 3D print finish
TOLERANCES:
LINEAR: 0.05 (print set to given dimentions regardless)
ANGULAR: 0.05
FINISH: Left with material finish by FormLabs Form 2 SLA 3D printer unless obstructed by remnants of support structures
Remove 3D Printer Support Structures and Sand Smooth
REVISION F
Energy Harvest
NAME
SIGNATURE
DATE
DRAWN
Dylan Santana
21 Mar 2018
CHK'D
Joe O'Bryan
21 Mar 2018
TITLE:
Fixture for Wax
MATERIAL: Tough V4 Resin for FormLabs 3D Printer
DWG NO.
D1
A3
SCALE: 4:1
SHEET 1 OF 1
A
B
C
D
E
F
1
2
3
4
5
6
7
8

Figure 32: Detailed Mechanical Drawing of Modular TEM-Heat Sink Interface.

9.5 Patent Classification

The scope of our device puts the concept of our project within a few possible patent classifications based on our different subsystems. These patent classes are: Closure Fasteners, Electricity: Batteries Charging or Discharging, and Batteries: Thermoelectric and Photovoltaic[22].

The patent classification that our assembly housing, as described earlier in this passband, most closely falls under is patent class 292, Closure Fasteners. The patent class covers everything that has to do with holding two or more materials or devices together. Our assembly housing holds together a thermoelectric module and a heat sink with intermediary thermal wax between the two. The housing which was uniquely designed using computer aided design software then 3D printed over several iterations acts to maintain this fit using structural pressure while also having side bars for easy interconnection. The patent class subclasses which most closely resembles our concepts include: portable clamps, and bendable securers[22].

The patent class that most closely fits our battery charging subsystem concepts is patent class 320, Electricity: Batteries Charging or Discharging [22]. This patent class covers novel methods of both charging and discharging. Our device uniquely harvests thermal heat in order and regulates the output using a boost converter to charge the battery of a mobile electrocardiograph monitor. Similar patent subclass categories within this patent class include: thermal cell source, and battery charging with pulsed DC-DC converter[22].

Along a similar vein, the concepts in our thermal harvesting and voltage boost subsystems fit into patent class 136, Batteries: Thermoelectric and Photovoltaic [22]. This patent class covers devices and phenomena relating to both thermoelectric and photovoltaic energy generation. Our device uniquely explored the effect of using multiple thermoelectric module combined with serial and parallel connections. For our final prototype we were able to determine that using a combination of four thermoelectric modules connected with both electrical connection types is idyllic for mobile energy harvesting. Similar patent subclass categories include: Peltier effect devices, thermoelectric processes, and thermoelectrics having housing, mounting, or support[22].

9.6 Review of Prior Art

US20060151021A1 is the patent for thermoelectric module being used for power generation. It describes a potted TEM with a series of N-type and P-type bismuth telluride-based semiconductor legs. The patent covers a variable thickness of 10-100 microns and a with of 10-100 microns, and length of 100-500 microns. The alternating N-type and P-type legs are electrically connected in series and thermally connected in parallel so that the temperature differential between the top and bottom plates results in the generation of power [19]. This patent is extremely important to our project since it defines the TEM's available on the market from which to generate power from. Our device differs form this general patent however in the optimization of power generation with the appropriately optimized heat sink, and the electrical arrangement of these TEMS in series and in parallel. In future work, our method to optimize TEM dimensions as to find a maximum sea beck coefficient can lie outside of these patented bounds depending on the final size of the final TEM.

US8527038B2 is the patent for a wired EKG that delivers data to a wrist or arm worn device. This device is battery powered and can read out the EKG signal which is plugged into the processing unit of the wristwatch like device. This device will prompt the user when the battery needs to be replaced and when the system needs to be reset. For the purposes of our device, we chose to power a wearable EKG which does not rely on wired electrodes rather PPG and EKG chip based technology. As these surrogates continue to develop and become clinically translated, they will continue the their trend and overtake the wired electrode gold standard. This will allow for the enhanced wear ability and comfort of the user. The device we chose can also transfer the data to an app enabled device to process the EKG signal. This allows the processed signal to be easily exported and shared. This patented device can also transfer data through wifi to external devices, or through the use of a serial port. The shortcomings are in the limited processing power of the wearable device. Devices which process data externally can benefit form a greater processing power of said external device. Another difference of our device is the powering of the EKG. The patented device initiated a sequence when the battery is to be replaced; first the user is prompted, then the memory is saved, the monitoring stops, the battery is replaced, and monitoring and connection are restored again. Our TEM based power system will eliminate the need to replace the battery and as a result break the continuity of the device monitoring [12].

US20140096807A1 is the patent pending titled “Thermoelectric assembly using a cartridge support fixture” for a TEM fixture or casing that allows the TEM to move relative to temperature changes in the system. The Abstract of the pending patent reads, “A thermoelectric power generator (TEG) assembly and a method of fabrication are provided. The TEG assembly includes at least one thermoelectric (TE) module, a casing containing the at least one TE module, and at least one support fixture mechanically coupling the at least one TE module to the casing. The at least one support fixture is coupled to the at least one TE module. The at least one portion of the at least one TE module is configured to move relative to the casing in response to temperature-induced dimensional changes of at least a portion of the at least one TE module or at least a portion of the casing.” [15]. The device is similar to our in that it is a patent casing or fixture that holds the TEM into place for a particular reason. The difference is its use. The fixture called Modular TEM-Heat

Sink Interface is an interface structure for holding the TEM and heat sink together in consistent and reproducible arrangements, with consistent and reproducible thermal characteristics. This differs significantly from the claims of US20140096807A1.

US6438964B1 is a patent granted for a device titled “Thermoelectric heat pump appliance with carbon foam heat sink.” It is a device designed to use the Peltier effect to heat or cool a part of a person’s body with thermoelectric modules. The Abstract reads, “A personal thermoelectric Peltier effect heating and cooling device for heating or cooling a portion of a user’s body utilizes a porous carbon foam heat sink secured to one surface of a Peltier thermovoltaic member. The heat sink is formed of a thermally conductive open cell foam medium through which air can pass and is partially enclosed by a shroud and a surrounding air filter...An on/off switch on the enclosure selectively energizes the air pump and the Peltier thermovoltaic member. A polarity reversing switch on the enclosure supplies selected polarized electrical energy to the Peltier thermovoltaic member for cooling or heating.” [7]. The device described utilized a sort of fixture that holds the TEM and heat sink, however this is a fully covered casing around the electronics containing the thermoelectric assembly. The Modular TEM-Heat Sink Interface differs in that it is placed such that the material holds the sides of the TEM and heat sink, allowing the thermoelectric module “hot side” and the heat sink to be fully exposed to the skin and air, respectively. The purpose of the the device described in US6438964B1 is significantly unlike that of the Modular TEM-Heat Sink Interface developed by the wearable thermoelectric power generation team.

Copies of these patents can be found in the Appendix

9.7 Conclusion

The housing for our heat sink and thermoelectric module assemblies is the most patentable concept found in our project. In order to patent this housing we would need to isolate the unique design features for the housing. Specifically, the ridges used to hold the heat sink and the body shape of the housing which protects and fastens the assembly in place while allowing for serial and parallel configurations. These must be demonstrated as being completely singular in comparison to existing wearable energy harvesting device housings. Other areas of possible patents related to our charging method and circuit configurations for charging a battery when boosting multiple thermoelectric modules.

Chapter 10

Engineering Standards and Realistic Constraints

10.1 Cost

The product must keep the buyer in mind at every stage of its use, including the initial purchase. Although health insurance and healthcare are available in many developed countries that can mitigate the cost of this device, we need to take into consideration buyers living under governments that do not provide assistance or locations where reasonable health insurance is hard to obtain. Being used to primarily power medical devices, it is understood that the buyers may already be burdened by the cost of healthcare or by their ailment itself, and the added stress of a device out of budget that will increase the quality of their recovery is unnecessary. Eliminating wasted costs on unnecessary components or unnecessary quality enhancements can make it affordable to more individuals needing a locally generated low-voltage output for a medical device. As the product is iterated through more versions, the most unnecessary components can be analyzed and their necessity called into question. Repeating this design process increases the cost effectiveness of the product.

10.2 Health and Safety

Our main priority with the development of the device and its implementation with other technologies is the safety of the user, engineers developing the technology, manufacturers, and all others involved in the production, sale, and use of Wearable Thermoelectric Power Generation. Every step of the way, the safety of all involved was prioritized above anything else. In terms of the safety of the user, the electrical components are insulated and the product is built with total security of the components, with minimal possibility of a break in electrical travel or physical break of a component or the system. Proper safety procedure was followed while developing and constructing the prototype by all involved in this process.

10.3 Manufacturability and Repairability

Increasing manufacturability means not carelessly requiring abstract means of producing simple products. This is important to wearable thermoelectric power generation because this can decrease the cost of the end product drastically. Simple injection-molding plastic parts, or easy machine-automated fabric production is necessary for full cost efficiency. Although the first iterations of the device will not meet these desired goals, any marketable production iteration would meet these goals and ensure cost is low while maintaining full efficient function of the device.

Repairability is defined by how easy it is for a broken or non-functioning component to be replaced with as little help from the company's support as possible. Like a LEGO^{TM} set, the components should be as "plug-and-play" replaceable and and repairable as possible. This is important because this allows for the product to reach much further as there is less of a need for the company to support the buyer after the sale. It also reduced the cost of the repair, replacing only one single part rather than the entire non-functioning product. This is being achieved with the Modular TEM-Heat Sink Interface housing fixture for the TEM-heat sink assembly. The single-piece assemblies have bars on the side for easy detachment and reattachment for replacement of an assembly that may be damaged or non-functional. This increases the speed of repairs and will bring piece-of-mind to the user for there is less worry of repairs that would cost more than the total worth of the device.

10.4 Sustainability

One of the most attractive benefits of thermoelectric power generation is the minimal waste produced. The power is not generated from chemical reactions like most other forms of generation, therefore no waste product is produced by the thermoelectric modules. Heat flow produces no carbon dioxide or radioactivity. The amount of waste that is produced, however, is comprised of discarded thermoelectric modules and electrical components. The wearable thermoelectric power generation team followed all local, state, federal, and international guidelines, as well as those given by the manufacturer, for all electronics. A definitive plan for managing waste would be devised in the event of large scale manufacturing. Regardless, the minimal amount of waste is unparalleled for small scale generation, and wearable thermoelectric power generation hopes to maintain this level of sustainability in all parts of the development, production, and maintenance processes for the product.

10.5 Ethical Considerations

The ethical implications of the device can be very significant depending on the device being charged with wearable thermoelectric power generation. Medical devices such as EKGs, insulin pumps, glucose monitors, hearing aides, and others have significant impacts in the daily lives of users, and although our goal is to increase quality of life and access to medical devices through thermoelectric power generation, should our device fail while in use, it should not pose a danger to users. Fail-safes such as a backup battery would be in place to prevent users from being without their potentially life-saving devices in the event of a thermoelectric power generation failure.

In the event of producing our device to be distributed to medical device users, the team would work with the American Red Cross, the U.S. Department of Health and Human Services, and member groups of the World Health Organization in terms of standards to be set for safe use of our device. Additionally, with recommendation from the previously mentioned groups, clear understanding of the limitations of the device, its possible dangers, and ways of properly using the device will be communicated to every user to minimize risk.

Chapter 11

Conclusion

11.1 Summary

Wearable medical devices offer vast benefits to users that range from improving quality of their lives to saving their lives. However, powering these medical devices is a constant concern as battery replacement and frequent charging is necessary, limiting the freedom of users. Additionally, lack of access to electricity prevents a significant portion of the world from benefiting from wearable medical devices as they are unable to provide power for them. We are developing a wearable thermoelectric power generator in the form of a wristband that charges the battery of a medical device in order to increase medical device users peace of mind and freedom and grant wearable medical device access to those who live without electricity.

Our design solution utilizes thermoelectric technology to generate off-the-grid electric power from users' body heat. Body heat from the wrist heats up the bottom of thermoelectric modules while heat sinks dissipate heat away from the top of modules. This temperature difference across the modules generates electricity which is boosted to 4.1 [V] through the use of a boost converter, and this electrical output is used to charge the battery of a wearable medical device. We are developing a prototype that charges a wrist EKG which has successfully generated the 4.1 [V] required by the EKG battery in room temperature or colder conditions. Further development and optimization of thermoelectric module design and heat dissipation method is necessary to generate a current sufficient for useful battery charging. Significant design challenges were faced due to the limitations of available thermoelectric modules on the market, the size constraints for our device, and the interdependent electrical input requirements for our boost converter.

11.2 Future Improvements

Regarding future design improvements in order to achieve more consistent performance, the first and most effective action to be taken would be further optimization of the power generation subsystem, specifically the TEM model used within it. However, due to market limitations, further B factor optimization is only attainable through the design of a custom TEM. By designing the TEM and choosing its geometric characteristics, our team would truly have control over the performance characteristics of the module. The plot shown in Figure 33 is the same plot from Figure 14 with number of leg pairs (N) taken into consideration as well. As N decreases, the theoretical power output of the TEM increases thus showing the module's performance can be directly optimized by adjusting its geometric characteristic. By designing a custom TEM, we could not only perfectly match the desired effective B factor but could further increase the TEM's output by adjusting geometries while maintaining the desired B_{eff} value.

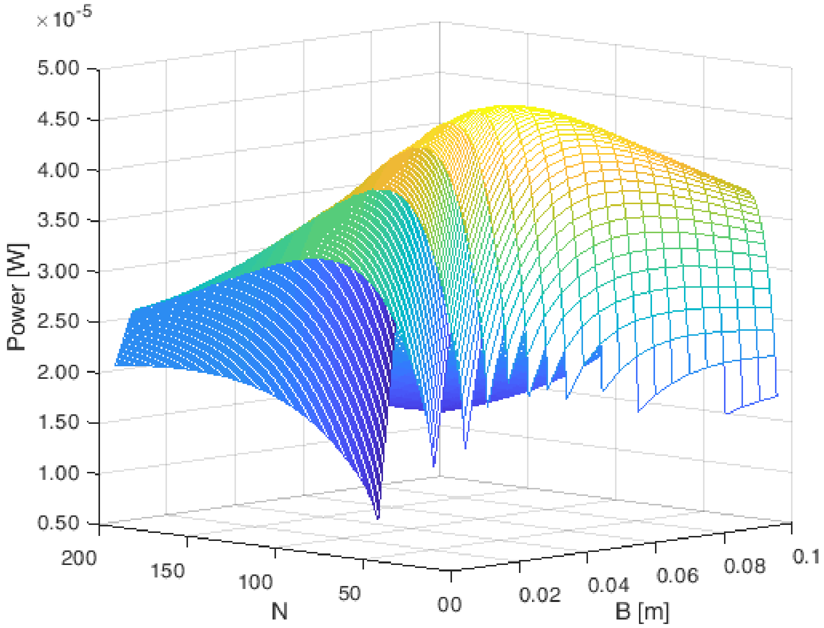

Figure 33: TEM theoretical power output versus N versus B_{eff}, courtesy of Tom Watson, SCU.

An additional future change is to increase TEM performance with improved heat dissipation. Increasing the height or base area of the current heat sinks would certainly violate size constraints. However, the following more creative heat dissipation methods could improve heat dissipation while reducing overall profile and increasing aesthetic value of the device:

1. Integrate the heat sinks into body of wristband. Custom machined aluminum parts could make up significant segments of the wristband body, rather then full elastic, and detailing of these parts, such as surface texture and geometry, could be optimized to dissipate heat.

2. Explore flexible heat sinks. Copper mesh or thin plates can be used to spread heat from the TEMs over a larger area, and flexible woven metal “fabrics” could be placed on top of this to dissipate heat from these copper surfaces.

11.3 Final Thoughts

Overall, development of our wearable thermoelectric power generation wristband prototype made significant progress towards the goal of powering a wearable medical device with body heat through thermoelectric technology, and it allowed us to learn much about the relatively unexplored field of wearable thermoelectric power generation and the engineering design process in general. We believe that our current progress and implementation of suggested future improvements make wearable thermoelectric power generation a viable option for charging a medical device without grid-power, making a significant impact in the lives of medical device users.

References

[1] "Access to electricity (% of population)." 2016, from `https://data.worldbank.org/indicator/EG.ELC.ACCS.ZS`.

[2] Agarwal, Tarun, n.d., "What is a Heat Sink and its Importance." From `https://www.elprocus.com/different-types-of-heat-sinks-and-their-importance/`.

[3] "Breif History of Thermoelectrics." N.d.,`http://www.thermoelectrics.caltech.edu/thermoelectrics/history.html`

[4] "Cardiovascular Disease." 2017, from `http://www.who.int/cardiovascular$_$diseases/en/`.

[5] "The Difference Between TEC and TEG" N.d., from `http://www.europeanthermodynamics.com/news/difference-between-TEC-and-TEG`

[6] Francioso, L., De Pascali, C., Sglavo, V., Grazioli, A., Masieri, M., and Siciliano, P, 2017, "Modeling, Fabrication, and Experimental Testing of a Heatsink-free Wearable Thermoelectric Generator," Energy Conversion & Management, Vol. 145, pp. 204-213.

[7] Giblin, P., 2001. "Thermoelectric heat pump appliance with carbon foam heat sink," U.S. Patent US6438964B1.

[8] "Heat Sink Considerations." N.d., from `https://thermal.ferrotec.com/technology/thermoelectric-reference-guide/thermalref05/`.

[9] Huang, S. and Xu, X, 2016, Parametric Optimization of Thermoelectric Generators for Waste Heat Recovery. "Journal of Electronic Materials," Vol. 45 No. 10, pp. 5213-5222.

[10] "LTC3108 Ultralow Voltage Step-Up Converter and Power Manager." N.d., from `http://www.analog.com/media/en/technical-documentation/data-sheets/3108fc.pdf`.

[11] "Maximum Power Transfer."N.d., from `https://www.electronics-tutorials.ws/dccircuits/dcp$_9$.html`

[12] Moon, J., Visser, H., and Hunt, R., 2013, "Body-worn Vital Sign Monitor." U.S. Patent US8527038B2.

[13] "Passive Heat Sink." N.d., from `https://www.micforg.co.jp/en/cat$_$pass.html`..

[14] Pietrzyk, K., Ohara, B., Watson, T., Gee, M., Avalos, D., and Lee, H., 2016, "Thermoelectric module design strategy for solid-state refrigeration." Elsevir Energy Vol. 114, pp. 823-832.

[15] Renalli, M., 2014, "Thermoelectric assembly using a cartridge support fixture". U.S. Patent US20140096807A1.

[16] "Seiko Thermic." *Seiko.* N.d., From `https://museum.seiko.co.jp/en/collections/clock$_$watch/category3/collect041.html`.

[17] Siddique, A., Mahmud, S., and Heyst, B., 2017, A Review of the State of the Science on Wearable Thermoelectric Power Generators (TEGs) and their Existing Challenges. Renewable and Sustainable Energy Reviews, Vol. 73, pp. 730-744.

[18] Siouane, S., Jovanovic, S., and Poure, P. Equivalent Electrical Circuits of Thermoelectric Generators under Different Operating Conditions. Energies Vol. 10 No. 3 (2017): pp. 1-15.

[19] Stark, I., 2009, "Low Power Thermoelectric Generator." U.S. Patent US20060151021A1.

[20] "Technology: Thermal Engineering." N.d., From `https://www.matrixindustries.com/technology/`..

[21] "TE-65-0.6-1.5" N.d., from `https://tetech.com/product/te-65-0-6-1-5/`

[22] "US Classes by Number with Title". N.d., from `https://www.uspto.gov/web/patents/classification/selectnumwithtitle.htm`

[23] Wang, C., Hung, C., and Chen, W., 2010, "Design of Heat Sink for Improving the performance of Thermoelectric Generators Using Two-Stage Optimization." Sustainable Energy and Environmental Protection Vol. 39 No. 1,: pp. 236-245.

[24] Weng, S.F., Reps, J., Kai, J., Garibaldi, J.M., Qureshi, N., 2017, "Can machine-learning improve cardiovascular risk prediction using routine clinical data?" PLoS ONE. Vol. 12(4):e0174944.

Appenidx A: Selection Matrices

The matrix below lists the weightings of importance for different factors relating to each subsystem.

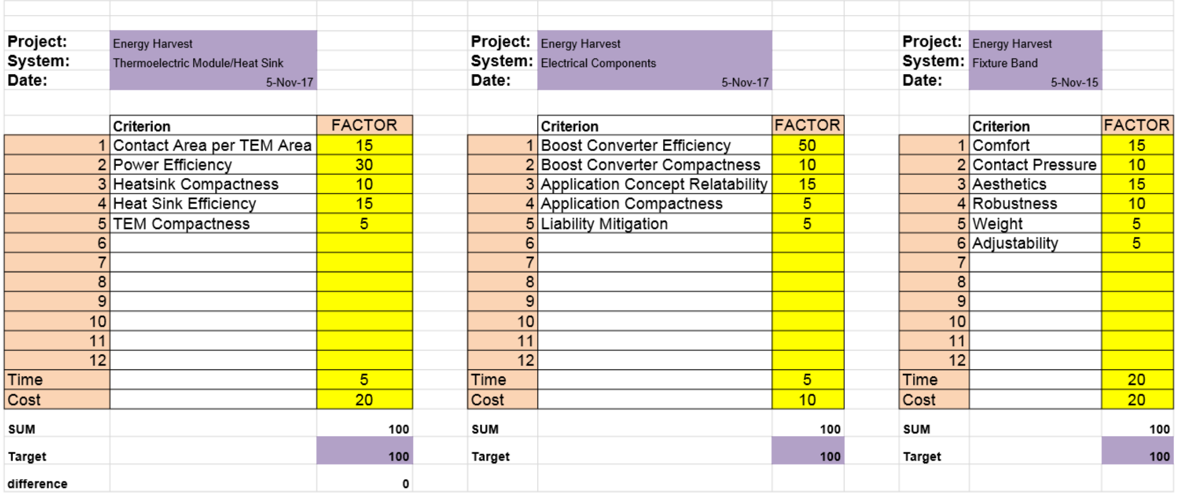

Project: Energy Harvest
System: Thermoelectric Module/Heat Sink
Date: 5-Nov-17

	Criterion	FACTOR
1	Contact Area per TEM Area	15
2	Power Efficiency	30
3	Heatsink Compactness	10
4	Heat Sink Efficiency	15
5	TEM Compactness	5
6		
7		
8		
9		
10		
11		
12		
Time		5
Cost		20
SUM		100
Target		100
difference		0

Project: Energy Harvest
System: Electrical Components
Date: 5-Nov-17

	Criterion	FACTOR
1	Boost Converter Efficiency	50
2	Boost Converter Compactness	10
3	Application Concept Relatability	15
4	Application Compactness	5
5	Liability Mitigation	5
6		
7		
8		
9		
10		
11		
12		
Time		5
Cost		10
SUM		100
Target		100

Project: Energy Harvest
System: Fixture Band
Date: 5-Nov-15

	Criterion	FACTOR
1	Comfort	15
2	Contact Pressure	10
3	Aesthetics	15
4	Robustness	10
5	Weight	5
6	Adjustability	5
7		
8		
9		
10		
11		
12		
Time		20
Cost		20
SUM		100
Target		100

Figure 34: Subsystem factor weighting matrix.

The matrices below list the rankings calculated from the factors of importance from Figure 34 along with individual factors ranging for each concept of the subsystem.

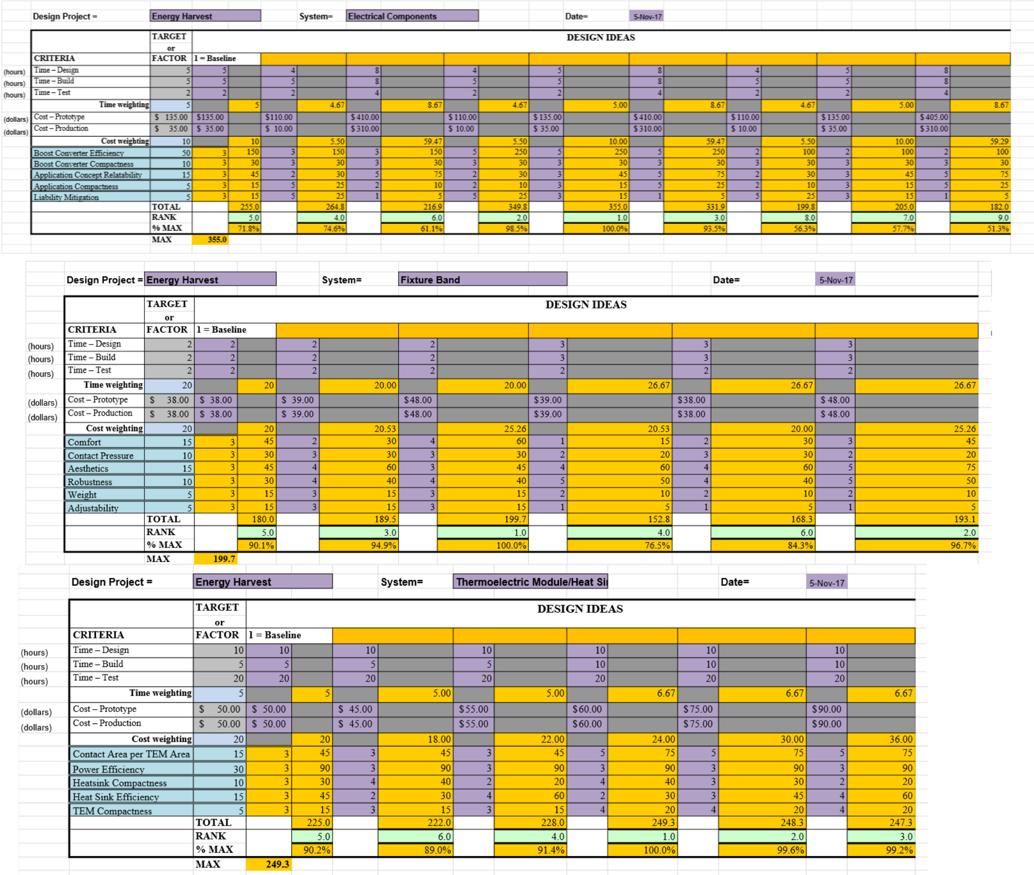

Design Project = Energy Harvest System= Electrical Components Date= 5-Nov-17

DESIGN IDEAS

	CRITERIA	TARGET or FACTOR	1 = Baseline																	
(hours)	Time – Design	5	5		4		8		4		5		8		4		5		8	
(hours)	Time – Build	5	5		5		8		5		5		8		5		5		8	
(hours)	Time – Test	2	2		2		4		2		2		4		2		2		4	
	Time weighting	5		5		4.67		8.67		4.67		5.00		8.67		4.67		5.00		8.67
(dollars)	Cost – Prototype	$ 135.00	$135.00		$110.00		$ 410.00		$ 110.00		$ 135.00		$ 410.00		$ 110.00		$ 135.00		$ 405.00	
(dollars)	Cost – Production	$ 35.00	$ 35.00		$ 10.00		$ 310.00		$ 10.00		$ 35.00		$ 310.00		$ 10.00		$ 35.00		$ 310.00	
	Cost weighting	10		10		5.50		59.47		5.50		10.00		59.47		5.50		10.00		59.29
	Boost Converter Efficiency	50	3	150	3	150	3	150	5	250	5	250	5	250	2	100	2	100	2	100
	Boost Converter Compactness	10	3	30	3	30	3	30	3	30	3	30	3	30	3	30	3	30	3	30
	Application Concept Relatability	15	3	45	2	30	5	75	2	30	3	45	5	75	2	30	3	45	5	75
	Application Compactness	5	3	15	5	25	2	10	2	10	3	15	5	25	2	10	3	15	5	25
	Liability Mitigation	5	3	15	5	25	1	5	5	25	3	15	1	5	5	25	3	15	1	5
		TOTAL		255.0		264.8		216.9		349.8		355.0		331.9		199.8		205.0		182.0
		RANK		5.0		4.0		6.0		2.0		1.0		3.0		8.0		7.0		9.0
		% MAX		71.8%		74.6%		61.1%		98.5%		100.0%		93.5%		56.3%		57.7%		51.3%
		MAX	**355.0**																	

Design Project = Energy Harvest System= Fixture Band Date= 5-Nov-17

DESIGN IDEAS

	CRITERIA	TARGET or FACTOR	1 = Baseline											
(hours)	Time – Design	2	2		2		2		3		3		3	
(hours)	Time – Build	2	2		2		2		3		3		3	
(hours)	Time – Test	2	2		2		2		2		2		2	
	Time weighting	20		20		20.00		20.00		26.67		26.67		26.67
(dollars)	Cost – Prototype	$ 38.00	$ 38.00		$ 39.00		$48.00		$39.00		$38.00		$ 48.00	
(dollars)	Cost – Production	$ 38.00	$ 38.00		$ 39.00		$48.00		$39.00		$38.00		$ 48.00	
	Cost weighting	20		20		20.53		25.26		20.53		20.00		25.26
	Comfort	15	3	45	2	30	4	60	1	15	2	30	3	45
	Contact Pressure	10	3	30	3	30	3	30	2	20	3	30	2	20
	Aesthetics	15	3	45	4	60	3	45	4	60	4	60	5	75
	Robustness	10	3	30	4	40	4	40	5	50	4	40	5	50
	Weight	5	3	15	3	15	3	15	2	10	2	10	2	10
	Adjustability	5	3	15	3	15	3	15	1	5	1	5	1	5
		TOTAL		180.0		189.5		199.7		152.8		168.3		193.1
		RANK		5.0		3.0		1.0		4.0		6.0		2.0
		% MAX		90.1%		94.9%		100.0%		76.5%		84.3%		96.7%
		MAX	**199.7**											

Design Project = Energy Harvest System= Thermoelectric Module/Heat Si Date= 5-Nov-17

DESIGN IDEAS

	CRITERIA	TARGET or FACTOR	1 = Baseline											
(hours)	Time – Design	10	10		10		10		10		10		10	
(hours)	Time – Build	5	5		5		5		10		10		10	
(hours)	Time – Test	20	20		20		20		20		20		20	
	Time weighting	5		5		5.00		5.00		6.67		6.67		6.67
(dollars)	Cost – Prototype	$ 50.00	$ 50.00		$ 45.00		$55.00		$60.00		$75.00		$90.00	
(dollars)	Cost – Production	$ 50.00	$ 50.00		$ 45.00		$55.00		$60.00		$75.00		$90.00	
	Cost weighting	20		20		18.00		22.00		24.00		30.00		36.00
	Contact Area per TEM Area	15	3	45	3	45	3	45	5	75	5	75	5	75
	Power Efficiency	30	3	90	3	90	3	90	3	90	3	90	3	90
	Heatsink Compactness	10	3	30	4	40	2	20	4	40	3	30	2	20
	Heat Sink Efficiency	15	3	45	2	30	4	60	2	30	3	45	4	60
	TEM Compactness	5	3	15	3	15	3	15	4	20	4	20	4	20
		TOTAL		225.0		222.0		228.0		249.3		248.3		247.3
		RANK		5.0		6.0		4.0		1.0		2.0		3.0
		% MAX		90.2%		89.0%		91.4%		100.0%		99.6%		99.2%
		MAX	**249.3**											

Figure 35: Subsystem concept ranking matrix.

Appendix B: PDS

A table listing the design requirements and constraints for this project is depicted above to outline device specifications for performance customer needs, safety limits, and maintenance is depicted below.

Table 10: PDS. Rev. 3, May 7, 2018.

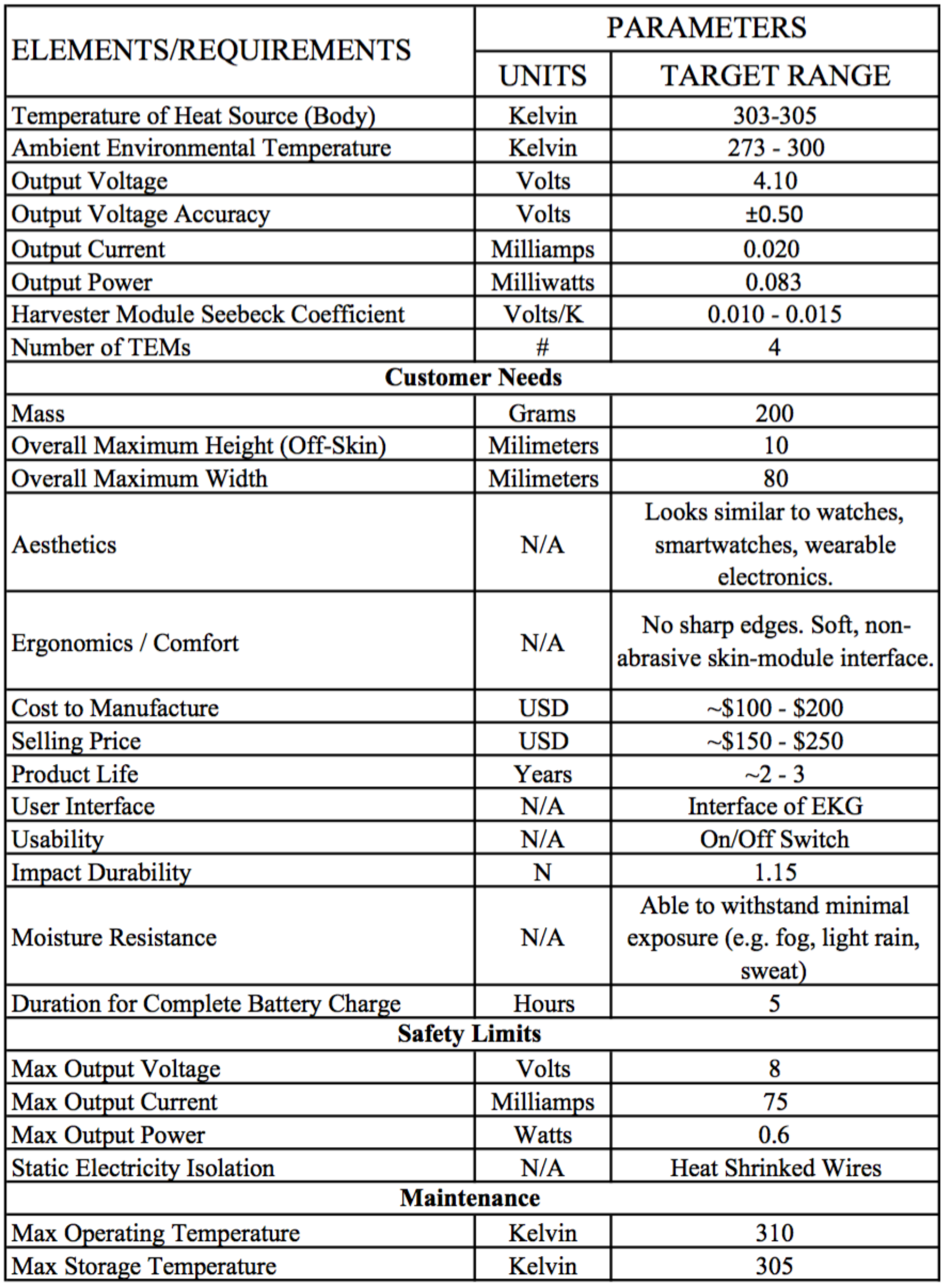

ELEMENTS/REQUIREMENTS	PARAMETERS	
	UNITS	TARGET RANGE
Temperature of Heat Source (Body)	Kelvin	303-305
Ambient Environmental Temperature	Kelvin	273 - 300
Output Voltage	Volts	4.10
Output Voltage Accuracy	Volts	±0.50
Output Current	Milliamps	0.020
Output Power	Milliwatts	0.083
Harvester Module Seebeck Coefficient	Volts/K	0.010 - 0.015
Number of TEMs	#	4
Customer Needs		
Mass	Grams	200
Overall Maximum Height (Off-Skin)	Milimeters	10
Overall Maximum Width	Milimeters	80
Aesthetics	N/A	Looks similar to watches, smartwatches, wearable electronics.
Ergonomics / Comfort	N/A	No sharp edges. Soft, non-abrasive skin-module interface.
Cost to Manufacture	USD	~$100 - $200
Selling Price	USD	~$150 - $250
Product Life	Years	~2 - 3
User Interface	N/A	Interface of EKG
Usability	N/A	On/Off Switch
Impact Durability	N	1.15
Moisture Resistance	N/A	Able to withstand minimal exposure (e.g. fog, light rain, sweat)
Duration for Complete Battery Charge	Hours	5
Safety Limits		
Max Output Voltage	Volts	8
Max Output Current	Milliamps	75
Max Output Power	Watts	0.6
Static Electricity Isolation	N/A	Heat Shrinked Wires
Maintenance		
Max Operating Temperature	Kelvin	310
Max Storage Temperature	Kelvin	305

Appendix C: Timeline

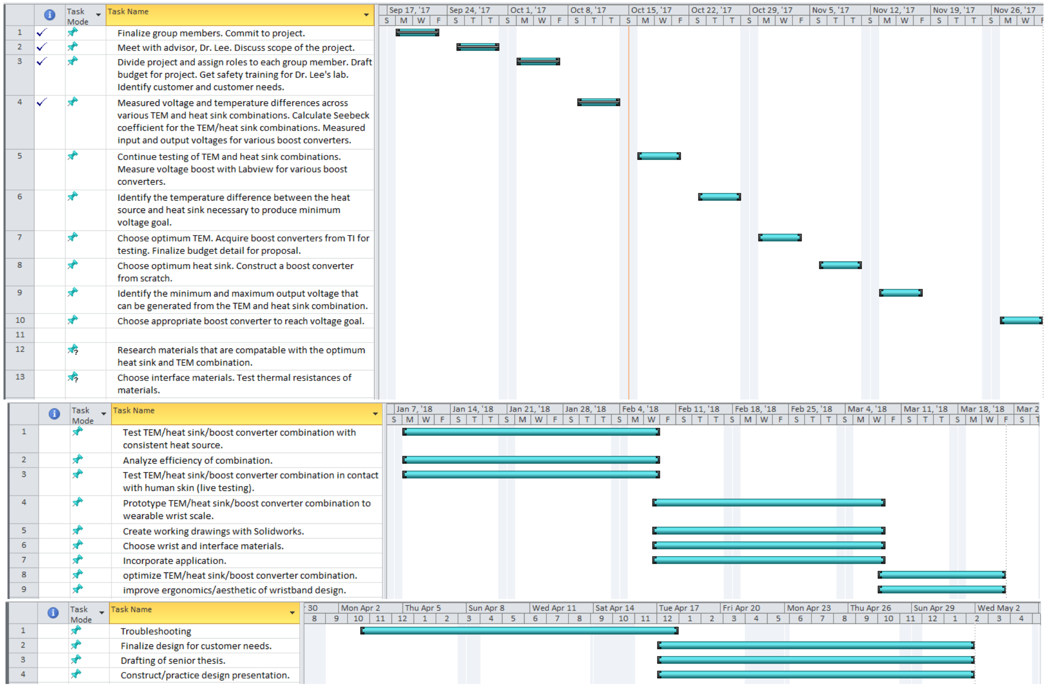

	ℹ	Task Mode	Task Name
1	✓	📌	Finalize group members. Commit to project.
2	✓	📌	Meet with advisor, Dr. Lee. Discuss scope of the project.
3	✓	📌	Divide project and assign roles to each group member. Draft budget for project. Get safety training for Dr. Lee's lab. Identify customer and customer needs.
4	✓	📌	Measured voltage and temperature differences across various TEM and heat sink combinations. Calculate Seebeck coefficient for the TEM/heat sink combinations. Measured input and output voltages for various boost converters.
5		📌	Continue testing of TEM and heat sink combinations. Measure voltage boost with Labview for various boost converters.
6		📌	Identify the temperature difference between the heat source and heat sink necessary to produce minimum voltage goal.
7		📌	Choose optimum TEM. Acquire boost converters from TI for testing. Finalize budget detail for proposal.
8		📌	Choose optimum heat sink. Construct a boost converter from scratch.
9		📌	Identify the minimum and maximum output voltage that can be generated from the TEM and heat sink combination.
10		📌	Choose appropriate boost converter to reach voltage goal.
11			
12		📌?	Research materials that are compatable with the optimum heat sink and TEM combination.
13		📌?	Choose interface materials. Test thermal resistances of materials.

	ℹ	Task Mode	Task Name
1		📌	Test TEM/heat sink/boost converter combination with consistent heat source.
2		📌	Analyze efficiency of combination.
3		📌	Test TEM/heat sink/boost converter combination in contact with human skin (live testing).
4		📌	Prototype TEM/heat sink/boost converter combination to wearable wrist scale.
5		📌	Create working drawings with Solidworks.
6		📌	Choose wrist and interface materials.
7		📌	Incorporate application.
8		📌	optimize TEM/heat sink/boost converter combination.
9		📌	improve ergonomics/aesthetic of wristband design.

	ℹ	Task Mode	Task Name
1		📌	Troubleshooting
2		📌	Finalize design for customer needs.
3		📌	Drafting of senior thesis.
4		📌	Construct/practice design presentation.

Figure 36: Gantt charts for Fall, Winter, and Spring.

Appendix D: Calculations

Heat Sink Hand Calculations

The calculations below depict the thermal equivalent circuit and heat dissipation by the N19-10B heat sink.

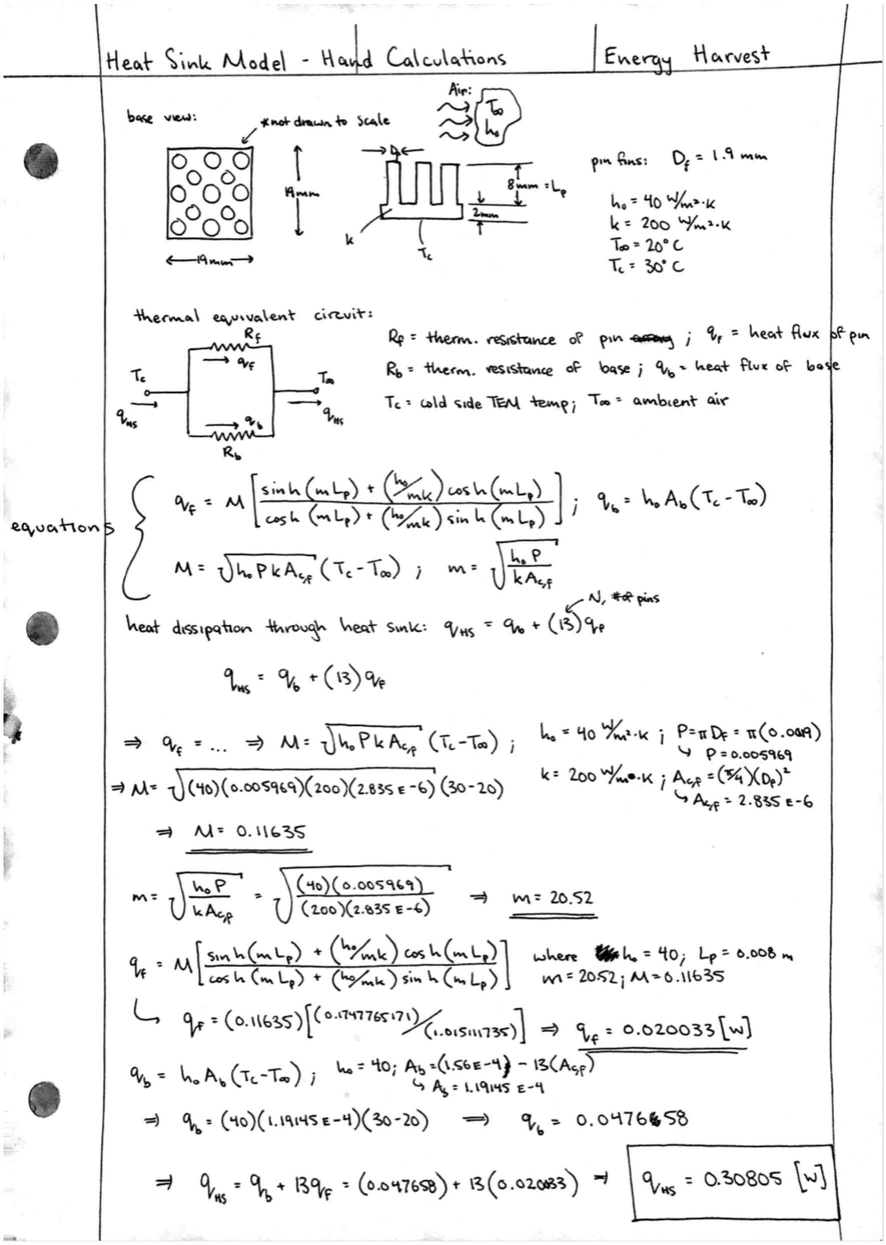

Heat Sink Model - Hand Calculations | Energy Harvest

base view:

*not drawn to scale

19mm
19mm
D_f
8mm $= L_p$
2mm
k
T_c
Air:
T_∞
h_o

pin fins: $D_f = 1.9$ mm

$h_o = 40\ W/m^2 \cdot K$

$k = 200\ W/m^2 \cdot K$

$T_\infty = 20°C$

$T_c = 30°C$

thermal equivalent circuit:

R_f
q_f
T_c
q_{HS}
q_b
R_b
T_∞
q_{HS}

R_f = therm. resistance of pin ; q_f = heat flux of pin

R_b = therm. resistance of base ; q_b = heat flux of base

T_c = cold side TEM temp ; T_∞ = ambient air

equations

$$q_f = M\left[\frac{\sinh(mL_p) + (h_o/mk)\cosh(mL_p)}{\cosh(mL_p) + (h_o/mk)\sinh(mL_p)}\right] ; \quad q_b = h_o A_b (T_c - T_\infty)$$

$$M = \sqrt{h_o P k A_{c,f}}\,(T_c - T_\infty) ; \quad m = \sqrt{\frac{h_o P}{k A_{c,f}}}$$

heat dissipation through heat sink: $q_{HS} = q_b + \overset{N,\ \#\text{ of pins}}{(13)}\, q_f$

$$q_{HS} = q_b + (13) q_f$$

$\Rightarrow q_f = \ldots \Rightarrow M = \sqrt{h_o P k A_{c,f}}\,(T_c - T_\infty)$; $\quad h_o = 40\ W/m^2 \cdot K$; $P = \pi D_f = \pi(0.0019)$ $\hookrightarrow P = 0.005969$

$\Rightarrow M = \sqrt{(40)(0.005969)(200)(2.835E-6)}\,(30-20)$ $\quad k = 200\ W/m \cdot K$; $A_{c,f} = (\pi/4)(D_f)^2$ $\hookrightarrow A_{c,f} = 2.835E-6$

$$\Rightarrow \underline{\underline{M = 0.11635}}$$

$$m = \sqrt{\frac{h_o P}{k A_{c,f}}} = \sqrt{\frac{(40)(0.005969)}{(200)(2.835E-6)}} \Rightarrow \underline{\underline{m = 20.52}}$$

$$q_f = M\left[\frac{\sinh(mL_p) + (h_o/mk)\cosh(mL_p)}{\cosh(mL_p) + (h_o/mk)\sinh(mL_p)}\right]$$ where $h_o = 40$; $L_p = 0.008$ m; $m = 20.52$; $M = 0.11635$

$$\hookrightarrow q_f = (0.11635)\left[(0.1747765171)/(1.015111735)\right] \Rightarrow \underline{\underline{q_f = 0.020033\,[W]}}$$

$q_b = h_o A_b (T_c - T_\infty)$; $\quad h_o = 40$; $A_b = (1.56E-4) - 13(A_{c,f})$ $\hookrightarrow A_b = 1.19145E-4$

$$\Rightarrow q_b = (40)(1.19145E-4)(30-20) \Longrightarrow q_b = 0.047658$$

$$\Rightarrow q_{HS} = q_b + 13 q_f = (0.047658) + 13(0.02083) \Rightarrow \boxed{q_{HS} = 0.30805\,[W]}$$

Figure 37: N19-10B heat dissipation hand calculations.

The calculations below depict the total surface area of the N19-10B heat sink and the flux of heat entering the heat sink from the TEM and subsequently leaving the heat sink.

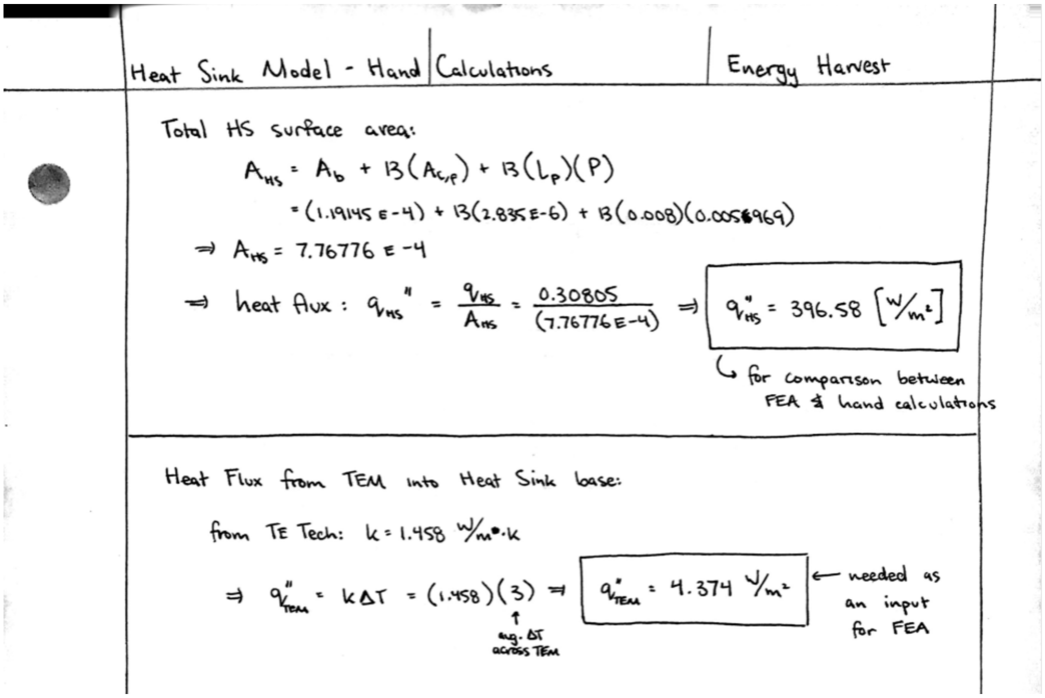

Heat Sink Model - Hand Calculations | Energy Harvest

Total HS surface area:

$$A_{HS} = A_b + 13(A_{c,f}) + 13(L_p)(P)$$

$$= (1.19145\text{E-}4) + 13(2.835\text{E-}6) + 13(0.008)(0.005\text{[illegible]}969)$$

$$\Rightarrow A_{HS} = 7.76776\text{E-}4$$

$$\Rightarrow \text{heat flux}: q_{HS}'' = \frac{q_{HS}}{A_{HS}} = \frac{0.30805}{(7.76776\text{E-}4)} \Rightarrow \boxed{q_{HS}'' = 396.58 \; [\text{W}/\text{m}^2]}$$

↳ for comparison between FEA & hand calculations

Heat Flux from TEM into Heat Sink base:

from TE Tech: $k = 1.458 \; \text{W}/\text{m}\cdot\text{K}$

$$\Rightarrow q_{TEM}'' = k\Delta T = (1.458)\underset{\substack{\uparrow \\ \text{avg. } \Delta T \\ \text{across TEM}}}{(3)} \Rightarrow \boxed{q_{TEM}'' = 4.374 \; \text{W}/\text{m}^2}$$

← needed as an input for FEA

Figure 38: N19-10B surface area and heat flux hand calculations.

Heat Sink FEA Analysis

Note: For the sake of conciseness, long strings of numerical data have been omitted from the report, and only the results are shown here.

```
Field Output Report, written Sun Mar 04 21:53:15 2018

Source 1
---------
   ODB: C:/temp/heat_sink_40.odb
   Step: heat transfer
   Frame: Increment      1: Step Time =    1.000

Loc 1 : Nodal values from source 1

Output sorted by column "Node Label".

Field Output reported at nodes for part: MERGED-1
   Computation algorithm: EXTRAPOLATE_COMPUTE_AVERAGE
   Averaged at nodes
   Averaging regions: ODB_REGIONS
   ---------------------------------------------------
     Node Label           NT11   HFL.Magnitude
                        @Loc 1          @Loc 1

  Minimum              21.0470         2.69345
         At Node             1            3815

  Maximum                  30.     1.07188E+03
         At Node         18539            3095

           Total     2.06456E+06     9.23853E+06

   ---------------------------------------------------
```

A visualization of the heat sink temperature distribution is depicted below. The heat sink is simulated to experience natural convection at the fins, a heat flux of 4.37 $\frac{W}{m^2K}$ at the bottom surface of the base, and a constant temperature of 30°C at the base. The heat sink is meshed at a seed size of 0.25 with triangle elements.

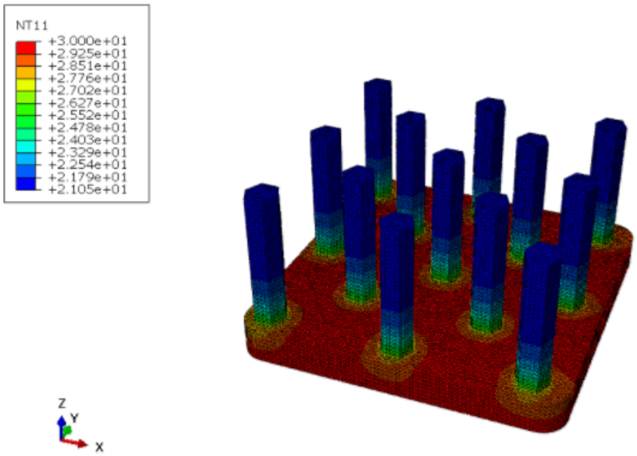

Figure 39: FEA temperature distribution model.

A visualization of the heat sink heat flux distribution is depicted above. The heat sink is simulated to experience natural convection at the fins, a heat flux of 4.37 $\frac{W}{m^2K}$ at the bottom surface of the base, and a constant temperature of 30°C at the base. The heat sink is meshed at a seed size of 0.25 with triangle elements.

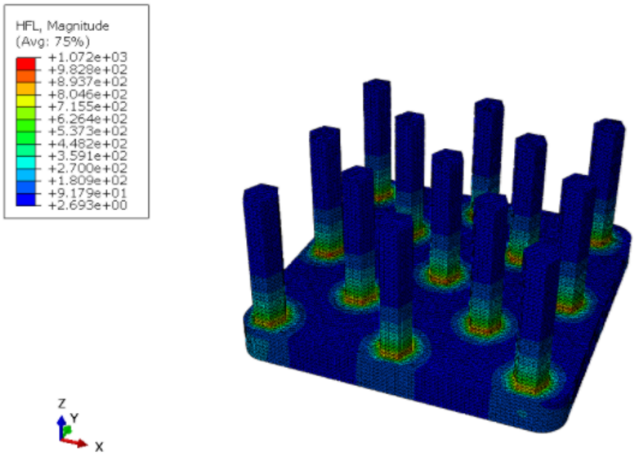

Figure 40: FEA heat flux model.

Appendix E: Drawings

Heat Sink

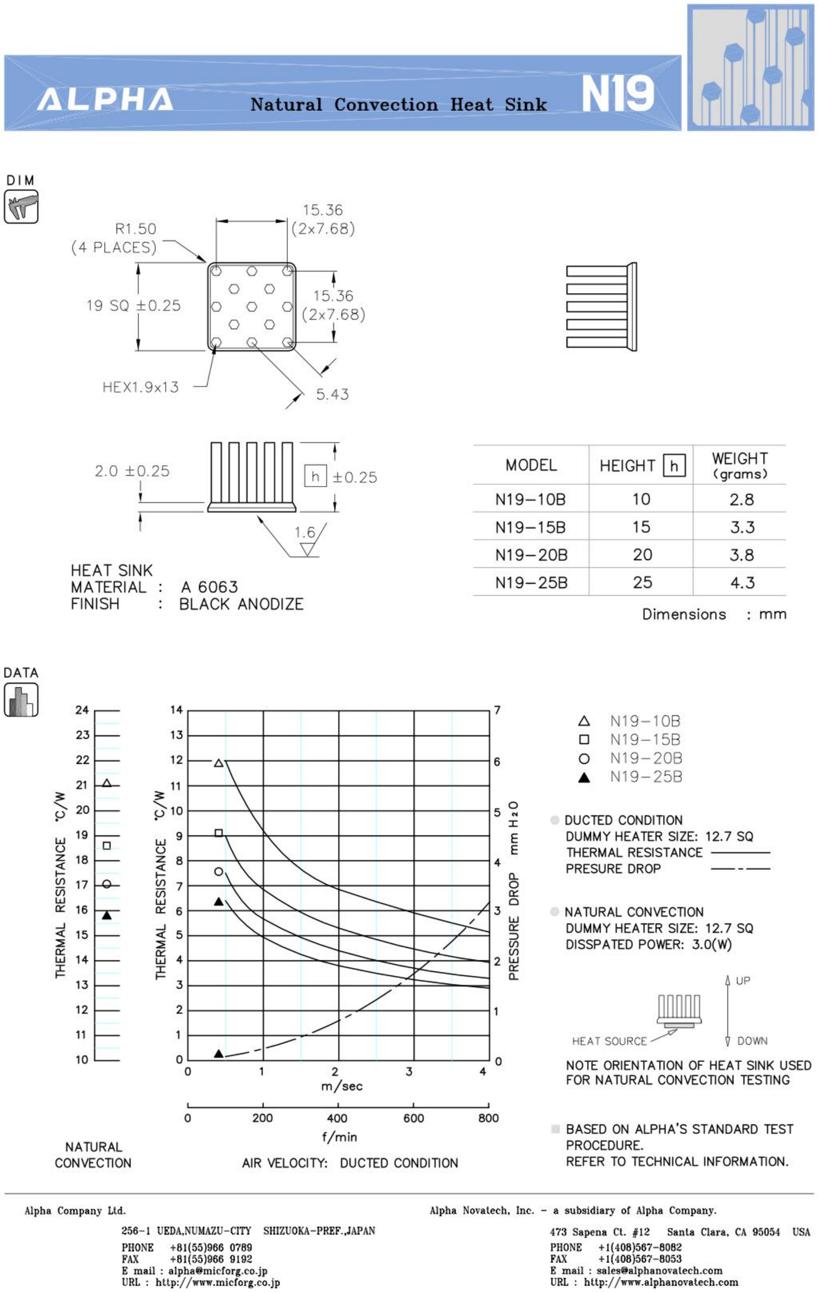

ALPHA Natural Convection Heat Sink **N19**

HEAT SINK
MATERIAL : A 6063
FINISH : BLACK ANODIZE

MODEL	HEIGHT h	WEIGHT (grams)
N19−10B	10	2.8
N19−15B	15	3.3
N19−20B	20	3.8
N19−25B	25	4.3

Dimensions : mm

△ N19−10B
□ N19−15B
○ N19−20B
▲ N19−25B

- DUCTED CONDITION
  DUMMY HEATER SIZE: 12.7 SQ
  THERMAL RESISTANCE ————
  PRESURE DROP —— - ——
- NATURAL CONVECTION
  DUMMY HEATER SIZE: 12.7 SQ
  DISSPATED POWER: 3.0(W)

NOTE ORIENTATION OF HEAT SINK USED FOR NATURAL CONVECTION TESTING

- BASED ON ALPHA'S STANDARD TEST PROCEDURE.
  REFER TO TECHNICAL INFORMATION.

Alpha Company Ltd.
256−1 UEDA,NUMAZU−CITY SHIZUOKA−PREF.,JAPAN
PHONE +81(55)966 0789
FAX +81(55)966 9192
E mail : alpha@micforg.co.jp
URL : http://www.micforg.co.jp

Alpha Novatech, Inc. − a subsidiary of Alpha Company.
473 Sapena Ct. #12 Santa Clara, CA 95054 USA
PHONE +1(408)567−8082
FAX +1(408)567−8053
E mail : sales@alphanovatech.com
URL : http://www.alphanovatech.com

Figure 41: N19-10B mechanical specifications, courtesy of Alpha Nova Tech.

Thermoelectric Module

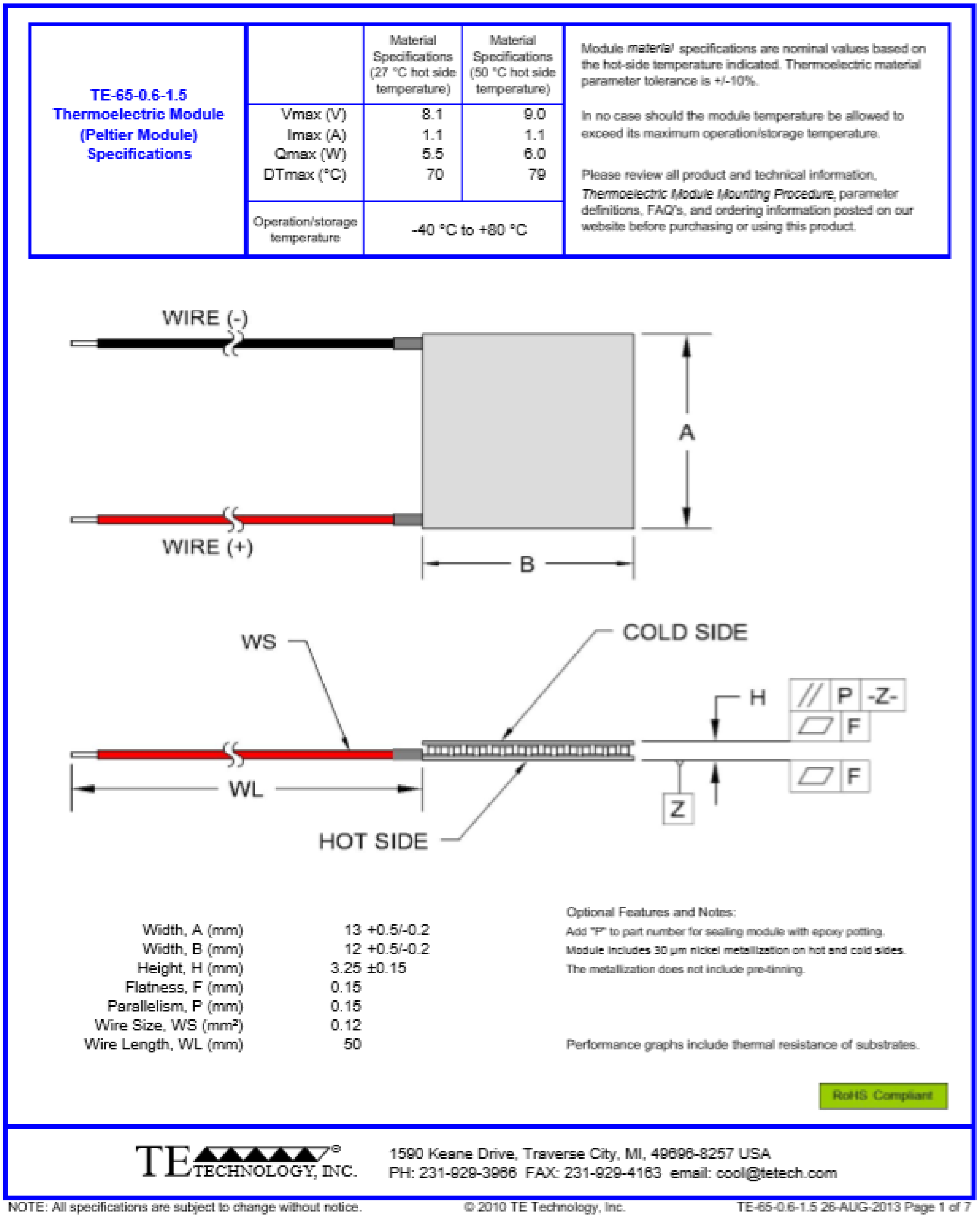

WIRE (-)
A
WIRE (+)
B
WS
COLD SIDE
H
// P -Z-
▱ F
WL
▱ F
Z
HOT SIDE

TE-65-0.6-1.5
Thermoelectric Module
(Peltier Module)
Specifications

	Material Specifications (27 °C hot side temperature)	Material Specifications (50 °C hot side temperature)
Vmax (V)	8.1	9.0
Imax (A)	1.1	1.1
Qmax (W)	5.5	6.0
DTmax (°C)	70	79
Operation/storage temperature	-40 °C to +80 °C	

Module *material* specifications are nominal values based on the hot-side temperature indicated. Thermoelectric material parameter tolerance is +/-10%.

In no case should the module temperature be allowed to exceed its maximum operation/storage temperature.

Please review all product and technical information, *Thermoelectric Module Mounting Procedure*, parameter definitions, FAQ's, and ordering information posted on our website before purchasing or using this product.

Width, A (mm)	13 +0.5/-0.2
Width, B (mm)	12 +0.5/-0.2
Height, H (mm)	3.25 ±0.15
Flatness, F (mm)	0.15
Parallelism, P (mm)	0.15
Wire Size, WS (mm²)	0.12
Wire Length, WL (mm)	50

Optional Features and Notes:
Add "F" to part number for sealing module with epoxy potting.
Module includes 30 μm nickel metallization on hot and cold sides.
The metallization does not include pre-tinning.

Performance graphs include thermal resistance of substrates.

RoHS Compliant

TE TECHNOLOGY, INC.®

1590 Keane Drive, Traverse City, MI, 49696-8257 USA
PH: 231-929-3966 FAX: 231-929-4163 email: cool@tetech.com

NOTE: All specifications are subject to change without notice. © 2010 TE Technology, Inc. TE-65-0.6-1.5 26-AUG-2013 Page 1 of 7

Figure 42: TE-65-0.6-1.5 detail drawing.

Housing

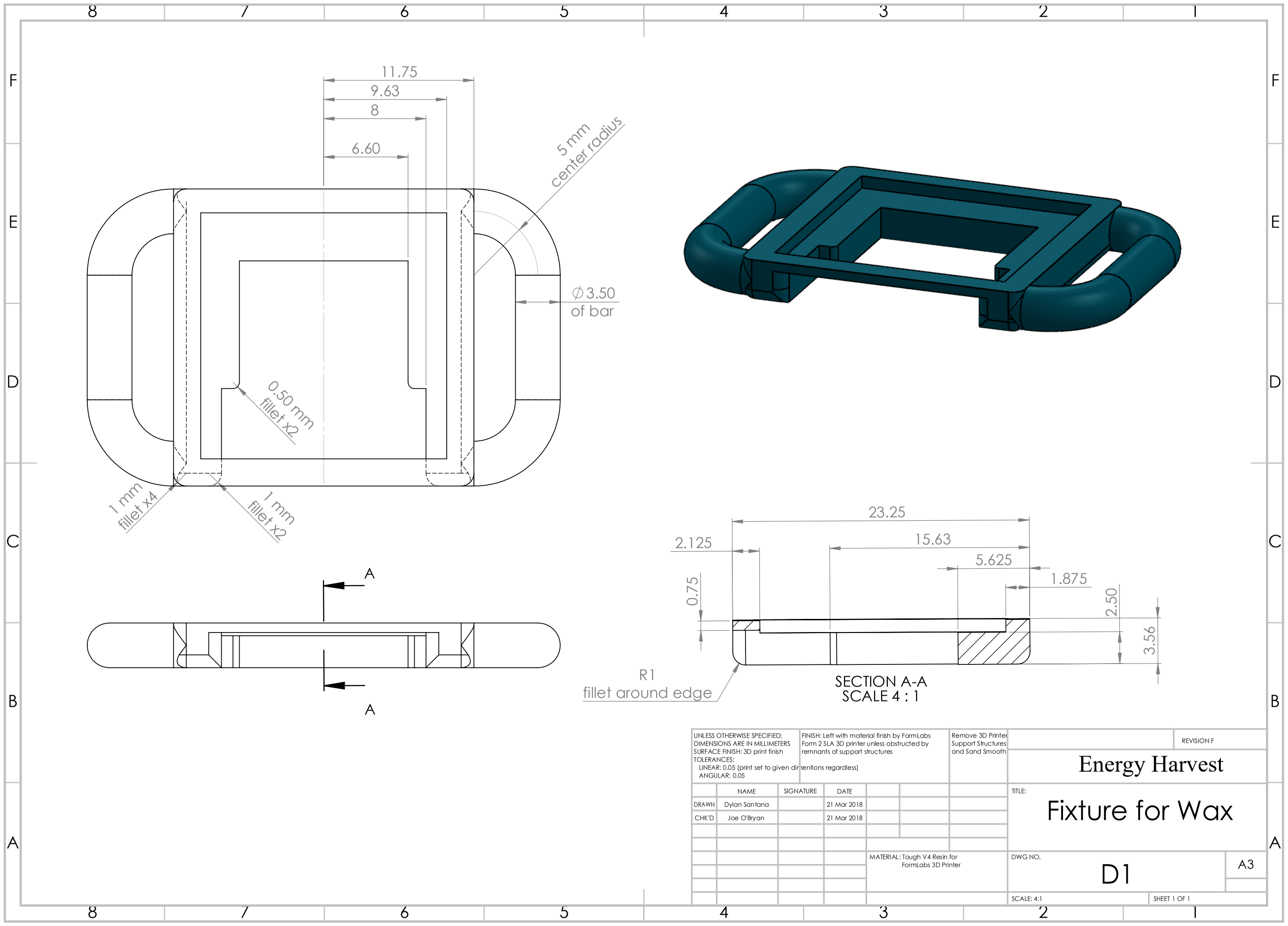
11.75
9.63
8
6.60
5 mm
center radius
∅3.50
of bar
0.50 mm
fillet x2
1 mm
fillet x4
1 mm
fillet x2
A
A
23.25
2.125
15.63
5.625
1.875
0.75
2.50
3.56
R1
fillet around edge
SECTION A-A
SCALE 4 : 1
UNLESS OTHERWISE SPECIFIED:
DIMENSIONS ARE IN MILLIMETERS
SURFACE FINISH: 3D print finish
TOLERANCES:
LINEAR: 0.05 (print set to given dimentions regardless)
ANGULAR: 0.05
FINISH: Left with material finish by FormLabs Form 2 SLA 3D printer unless obstructed by remnants of support structures
Remove 3D Printer Support Structures and Sand Smooth
REVISION F
Energy Harvest
NAME
SIGNATURE
DATE
DRAWN
Dylan Santana
21 Mar 2018
CHK'D
Joe O'Bryan
21 Mar 2018
TITLE:
Fixture for Wax
MATERIAL: Tough V4 Resin for FormLabs 3D Printer
DWG NO.
D1
A3
SCALE: 4:1
SHEET 1 OF 1
8
7
6
5
4
3
2
1
F
E
D
C
B
A

Figure 43: TEM-heat sink housing detail drawing.

Assembly Drawing

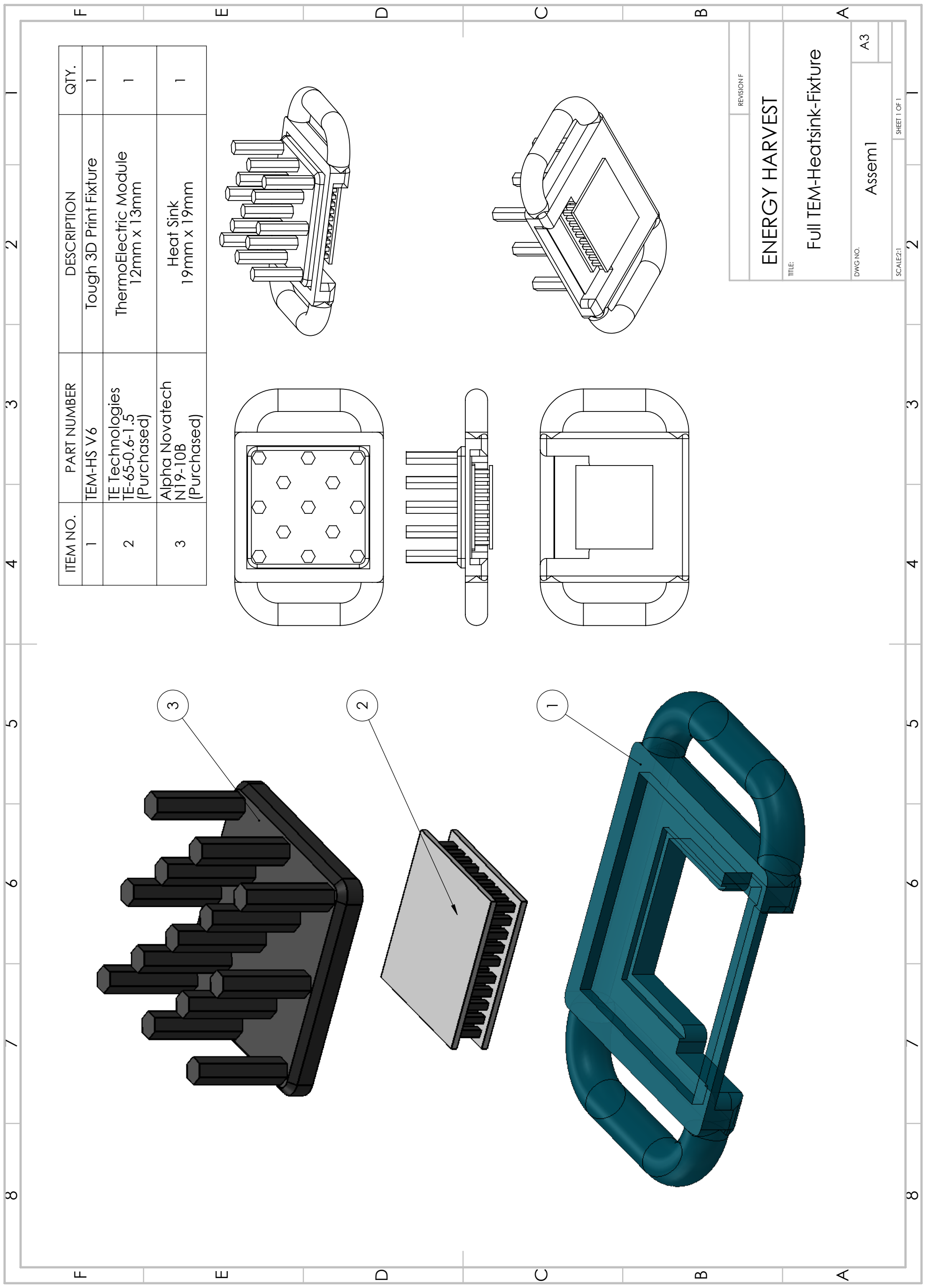

ITEM NO.	PART NUMBER	DESCRIPTION	QTY.
1	TEM-HS V6	Tough 3D Print Fixture	1
2	TE Technologies TE-65-0.6-1.5 (Purchased)	ThermoElectric Module 12mm x 13mm	1
3	Alpha Novatech N19-10B (Purchased)	Heat Sink 19mm x 19mm	1

Figure 44: TEM, heat sink, and housing assembly drawing.

Miscellaneous Drawings

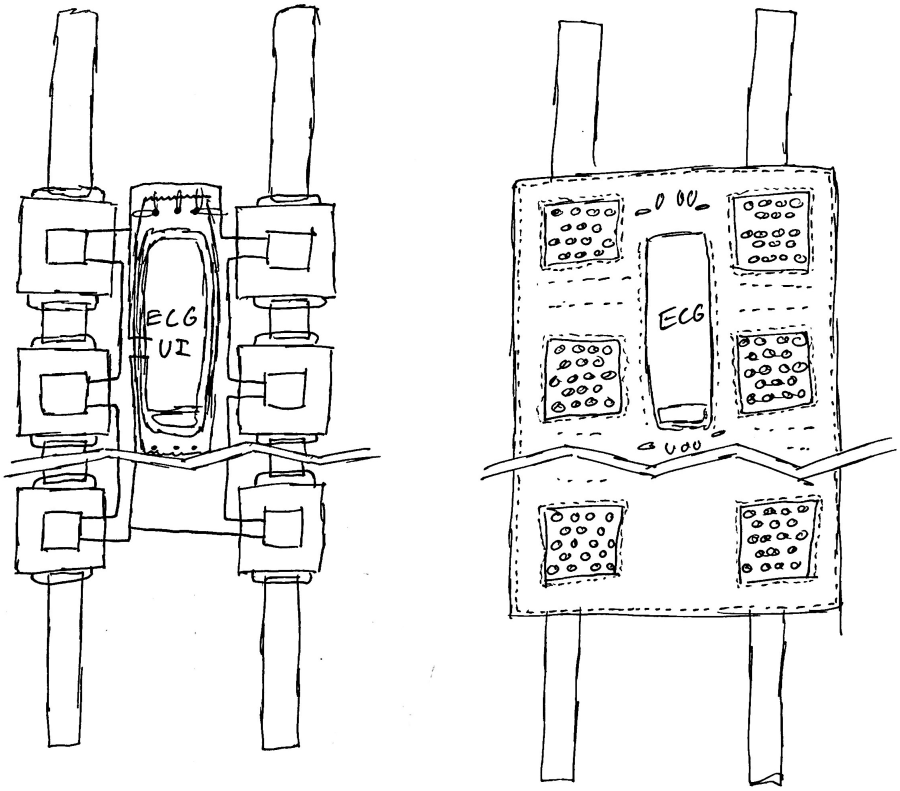

Figure 45: Assembly-in-wristband drawing, uncovered and covered, on left and right, respectively.

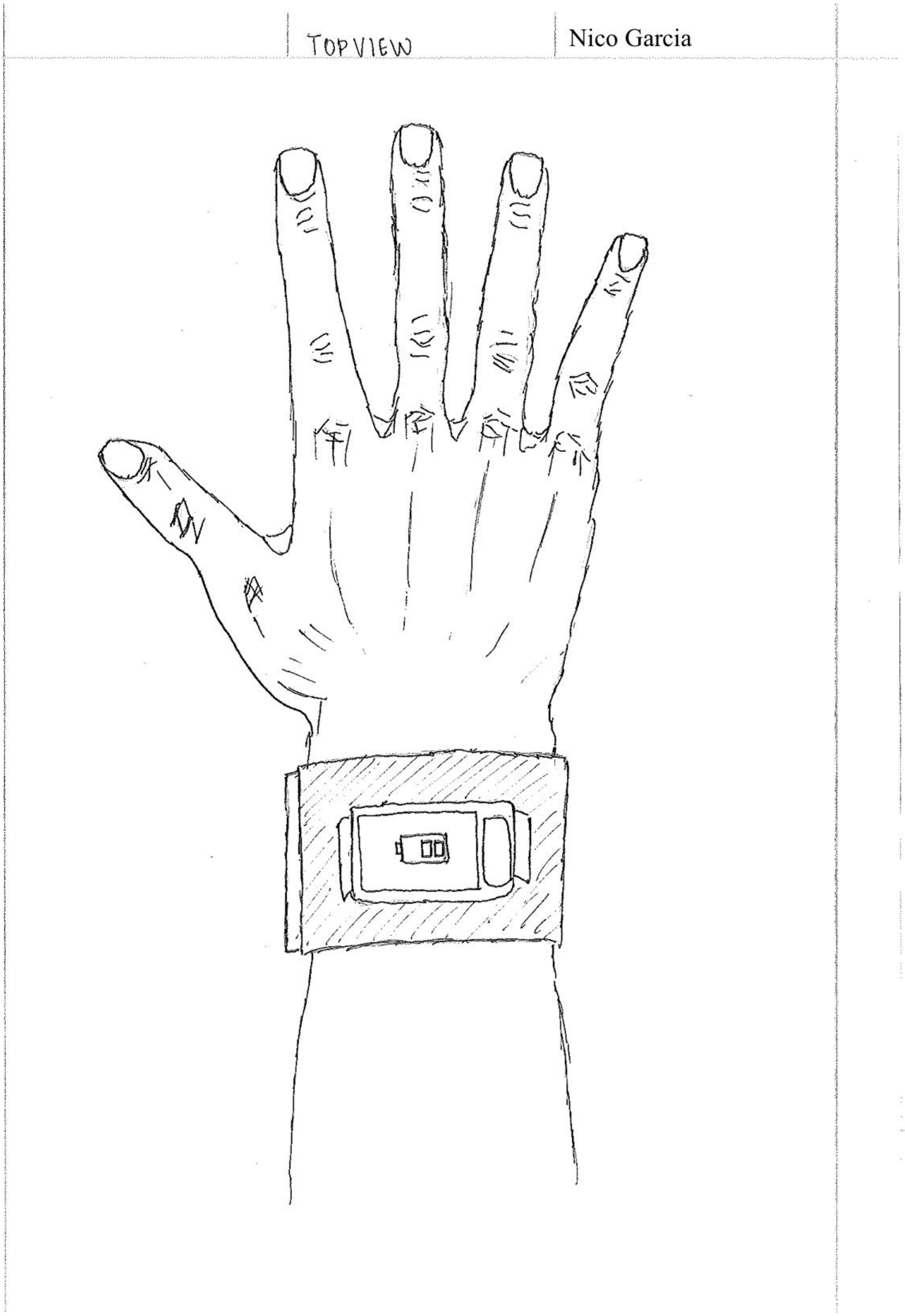

Figure 46: System sketch, top side of device.

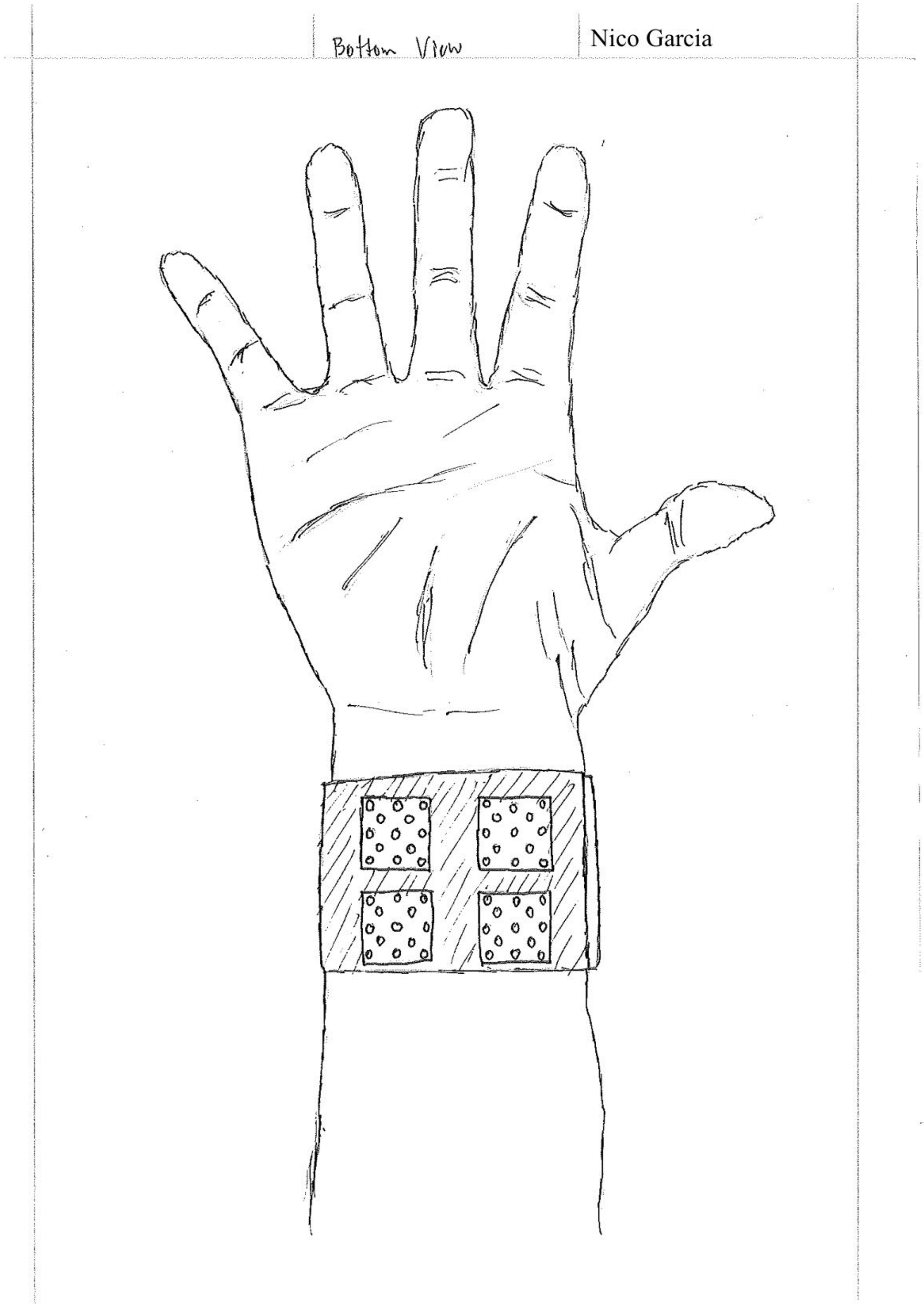

Figure 47: System sketch, bottom side of device.

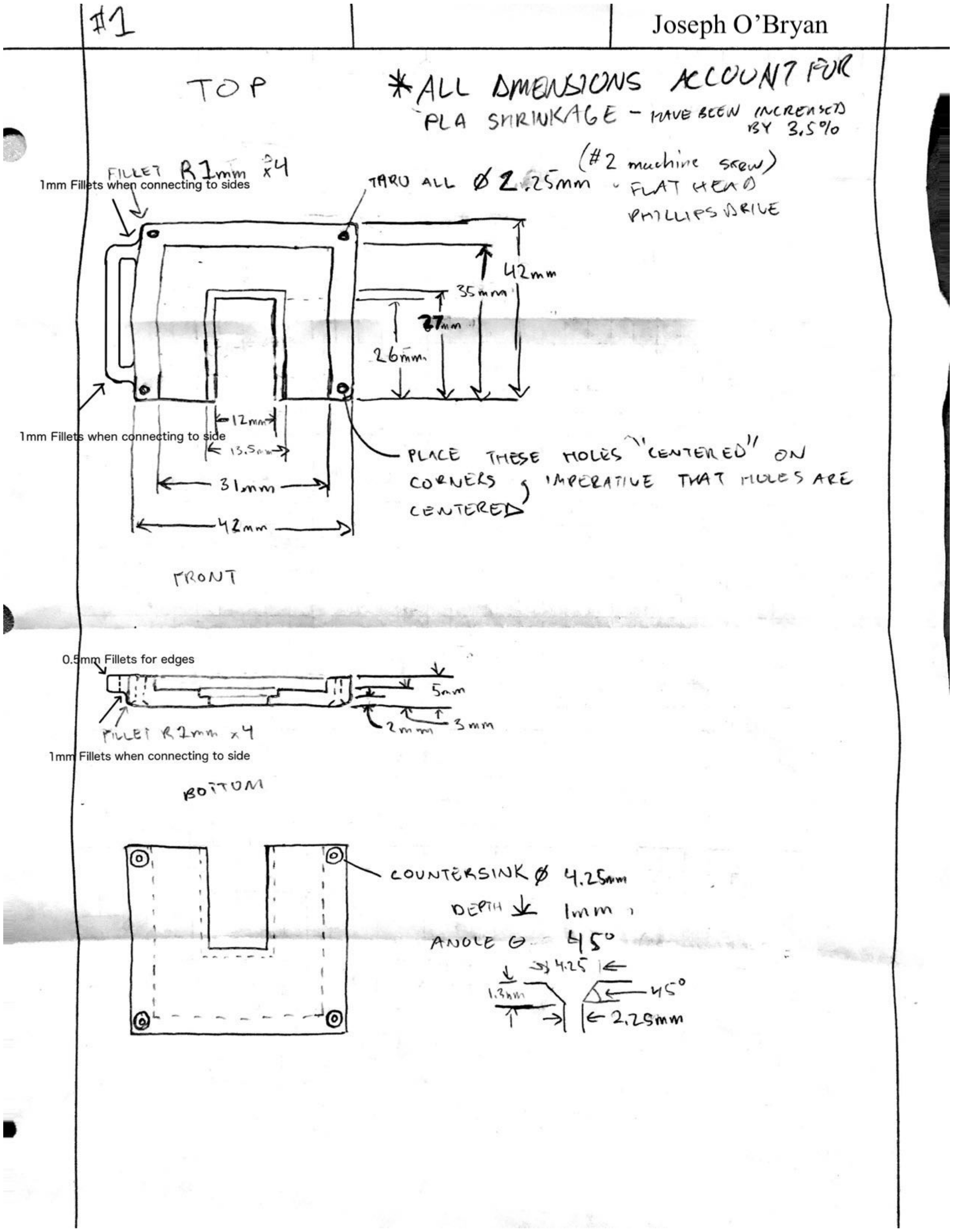
#1
Joseph O'Bryan
TOP
*ALL DIMENSIONS ACCOUNT FOR PLA SHRINKAGE - HAVE BEEN INCREASED BY 3.5%
FILLET R1mm x4
1mm Fillets when connecting to sides
THRU ALL Ø 2.25mm
(#2 machine screw)
FLAT HEAD
PHILLIPS DRIVE
42mm
35mm
27mm
26mm
12mm
13.5mm
31mm
42mm
1mm Fillets when connecting to side
PLACE THESE HOLES "CENTERED" ON CORNERS ; IMPERATIVE THAT HOLES ARE CENTERED
FRONT
0.5mm Fillets for edges
5mm
2mm
3mm
FILLET R2mm x4
1mm Fillets when connecting to side
BOTTOM
COUNTERSINK Ø 4.25mm
DEPTH ↓ 1mm
ANGLE θ 45°
4.25
1.3mm
45°
2.25mm

Figure 48: Screw-and-nut housing concept, hand sketch.

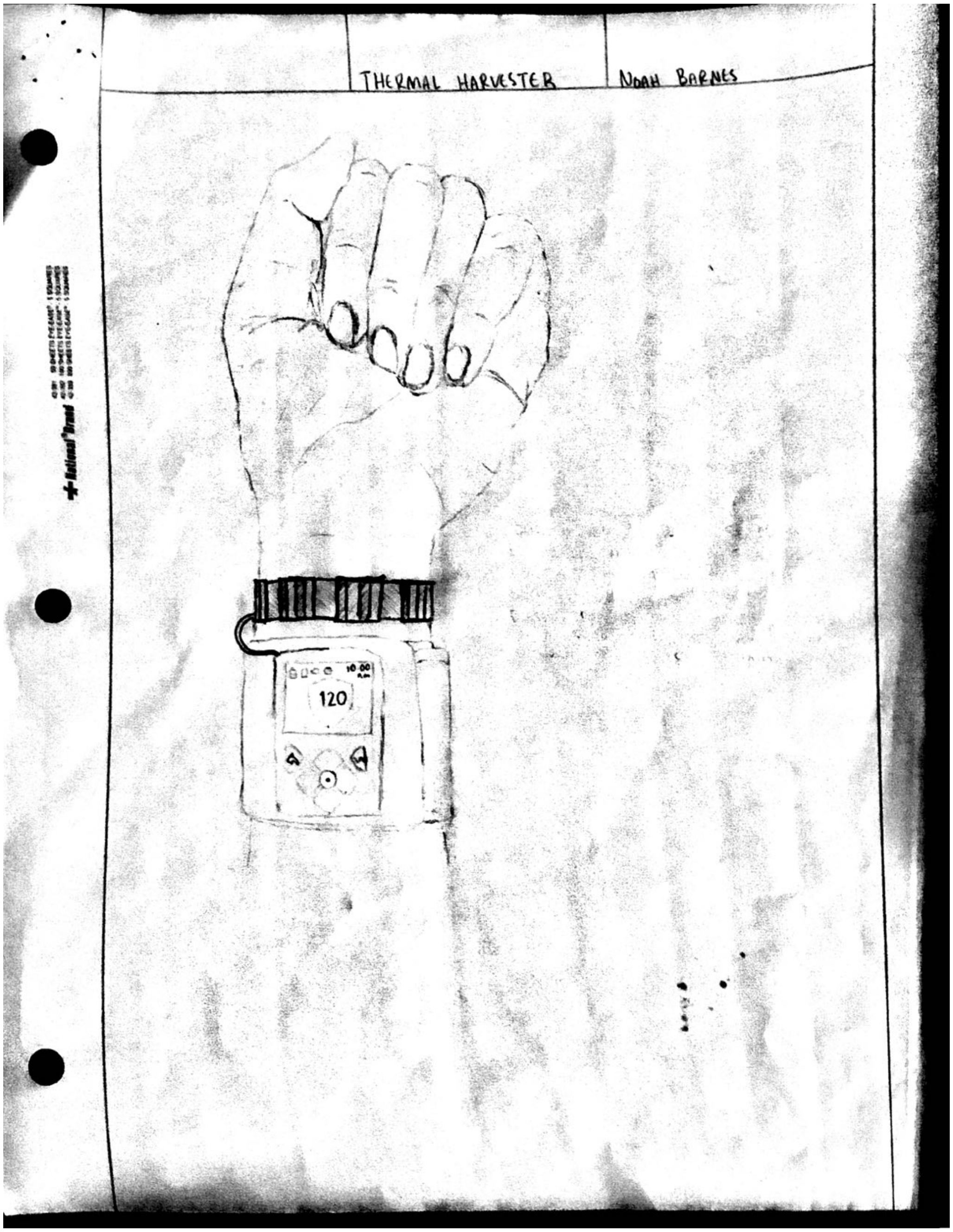

Figure 49: Thermoelectric power generator powering a medical device, hand sketch.

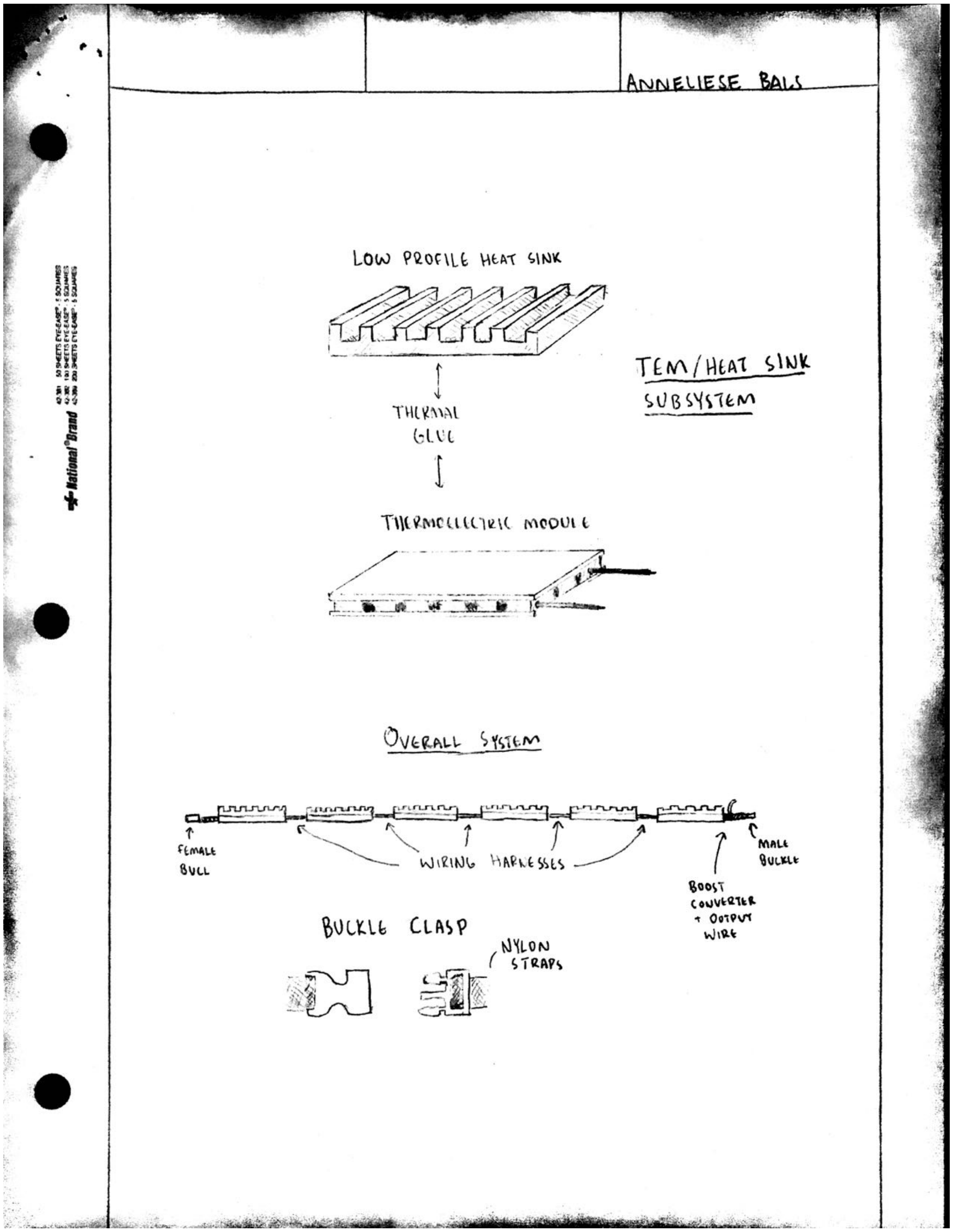

Figure 50: A watch band-esque thermoelectric power generator, hand sketch.

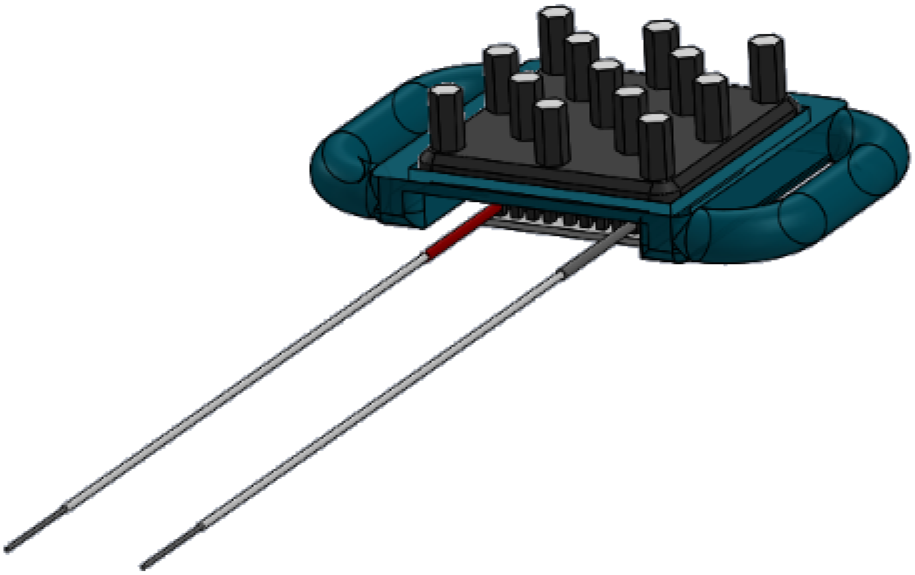

Figure 51: Orthographic view of full TEM, heat sink, and fixture assembly.

Appendix F: Budget Details

Table 11: Detailed proposed project budget.

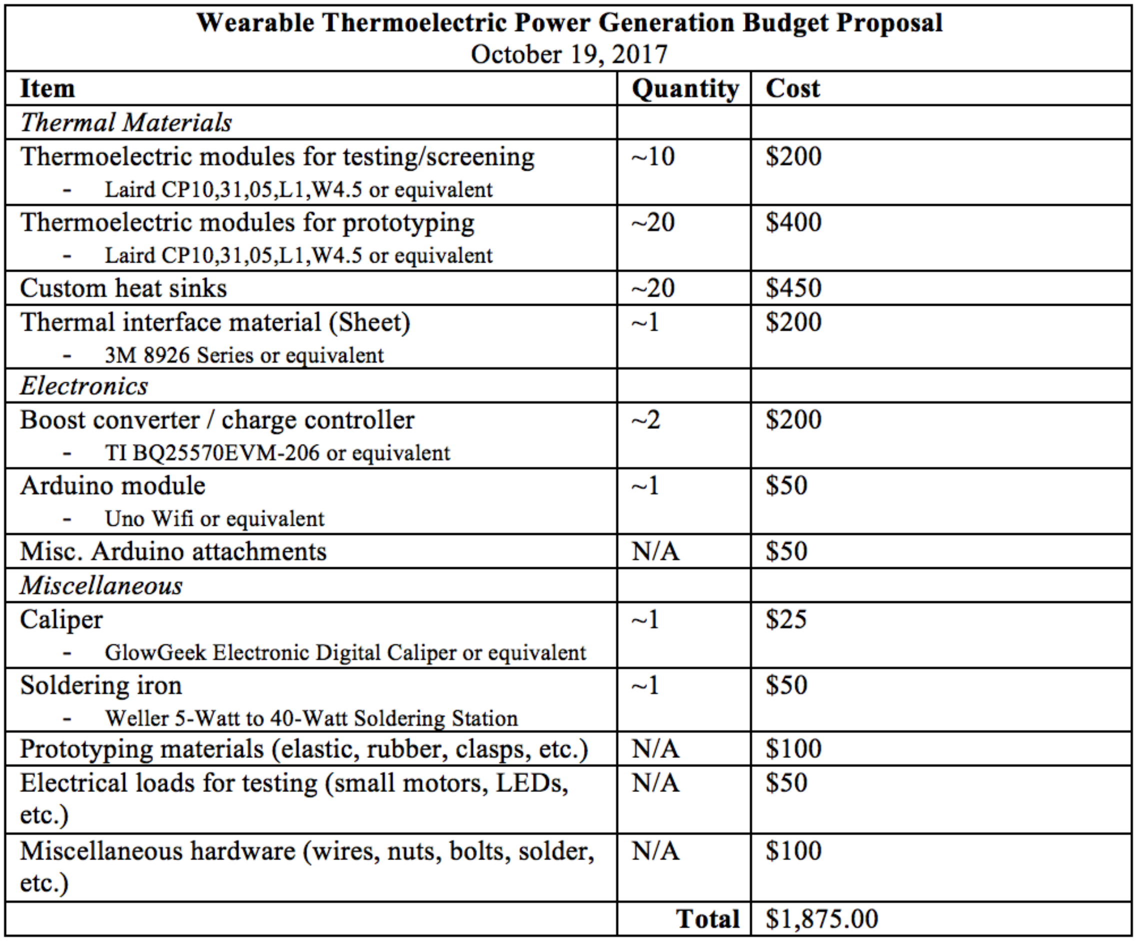

Wearable Thermoelectric Power Generation Budget Proposal
October 19, 2017

Item	**Quantity**	**Cost**
Thermal Materials		
Thermoelectric modules for testing/screening - Laird CP10,31,05,L1,W4.5 or equivalent	~10	$200
Thermoelectric modules for prototyping - Laird CP10,31,05,L1,W4.5 or equivalent	~20	$400
Custom heat sinks	~20	$450
Thermal interface material (Sheet) - 3M 8926 Series or equivalent	~1	$200
Electronics		
Boost converter / charge controller - TI BQ25570EVM-206 or equivalent	~2	$200
Arduino module - Uno Wifi or equivalent	~1	$50
Misc. Arduino attachments	N/A	$50
Miscellaneous		
Caliper - GlowGeek Electronic Digital Caliper or equivalent	~1	$25
Soldering iron - Weller 5-Watt to 40-Watt Soldering Station	~1	$50
Prototyping materials (elastic, rubber, clasps, etc.)	N/A	$100
Electrical loads for testing (small motors, LEDs, etc.)	N/A	$50
Miscellaneous hardware (wires, nuts, bolts, solder, etc.)	N/A	$100
	Total	$1,875.00

Table 12: Detailed project costs.

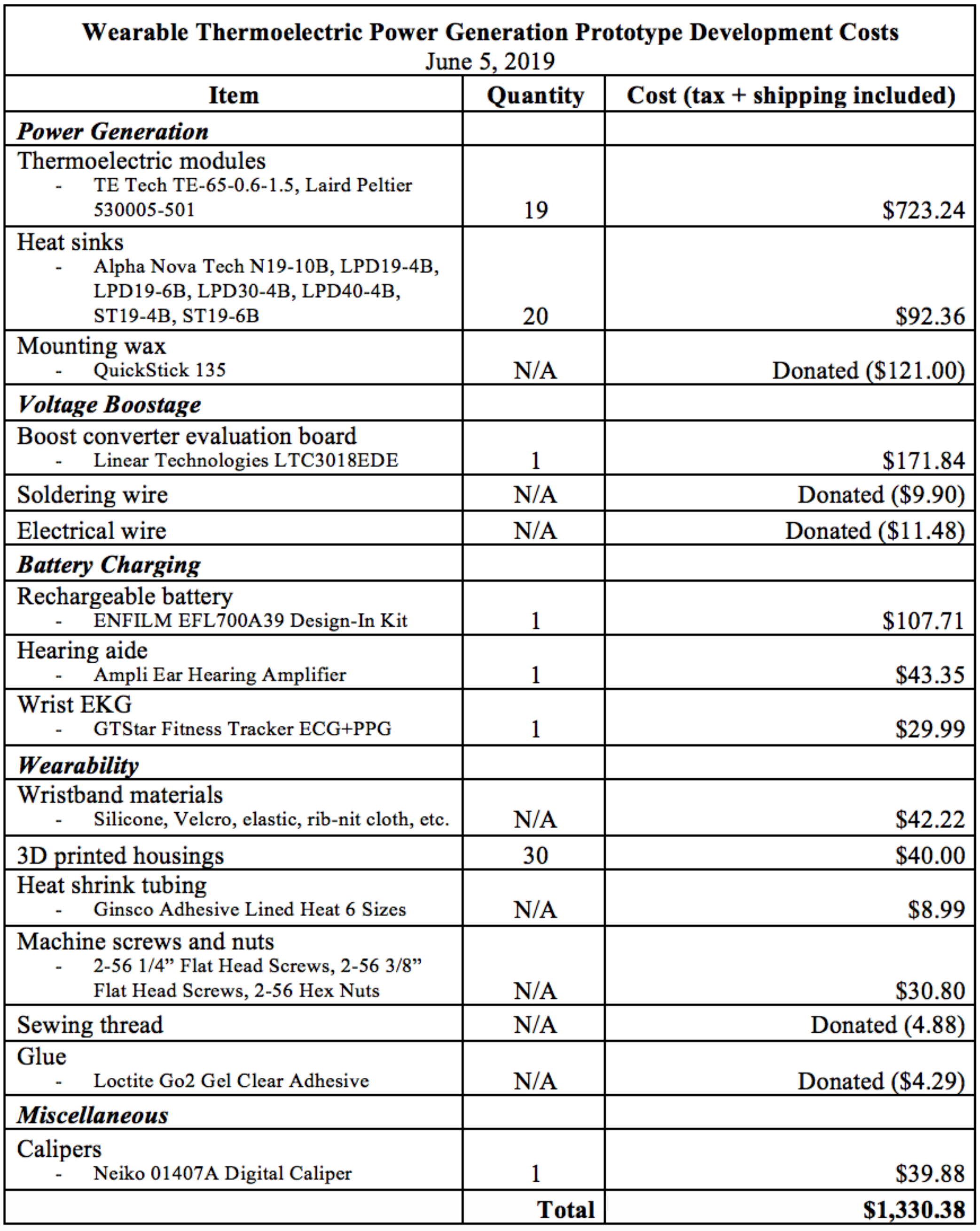

Wearable Thermoelectric Power Generation Prototype Development Costs
June 5, 2019

Item	**Quantity**	**Cost (tax + shipping included)**
Power Generation		
Thermoelectric modules - TE Tech TE-65-0.6-1.5, Laird Peltier 530005-501	19	$723.24
Heat sinks - Alpha Nova Tech N19-10B, LPD19-4B, LPD19-6B, LPD30-4B, LPD40-4B, ST19-4B, ST19-6B	20	$92.36
Mounting wax - QuickStick 135	N/A	Donated ($121.00)
Voltage Boostage		
Boost converter evaluation board - Linear Technologies LTC3018EDE	1	$171.84
Soldering wire	N/A	Donated ($9.90)
Electrical wire	N/A	Donated ($11.48)
Battery Charging		
Rechargeable battery - ENFILM EFL700A39 Design-In Kit	1	$107.71
Hearing aide - Ampli Ear Hearing Amplifier	1	$43.35
Wrist EKG - GTStar Fitness Tracker ECG+PPG	1	$29.99
Wearability		
Wristband materials - Silicone, Velcro, elastic, rib-nit cloth, etc.	N/A	$42.22
3D printed housings	30	$40.00
Heat shrink tubing - Ginsco Adhesive Lined Heat 6 Sizes	N/A	$8.99
Machine screws and nuts - 2-56 1/4” Flat Head Screws, 2-56 3/8” Flat Head Screws, 2-56 Hex Nuts	N/A	$30.80
Sewing thread	N/A	Donated (4.88)
Glue - Loctite Go2 Gel Clear Adhesive	N/A	Donated ($4.29)
Miscellaneous		
Calipers - Neiko 01407A Digital Caliper	1	$39.88
	Total	**$1,330.38**

Table 13: Detailed prototype costs.

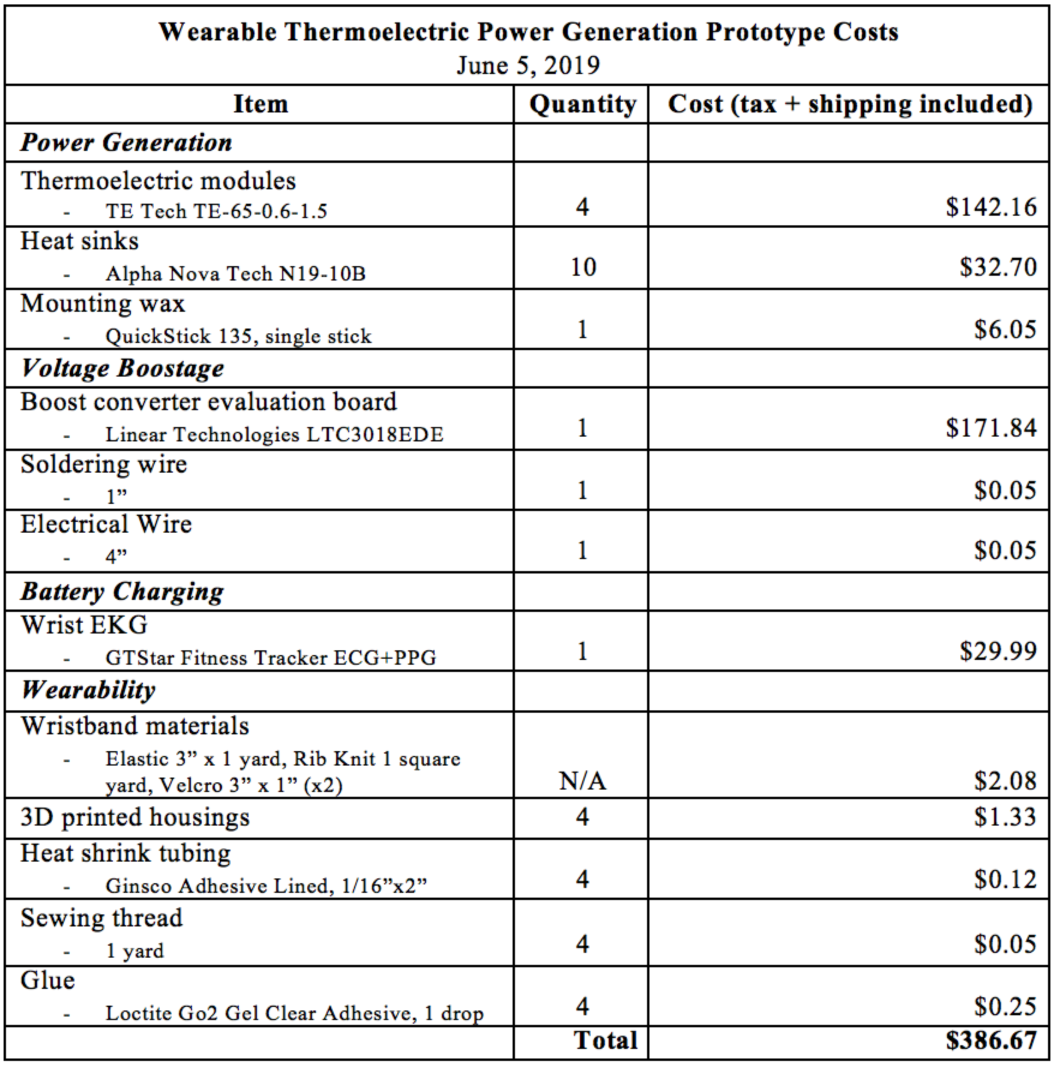

Wearable Thermoelectric Power Generation Prototype Costs
June 5, 2019

Item	**Quantity**	**Cost (tax + shipping included)**
Power Generation		
Thermoelectric modules - TE Tech TE-65-0.6-1.5	4	$142.16
Heat sinks - Alpha Nova Tech N19-10B	10	$32.70
Mounting wax - QuickStick 135, single stick	1	$6.05
Voltage Boostage		
Boost converter evaluation board - Linear Technologies LTC3018EDE	1	$171.84
Soldering wire - 1”	1	$0.05
Electrical Wire - 4”	1	$0.05
Battery Charging		
Wrist EKG - GTStar Fitness Tracker ECG+PPG	1	$29.99
Wearability		
Wristband materials - Elastic 3” x 1 yard, Rib Knit 1 square yard, Velcro 3” x 1” (x2)	N/A	$2.08
3D printed housings	4	$1.33
Heat shrink tubing - Ginsco Adhesive Lined, 1/16”x2”	4	$0.12
Sewing thread - 1 yard	4	$0.05
Glue - Loctite Go2 Gel Clear Adhesive, 1 drop	4	$0.25
	Total	**$386.67**

Appendix G: Senior Design Conference Presentation

Many people have a need for wearable medical devices, however, not everyone has access to constant and reliable power sources. With thermoelectric technology we can take advantage of our body heat and use it as a natural heat source to power wearable medical devices with low power needs. For our project we decided to power a wearable EKG; this device takes heartbeat information and forms a periodic function which can be analyzed to diagnose and detect onset of various forms of cardiovascular disease. We used thermoelectric modules to power the EKG. TEMs are small electrical devices capable of taking excess heat and converting it into a small power output. These modules do this by operating based on the Seebeck effect, which simply states that an electric current will be produced when two dissimilar metals are exposed to a temperature difference. Our device is composed of four subsystems: power generation, voltage boost, battery charging, and wearability.

The power generation subsystem consists of a heat sink, TEM, and heat source, which in our case is the body. We selected our heat sink after measuring and comparing the output voltage of a TEM, on a hot plate, matched with various heat sinks. After selecting our heat sink, we conducted finite element analysis and found that a majority of the heat flux occurs at the base of the pins allowing us to shorten the pin length. Our selection of the TEM was based on the B-factor, which is a calculation dependent on the dimensions of the module. After testing and optimization we chose to use TE-65.

The voltage boost subsystem is made up of the TEM circuitry to optimize the voltage output and a boost converter. The TEMs are arranged with two connected in series connected in parallel with two in series. The boost converter is a model from Linear Technologies called LTC 3108. The output of the TEMs is directly connected to the input of the boost converter.

The battery charging subsystem is consists of the boost converter output directly wired to the EKG rechargable battery. This subsystem is ideal for sensor applications or short bursts of power.

Lastly, the wearability subsystem consists of the wristband and fixtures holding the TEMs and heat sinks. This subsystem was broken down into seven qualities, based on the results of a survey we conducted in November 2017, that we considered during our design process. Of these qualities there are three main categories: performance, wearability, and safety. All things considered, we ranked safety as the most important quality to ensure the user was not at risk.

As far as future steps that can be taken with this project to achieve consistent performance, the first and most effective action that could be taken is to optimize the TEM module design as much as possible. Further B factor optimization could only be achieved by a team actually designing and building their own TEM, rather than purchasing one off the market. This way, you could truly control the performance characteristics of your module. Another area of improvement for the device is to increase the temperature difference present across the TEM, improving its performance. One way of doing this that we are looking towards is increasing the heat dissipation by the heat sinks by distributing the heat around the whole outer surface of the wristband, taking advantage of additional heat sinks, other dissipating materials, and the large surface area of the whole wristband. And finally, we are looking to lower the profile of the wristband by further lowering the height of the heat sinks and also we want to size down the 3d printed fixtures so they take up less area on the wrist. This will allow for either more TEMs to fit on a wrist, or with lass area we can choose for the wristband to take up less room on a wrist, making the wristband more comfortable.

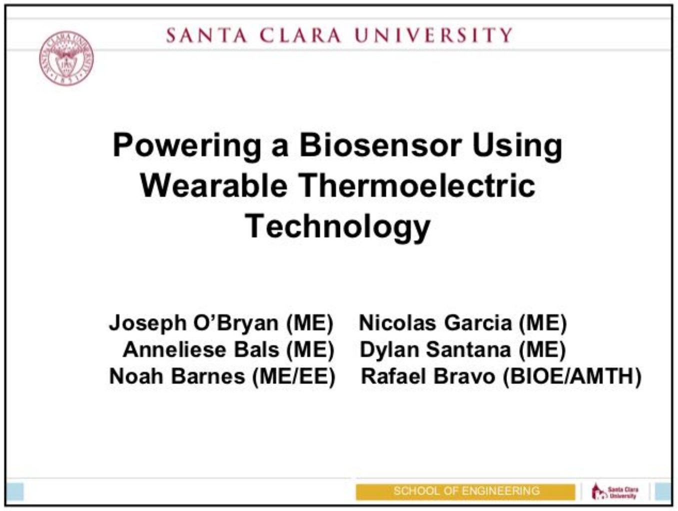

SANTA CLARA UNIVERSITY

Powering a Biosensor Using Wearable Thermoelectric Technology

Joseph O'Bryan (ME)	Nicolas Garcia (ME)
Anneliese Bals (ME)	Dylan Santana (ME)
Noah Barnes (ME/EE)	Rafael Bravo (BIOE/AMTH)

SCHOOL OF ENGINEERING

Santa Clara University

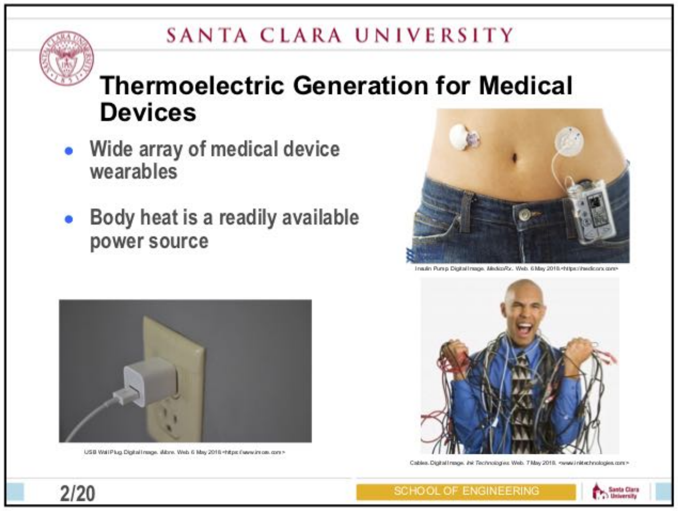

SANTA CLARA UNIVERSITY

Thermoelectric Generation for Medical Devices

- Wide array of medical device wearables
- Body heat is a readily available power source

Insulin Pump Digital Image. *MedicoRx*. Web. 6 May 2018.<https://medicorx.com>

USB Wall Plug Digital Image. *iMore*. Web. 6 May 2018 <https://www.imore.com>

Cables. Digital Image. *Ink Technologies*. Web. 7 May 2018. <www.inktechnologies.com>

SCHOOL OF ENGINEERING

Santa Clara University

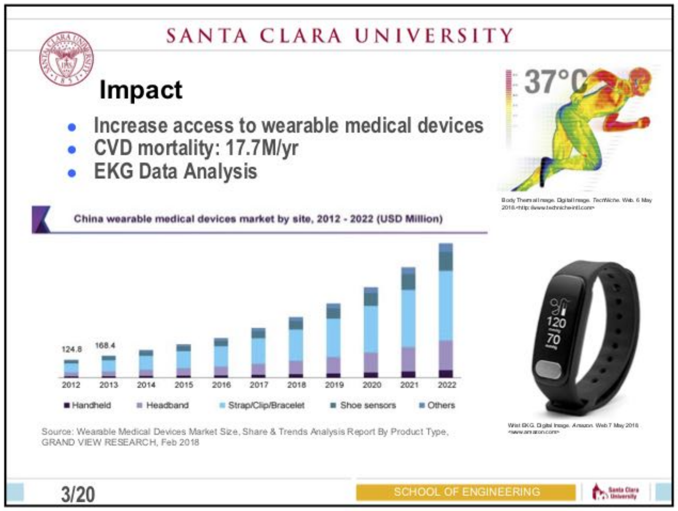

SANTA CLARA UNIVERSITY

Impact

- Increase access to wearable medical devices
- CVD mortality: 17.7M/yr
- EKG Data Analysis

China wearable medical devices market by site, 2012 - 2022 (USD Million)

124.8
168.4
2012
2013
2014
2015
2016
2017
2018
2019
2020
2021
2022
■ Handheld
■ Headband
■ Strap/Clip/Bracelet
■ Shoe sensors
■ Others
37°C
120
70

Source: Wearable Medical Devices Market Size, Share & Trends Analysis Report By Product Type, GRAND VIEW RESEARCH, Feb 2018

Body Thermal Image. Digital Image. *TechNiche*. Web. 6 May 2018.<http://www.techniche-intl.com>

Wrist EKG. Digital Image. *Amazon*. Web 7 May 2018 <www.amazon.com>

SCHOOL OF ENGINEERING

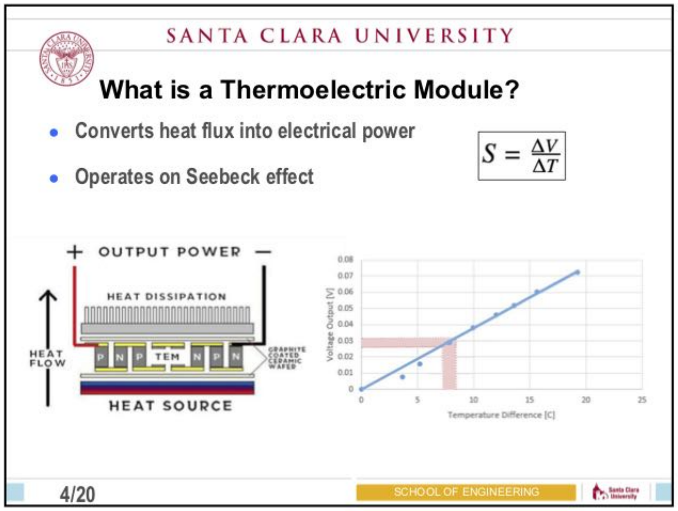

SANTA CLARA UNIVERSITY

What is a Thermoelectric Module?

- Converts heat flux into electrical power
- Operates on Seebeck effect

$$S = \frac{\Delta V}{\Delta T}$$

+ OUTPUT POWER −
HEAT DISSIPATION
HEAT FLOW
P N P TEM N P N
GRAPHITE COATED CERAMIC WAFER
HEAT SOURCE
Voltage Output [V]
0.08
0.07
0.06
0.05
0.04
0.03
0.02
0.01
0
0
5
10
15
20
25
Temperature Difference [C]

SCHOOL OF ENGINEERING

Santa Clara University

Examples of Existing Wearable Thermoelectric Generation in Use

Seiko Thermic (1998)

Matrix Power Watch (2017)

Voyager 1 (1977)

Seiko Thermic. Digital Image. *Rakuten*. Web. 4 May 2018. <global.rakuten.com>
Matrix Power Watch. Digital Image. *Engadget*. Web. 4 May 2018.
< www.engadget.com>
https://ideas.lego.com/projects/94639

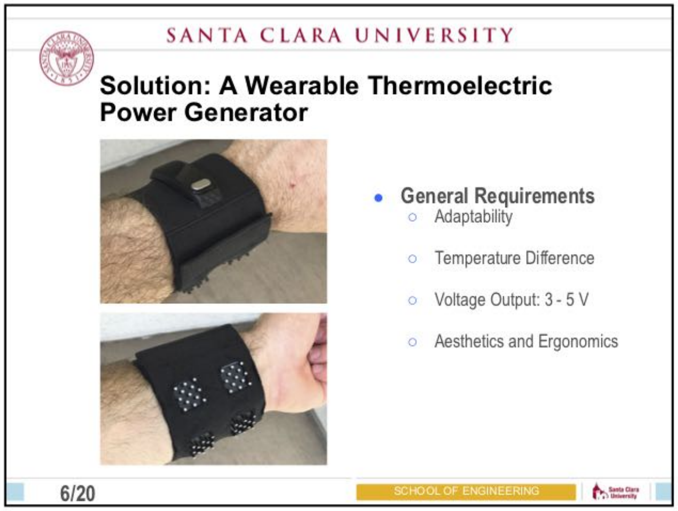

Solution: A Wearable Thermoelectric Power Generator

- General Requirements
  - Adaptability
  - Temperature Difference
  - Voltage Output: 3 - 5 V
  - Aesthetics and Ergonomics

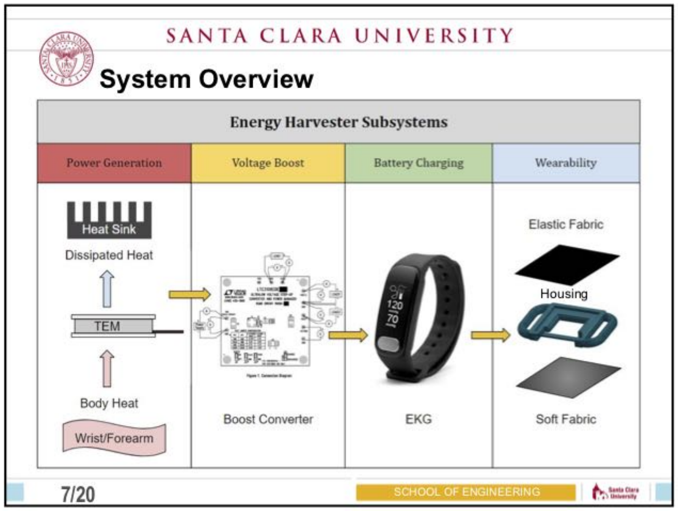

System Overview

Energy Harvester Subsystems

Power Generation

Voltage Boost

Battery Charging

Wearability

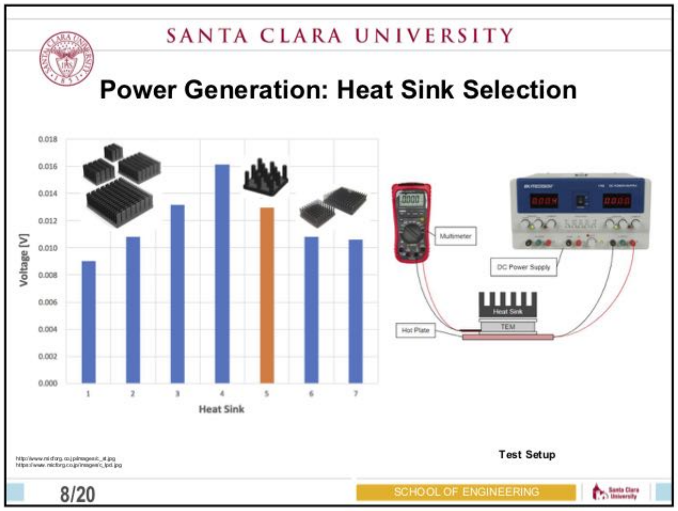

Power Generation: Heat Sink Selection

Test Setup

http://www.nidforg.co.jp/images/c_st.jpg
https://www.nidforg.co.jp/images/c_lpd.jpg

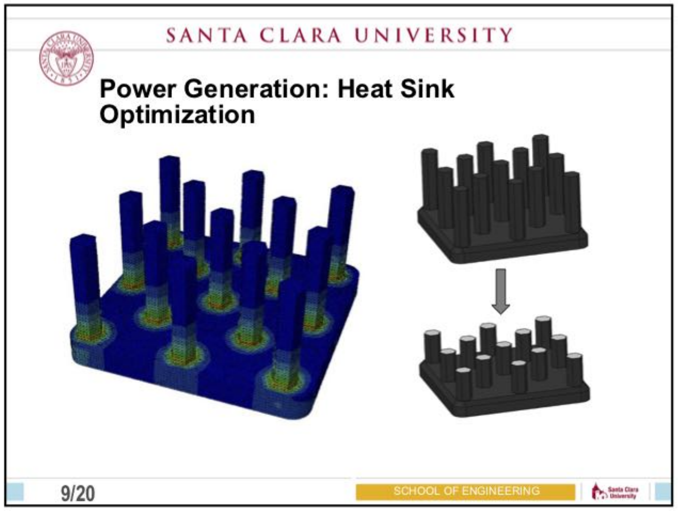

Power Generation: Heat Sink Optimization

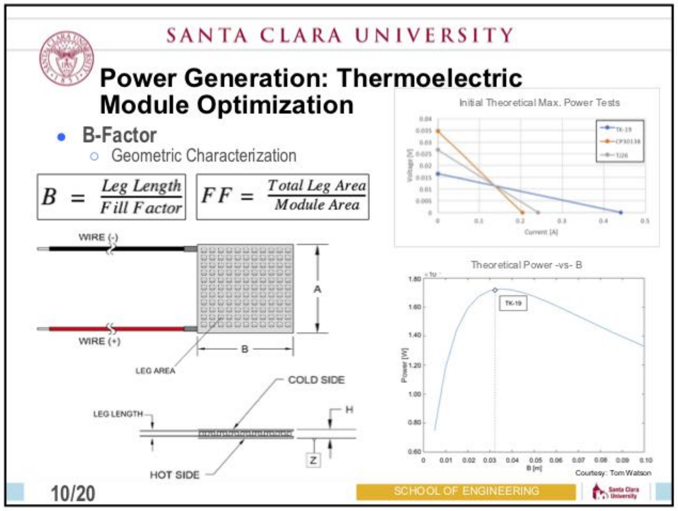

Power Generation: Thermoelectric Module Optimization

- B-Factor
  - Geometric Characterization

$$B = \frac{Leg\ Length}{Fill\ Factor} \qquad FF = \frac{Total\ Leg\ Area}{Module\ Area}$$

Courtesy: Tom Watson

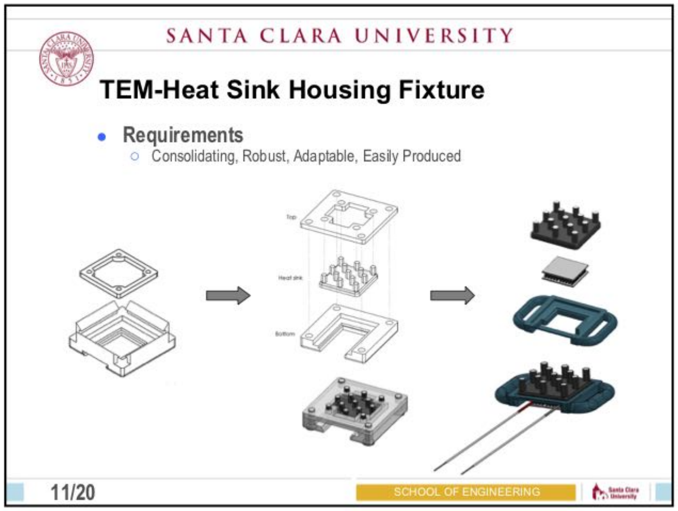

TEM-Heat Sink Housing Fixture

- Requirements
  - Consolidating, Robust, Adaptable, Easily Produced

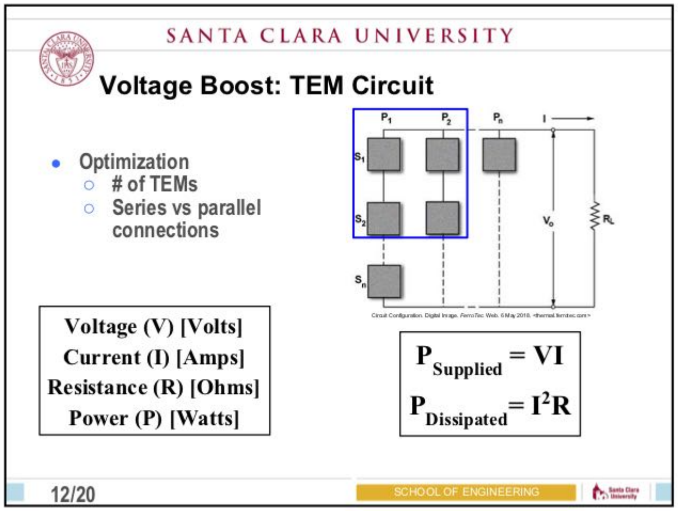

Voltage Boost: TEM Circuit

- Optimization
  - # of TEMs
  - Series vs parallel connections

Circuit Configuration. Digital Image. *FerroTec*. Web. 6 May 2016. <thermal.ferrotec.com>

Voltage (V) [Volts]
Current (I) [Amps]
Resistance (R) [Ohms]
Power (P) [Watts]

$$P_{Supplied} = VI$$
$$P_{Dissipated} = I^2R$$

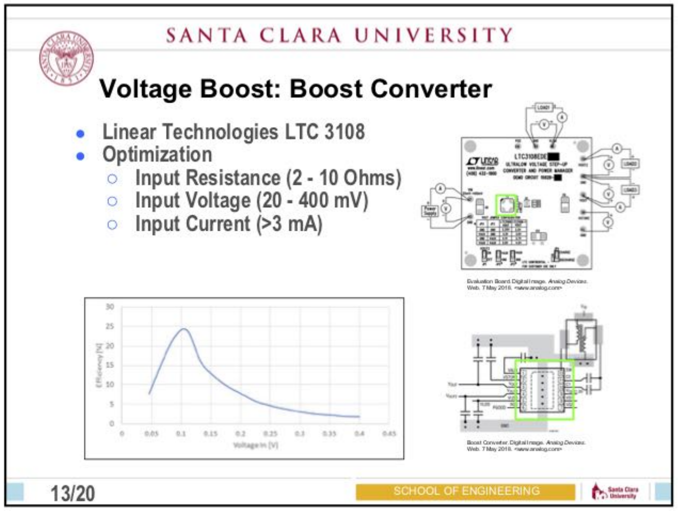

Voltage Boost: Boost Converter

- Linear Technologies LTC 3108
- Optimization
  - ○ Input Resistance (2 - 10 Ohms)
  - ○ Input Voltage (20 - 400 mV)
  - ○ Input Current (>3 mA)

Evaluation Board. Digital Image. *Analog Devices*. Web. 7 May 2018. <www.analog.com>

Boost Converter. Digital Image. *Analog Devices*. Web. 7 May 2018. <www.analog.com>

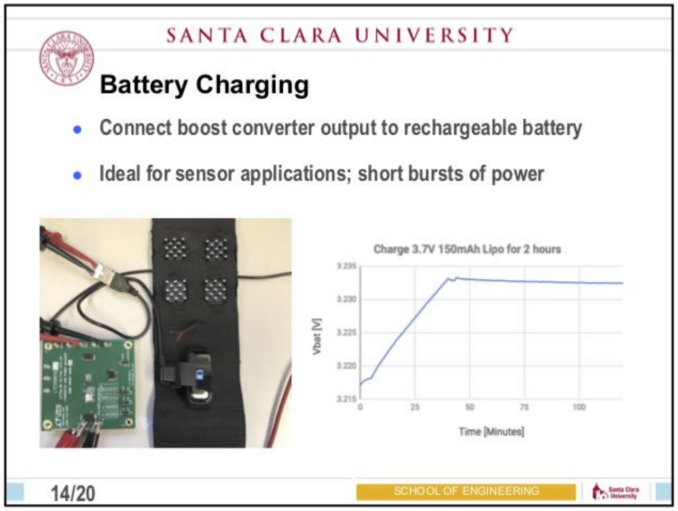

Battery Charging

- Connect boost converter output to rechargeable battery
- Ideal for sensor applications; short bursts of power

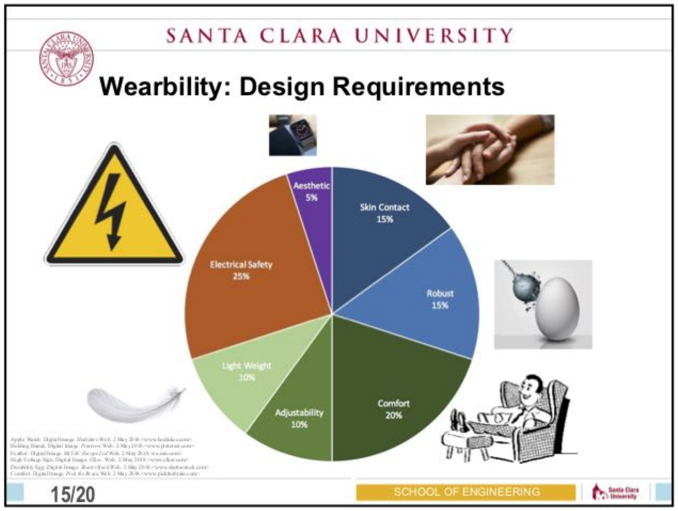

Wearability: Design Requirements

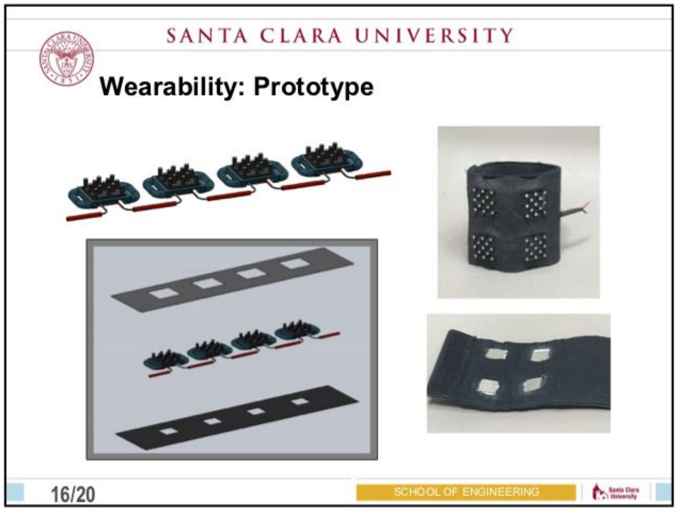

Wearability: Prototype

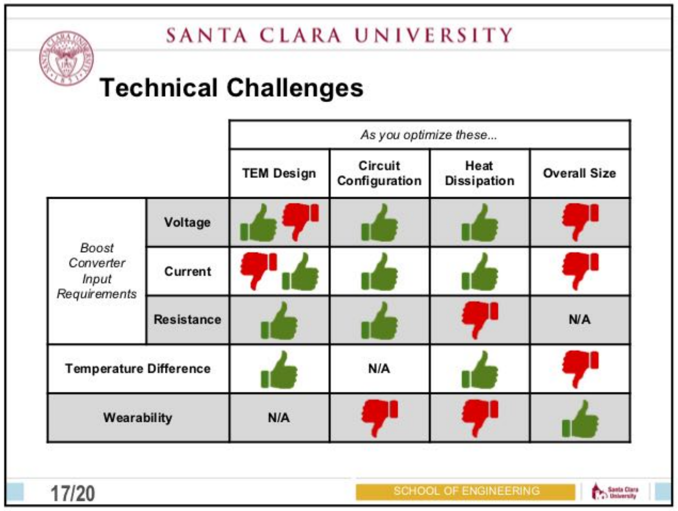

SANTA CLARA UNIVERSITY

Technical Challenges

		As you optimize these...			
		TEM Design	**Circuit Configuration**	**Heat Dissipation**	**Overall Size**
Boost Converter Input Requirements	**Voltage**	👍 👎	👍	👍	👎
	Current	👎 👍	👍	👍	👎
	Resistance	👍	👍	👎	N/A
Temperature Difference		👍	N/A	👍	👎
Wearability		N/A	👎	👎	👍

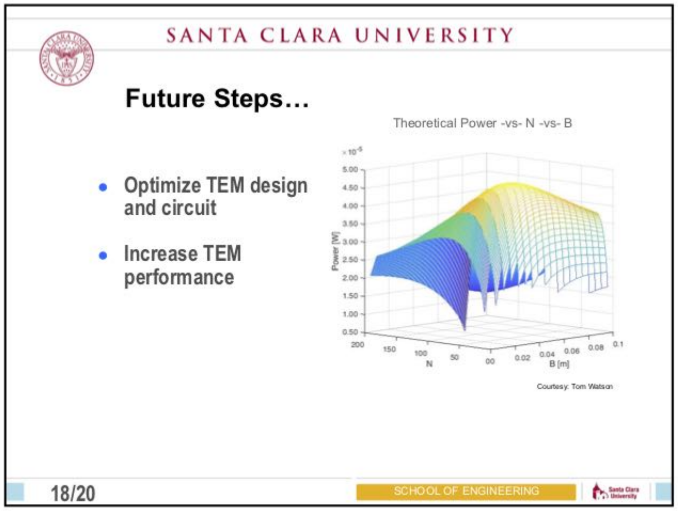

SANTA CLARA UNIVERSITY

Future Steps…

- Optimize TEM design and circuit
- Increase TEM performance

Theoretical Power -vs- N -vs- B

Courtesy: Tom Watson

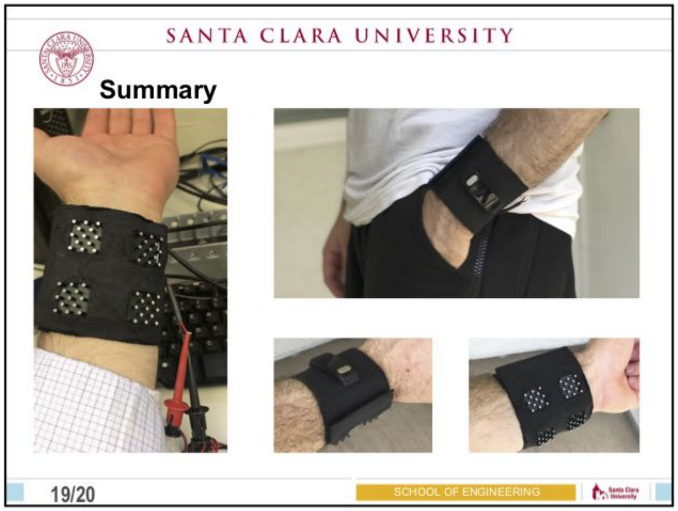

SANTA CLARA UNIVERSITY

Summary

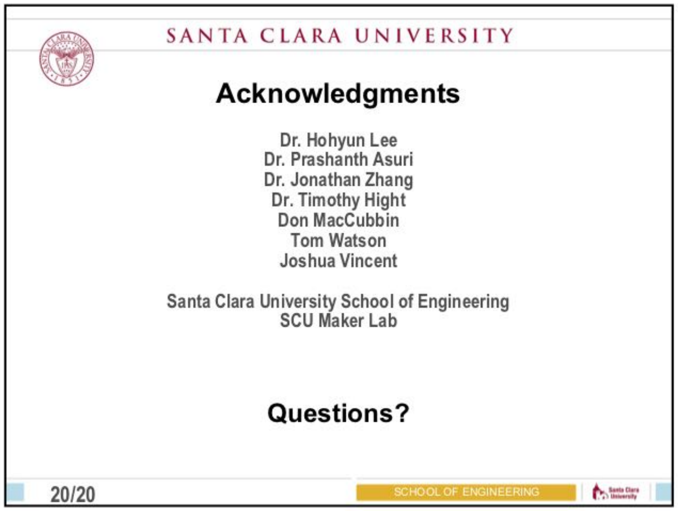

SANTA CLARA UNIVERSITY

Acknowledgments

Dr. Hohyun Lee
Dr. Prashanth Asuri
Dr. Jonathan Zhang
Dr. Timothy Hight
Don MacCubbin
Tom Watson
Joshua Vincent

Santa Clara University School of Engineering
SCU Maker Lab

Questions?

SANTA CLARA UNIVERSITY

references

[1] Thermic — Seiko Watches, THE SEIKO MUSEUM. https://museum.seiko.co.jp/e n/collections/clock watch/category3/collect041.html.

[2] Siddique, A., Mahmud, S., and Heyst, B. A Review of the State of the Science on Wearable Thermoelectric Power Generators (TEGs) and their Existing Challenges. Renewable and Sustainable Energy Reviews Vol. 73 (2017): pp. 730-744.

[3] Heinemann, L., & Krinelke, L. (2012). Insulin Infusion Set: The Achilles Heel of Continuous Subcutaneous Insulin Infusion. Journal of Diabetes Science and Technology, 6(4), 954–964.

[4] Walsh, J., Roberts, R., Weber, D., Faber-Heinemann, G., & Heinemann, L. (2015). Insulin Pump and CGM Usage in the United States and Germany: Results of a Real-World Survey With 985 Subjects. Journal of Diabetes Science and Technology, 9(5), 1103–1110. http://doi.org/10.1177/1932296815588945

Appendix H: Relevant Patents

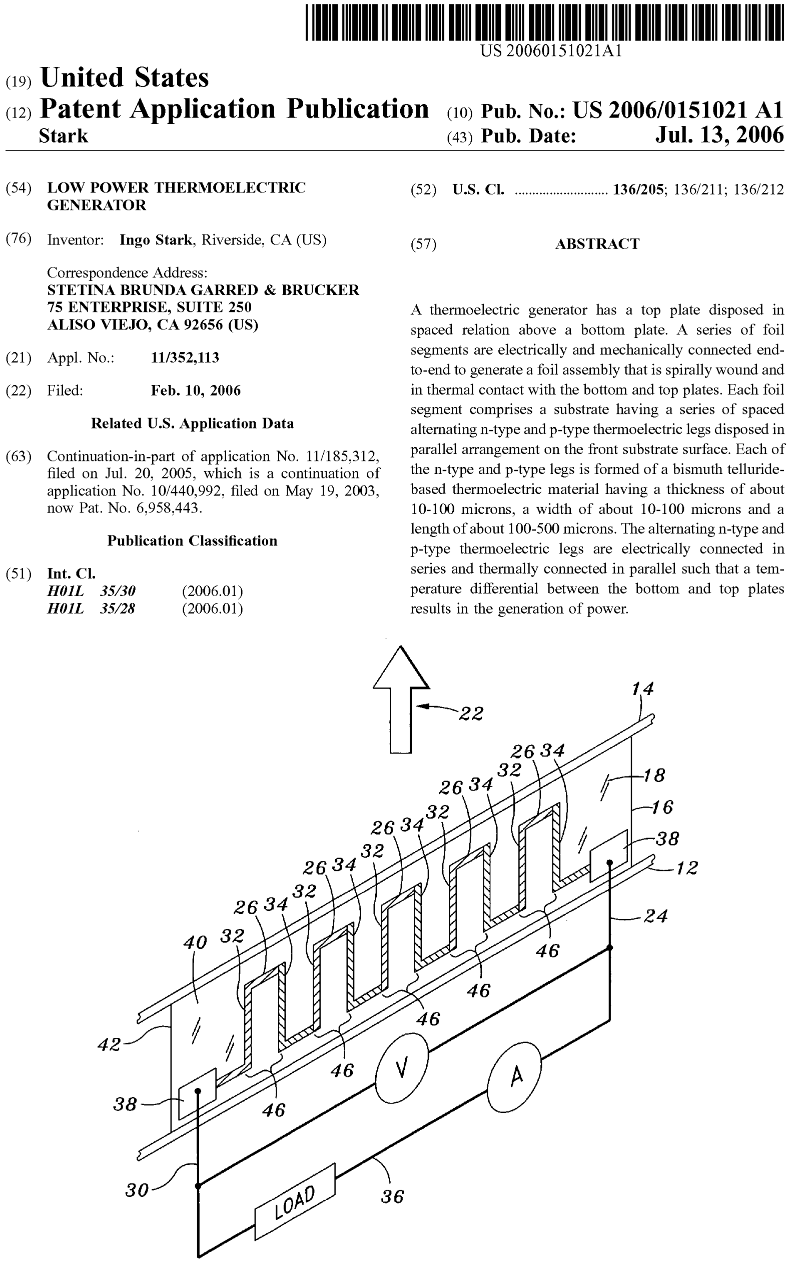

US 20060151021A1

(19) **United States**
(12) **Patent Application Publication**
Stark

(10) **Pub. No.: US 2006/0151021 A1**
(43) **Pub. Date: Jul. 13, 2006**

(54) **LOW POWER THERMOELECTRIC GENERATOR**

(76) Inventor: **Ingo Stark**, Riverside, CA (US)

Correspondence Address:
STETINA BRUNDA GARRED & BRUCKER
75 ENTERPRISE, SUITE 250
ALISO VIEJO, CA 92656 (US)

(21) Appl. No.: **11/352,113**

(22) Filed: **Feb. 10, 2006**

Related U.S. Application Data

(63) Continuation-in-part of application No. 11/185,312, filed on Jul. 20, 2005, which is a continuation of application No. 10/440,992, filed on May 19, 2003, now Pat. No. 6,958,443.

Publication Classification

(51) **Int. Cl.**
H01L 35/30 (2006.01)
H01L 35/28 (2006.01)

(52) **U.S. Cl.** **136/205**; 136/211; 136/212

(57) **ABSTRACT**

A thermoelectric generator has a top plate disposed in spaced relation above a bottom plate. A series of foil segments are electrically and mechanically connected end-to-end to generate a foil assembly that is spirally wound and in thermal contact with the bottom and top plates. Each foil segment comprises a substrate having a series of spaced alternating n-type and p-type thermoelectric legs disposed in parallel arrangement on the front substrate surface. Each of the n-type and p-type legs is formed of a bismuth telluride-based thermoelectric material having a thickness of about 10-100 microns, a width of about 10-100 microns and a length of about 100-500 microns. The alternating n-type and p-type thermoelectric legs are electrically connected in series and thermally connected in parallel such that a temperature differential between the bottom and top plates results in the generation of power.

Figure 52: Patent of TEM module used for low power generation.

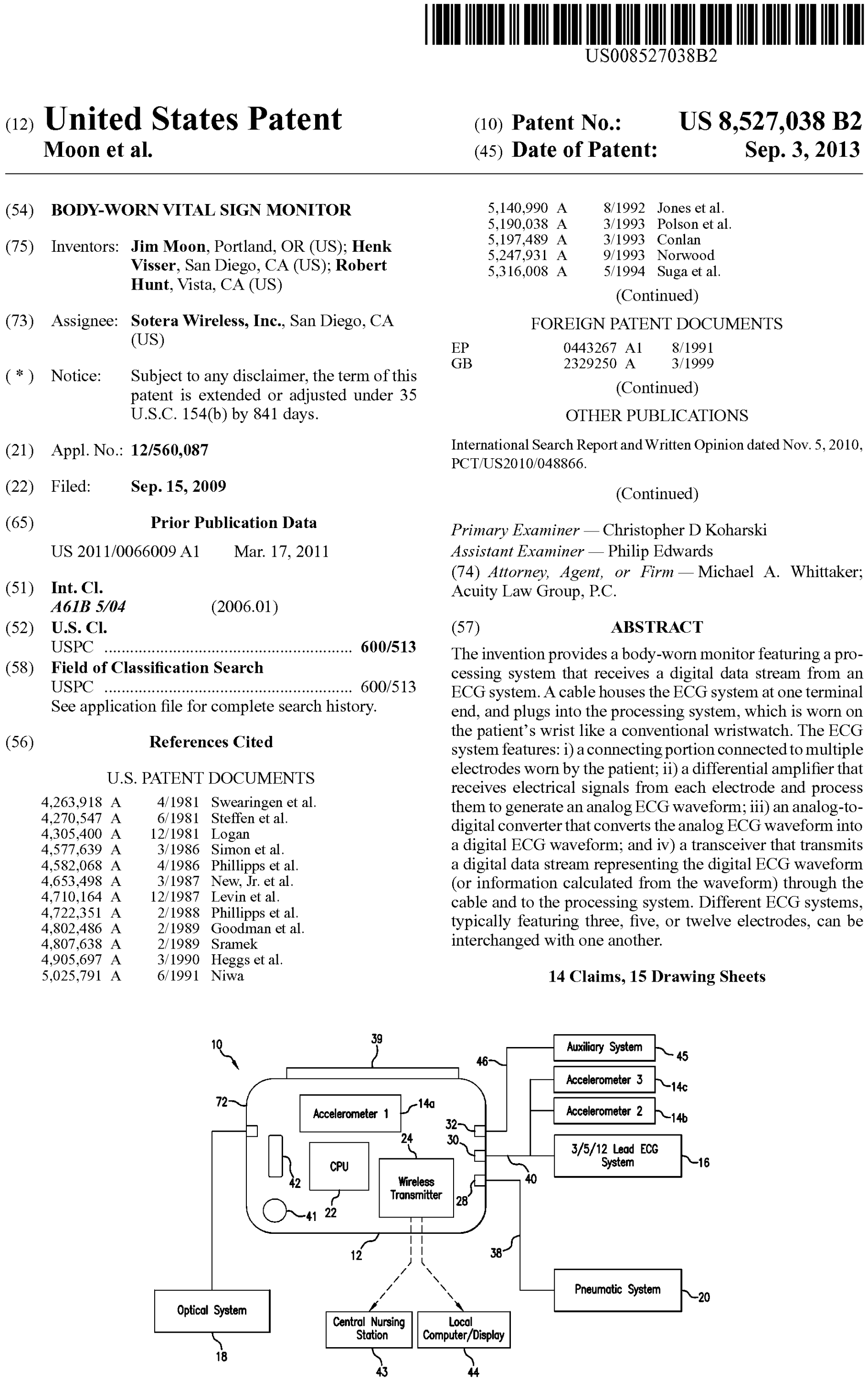

US008527038B2

(12) **United States Patent**
Moon et al.

(10) **Patent No.: US 8,527,038 B2**
(45) **Date of Patent: Sep. 3, 2013**

(54) **BODY-WORN VITAL SIGN MONITOR**

(75) Inventors: **Jim Moon**, Portland, OR (US); **Henk Visser**, San Diego, CA (US); **Robert Hunt**, Vista, CA (US)

(73) Assignee: **Sotera Wireless, Inc.**, San Diego, CA (US)

(*) Notice: Subject to any disclaimer, the term of this patent is extended or adjusted under 35 U.S.C. 154(b) by 841 days.

(21) Appl. No.: **12/560,087**

(22) Filed: **Sep. 15, 2009**

(65) **Prior Publication Data**

US 2011/0066009 A1 Mar. 17, 2011

(51) **Int. Cl.**
A61B 5/04 (2006.01)

(52) **U.S. Cl.**
USPC **600/513**

(58) **Field of Classification Search**
USPC 600/513
See application file for complete search history.

(56) **References Cited**

U.S. PATENT DOCUMENTS

4,263,918	A	4/1981	Swearingen et al.
4,270,547	A	6/1981	Steffen et al.
4,305,400	A	12/1981	Logan
4,577,639	A	3/1986	Simon et al.
4,582,068	A	4/1986	Phillipps et al.
4,653,498	A	3/1987	New, Jr. et al.
4,710,164	A	12/1987	Levin et al.
4,722,351	A	2/1988	Phillipps et al.
4,802,486	A	2/1989	Goodman et al.
4,807,638	A	2/1989	Sramek
4,905,697	A	3/1990	Heggs et al.
5,025,791	A	6/1991	Niwa
5,140,990	A	8/1992	Jones et al.
5,190,038	A	3/1993	Polson et al.
5,197,489	A	3/1993	Conlan
5,247,931	A	9/1993	Norwood
5,316,008	A	5/1994	Suga et al.

(Continued)

FOREIGN PATENT DOCUMENTS

EP	0443267	A1	8/1991
GB	2329250	A	3/1999

(Continued)

OTHER PUBLICATIONS

International Search Report and Written Opinion dated Nov. 5, 2010, PCT/US2010/048866.

(Continued)

Primary Examiner — Christopher D Koharski
Assistant Examiner — Philip Edwards
(74) *Attorney, Agent, or Firm* — Michael A. Whittaker; Acuity Law Group, P.C.

(57) **ABSTRACT**

The invention provides a body-worn monitor featuring a processing system that receives a digital data stream from an ECG system. A cable houses the ECG system at one terminal end, and plugs into the processing system, which is worn on the patient's wrist like a conventional wristwatch. The ECG system features: i) a connecting portion connected to multiple electrodes worn by the patient; ii) a differential amplifier that receives electrical signals from each electrode and process them to generate an analog ECG waveform; iii) an analog-to-digital converter that converts the analog ECG waveform into a digital ECG waveform; and iv) a transceiver that transmits a digital data stream representing the digital ECG waveform (or information calculated from the waveform) through the cable and to the processing system. Different ECG systems, typically featuring three, five, or twelve electrodes, can be interchanged with one another.

14 Claims, 15 Drawing Sheets

Figure 53: Patent of wrist wearable EKG device.

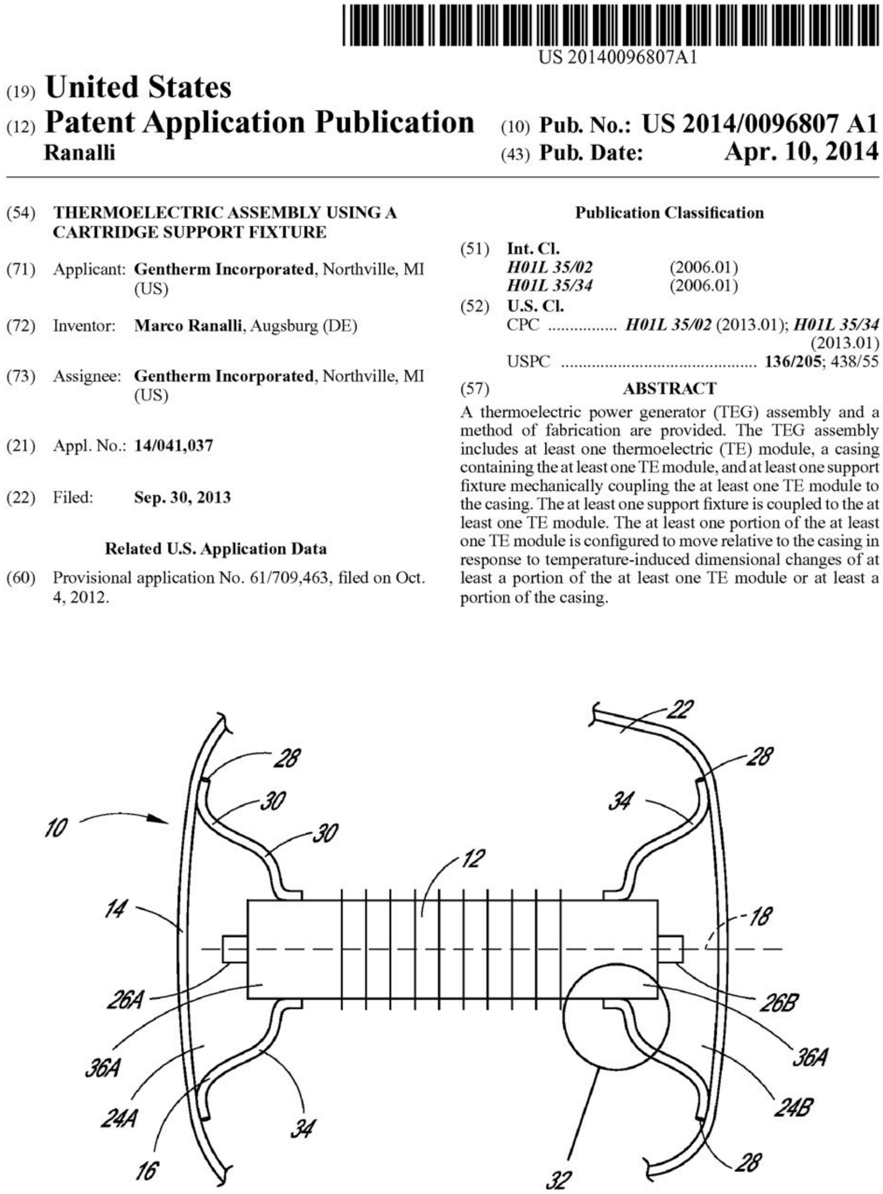

US 20140096807A1

(19) **United States**

(12) **Patent Application Publication** (10) **Pub. No.: US 2014/0096807 A1**

Ranalli (43) **Pub. Date: Apr. 10, 2014**

(54) **THERMOELECTRIC ASSEMBLY USING A CARTRIDGE SUPPORT FIXTURE**

(71) Applicant: **Gentherm Incorporated**, Northville, MI (US)

(72) Inventor: **Marco Ranalli**, Augsburg (DE)

(73) Assignee: **Gentherm Incorporated**, Northville, MI (US)

(21) Appl. No.: **14/041,037**

(22) Filed: **Sep. 30, 2013**

Related U.S. Application Data

(60) Provisional application No. 61/709,463, filed on Oct. 4, 2012.

Publication Classification

(51) **Int. Cl.**

H01L 35/02 (2006.01)

H01L 35/34 (2006.01)

(52) **U.S. Cl.**

CPC ***H01L 35/02*** (2013.01); ***H01L 35/34*** (2013.01)

USPC **136/205**; 438/55

(57) **ABSTRACT**

A thermoelectric power generator (TEG) assembly and a method of fabrication are provided. The TEG assembly includes at least one thermoelectric (TE) module, a casing containing the at least one TE module, and at least one support fixture mechanically coupling the at least one TE module to the casing. The at least one support fixture is coupled to the at least one TE module. The at least one portion of the at least one TE module is configured to move relative to the casing in response to temperature-induced dimensional changes of at least a portion of the at least one TE module or at least a portion of the casing.

Figure 54: Patent of thermoelectric assembly using cardtridge support fixture.

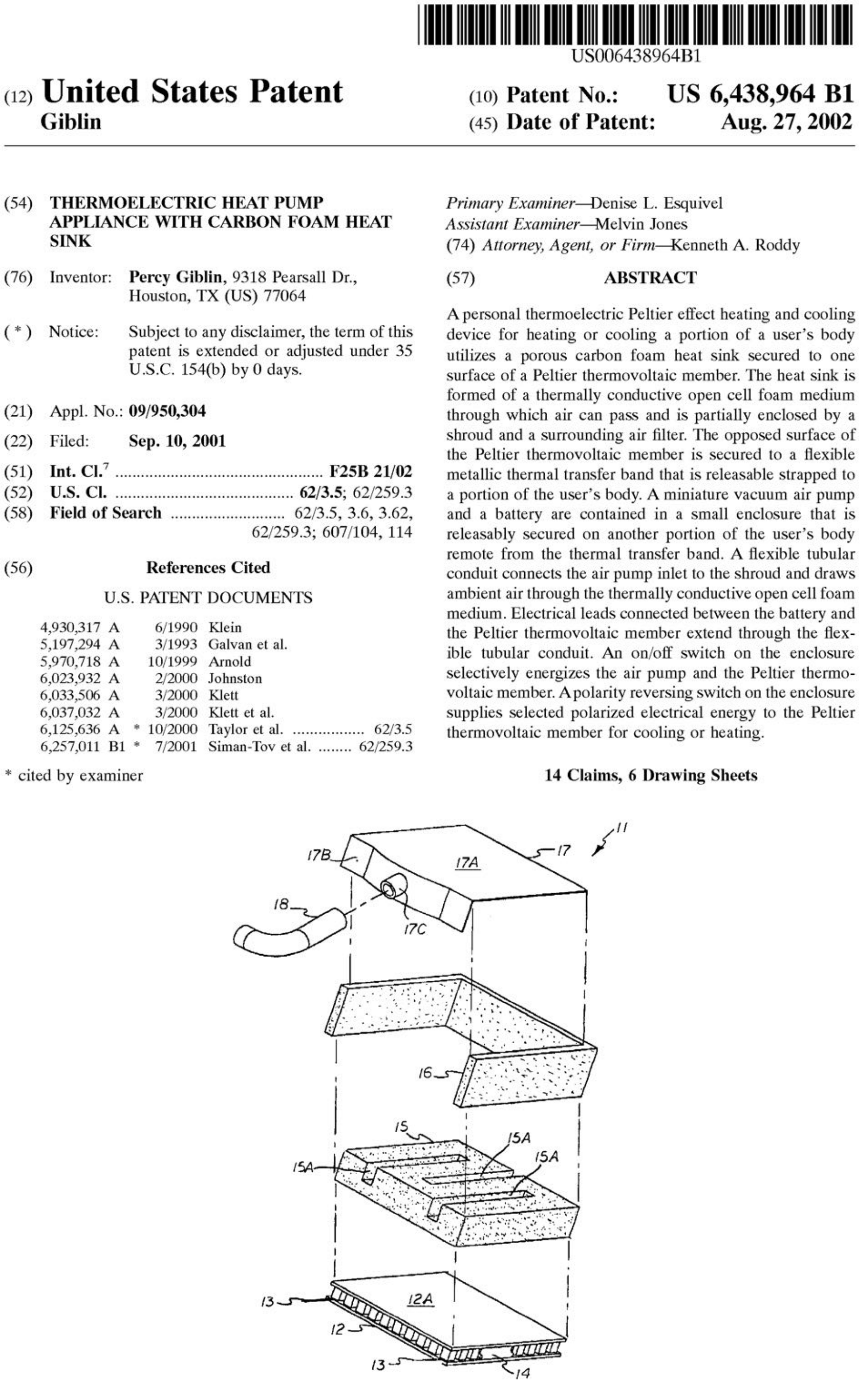

US006438964B1

(12) **United States Patent**
Giblin

(10) **Patent No.: US 6,438,964 B1**
(45) **Date of Patent: Aug. 27, 2002**

(54) **THERMOELECTRIC HEAT PUMP APPLIANCE WITH CARBON FOAM HEAT SINK**

(76) Inventor: **Percy Giblin**, 9318 Pearsall Dr., Houston, TX (US) 77064

(*) Notice: Subject to any disclaimer, the term of this patent is extended or adjusted under 35 U.S.C. 154(b) by 0 days.

(21) Appl. No.: **09/950,304**

(22) Filed: **Sep. 10, 2001**

(51) **Int. Cl.**^{7} **F25B 21/02**
(52) **U.S. Cl.** **62/3.5**; 62/259.3
(58) **Field of Search** 62/3.5, 3.6, 3.62, 62/259.3; 607/104, 114

(56) **References Cited**

U.S. PATENT DOCUMENTS

4,930,317	A		6/1990	Klein	
5,197,294	A		3/1993	Galvan et al.	
5,970,718	A		10/1999	Arnold	
6,023,932	A		2/2000	Johnston	
6,033,506	A		3/2000	Klett	
6,037,032	A		3/2000	Klett et al.	
6,125,636	A	*	10/2000	Taylor et al.	62/3.5
6,257,011	B1	*	7/2001	Siman-Tov et al.	62/259.3

* cited by examiner

Primary Examiner—Denise L. Esquivel
Assistant Examiner—Melvin Jones
(74) *Attorney, Agent, or Firm*—Kenneth A. Roddy

(57) **ABSTRACT**

A personal thermoelectric Peltier effect heating and cooling device for heating or cooling a portion of a user's body utilizes a porous carbon foam heat sink secured to one surface of a Peltier thermovoltaic member. The heat sink is formed of a thermally conductive open cell foam medium through which air can pass and is partially enclosed by a shroud and a surrounding air filter. The opposed surface of the Peltier thermovoltaic member is secured to a flexible metallic thermal transfer band that is releasable strapped to a portion of the user's body. A miniature vacuum air pump and a battery are contained in a small enclosure that is releasably secured on another portion of the user's body remote from the thermal transfer band. A flexible tubular conduit connects the air pump inlet to the shroud and draws ambient air through the thermally conductive open cell foam medium. Electrical leads connected between the battery and the Peltier thermovoltaic member extend through the flexible tubular conduit. An on/off switch on the enclosure selectively energizes the air pump and the Peltier thermovoltaic member. A polarity reversing switch on the enclosure supplies selected polarized electrical energy to the Peltier thermovoltaic member for cooling or heating.

14 Claims, 6 Drawing Sheets

Figure 55: Patent of thermoelectric heat pump.